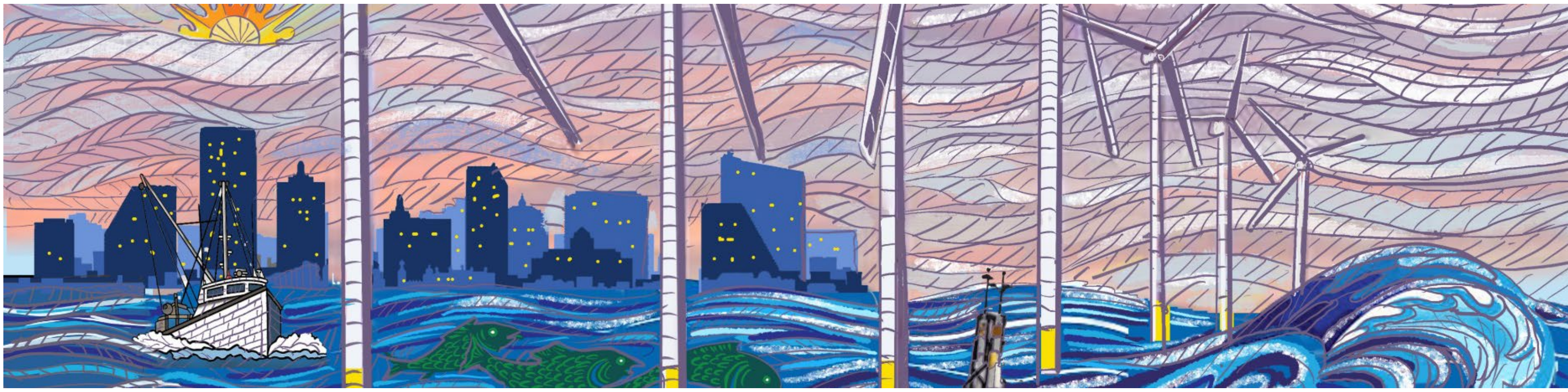

Appendix II-J3

Sediment Dispersion Modeling Report

May 2024

TECHNICAL REPORT

SEDIMENT TRANSPORT MODELING

Atlantic Shores Offshore Project Area Cable Installation

Prepared by:

RPS

Jill Rowe, Heather Weitzner, Missy Gloekler

55 Village Square Drive
South Kingstown RI 02879

T +1 401 789 6224
E Jill.Rowe@rpsgroup.com

Prepared for:

EDR

RPS Project: P-19-208506
Report Version: 2
December 16, 2021

Contents

Figures

Tables

Appendices

List of Acronyms

BOEM	Bureau of Ocean Energy Management
COP	Construction and Operations Plan
ECC	Export Cable Corridor
EDR	Environmental Design & Research
GIS	Geographic Information System
HDD	Horizontal Directional Drilling
HVAC	High Voltage Alternating Current
HVDC	High Voltage Direct Current
IAC	Inter-Array Cable
IACC	Inter-Array Cable Corridor
NDBC	National Data Buoy Center
NEPA	National Environmental Policy Act
NOAA	National Oceanic and Atmospheric Administration
OCS	Outer Continental Shelf
O&M	Operations and Maintenance
PDE	Project Design Envelope
POI	Point of Interconnection
SSFATE	Suspended Sediment FATE
TSS	Total Suspended Solids
USGS	United States Geological Survey
WEA	Wind Energy Area
WTA	Wind Turbine Area
WTG	Wind Turbine Generator

EXECUTIVE SUMMARY

Atlantic Shores Offshore Wind, LLC (Atlantic Shores), a 50/50 joint venture between EDF-RE Offshore Development, LLC, a wholly owned subsidiary of EDF Renewables, Inc. (EDF Renewables) and Shell New Energies US LLC (Shell), are proposing to develop offshore wind energy generation projects (the Projects) within the southern portion of Lease Area OCS-A 0499 (the Lease Area). The Lease Area is approximately 183,253 acres (742 km^2) in size and is located on the Outer Continental Shelf (OCS) within the New Jersey Wind Energy Area (WEA). The New Jersey WEA was identified as suitable for offshore renewable energy development by the Bureau of Ocean Energy Management (BOEM) through a multi-year, public environmental review process. Through this review process, the New Jersey WEA was sited to exclude areas of high value habitat and conflicting water and air space uses.

The Construction and Operations Plan (COP) has been developed in accordance with 30 CFR § 585 and the stipulations in Atlantic Shores' Lease Agreement OCS-A 0499. Atlantic Shores is requesting BOEM's review and authorization of the Projects in accordance with BOEM's (2018) Project Design Envelope (PDE) guidance. A PDE provides a reasonable range of designs for proposed components and installation techniques to deliver the Projects, which provides Atlantic Shores with the flexibility to optimize the Projects and take advantage of anticipated improvements in the rapidly-evolving offshore wind technology while providing BOEM with the information required to fulfill its expected role as the lead federal agency under the National Environmental Policy Act (NEPA). The COP will also inform the state and local regulatory processes.

Atlantic Shores' proposed offshore wind energy generation facilities will be located in an approximately 102,124-acre (413-km^2) Wind Turbine Area (WTA) located in the southern portion of the Lease Area. The WTA consists of two areas, Project 1 and Project 2. Project 1 is located in the western 54,175 acres (219.2 km^2) of the WTA and Project 2 is located in the eastern 31,847 acres (128.9 km^2) of the WTA, with a 16,102-acre (65.2-km^2) Overlap Area that could be used by either Project 1 or Project 2. In addition to the WTA, the PDE includes two offshore Export Cable Corridors (ECCs) within federal and New Jersey state waters as well as two onshore interconnection cable routes, onshore substation sites, and a proposed operations and maintenance (O&M) facility in New Jersey, each of which could be used by Project 1, Project 2, or both.

At its closest point, the WTA is approximately 8.7 miles (mi) (14 km) from the New Jersey shoreline. Within the WTA, the Projects will include up to 200 wind turbine generators[1] (WTGs) and up to 10 offshore substations (OSSs). The WTGs and OSSs will be connected by a system of 66 kV to 150 kV inter-array cables (IACs). OSSs within the WTA may be connected to each other by 66 kV to 275 kV inter-link cables.

Energy from the OSSs will be delivered to shore via 230 kV to 525 kV high voltage alternating current (HVAC) or high voltage direct current (HVDC) export cables. Up to five export cables could be installed within either of the ECCs (the Atlantic ECC and the Monmouth ECC); however, the total number of cables for both ECCs combined will be up to eight export cables. The export cables will traverse federal and state waters to deliver energy from the OSSs to landfall sites in New Jersey. The Atlantic ECC travels from the western tip of the WTA westward to the Atlantic Landfall Site in Atlantic City, NJ and has a total length of approximately 12 mi (19 km). The approximately 61 mi (98 km) long Monmouth ECC travels from the eastern corner of the WTA along the eastern edge of Lease Area OCS-A 0499 to the Monmouth Landfall Site in Sea Girt, NJ. At the Monmouth and Atlantic ECC Landfall Sites, horizontal directional drilling (HDD) will be employed to support each export cables' offshore-to-onshore transition. The HDD landfall technique has been selected both to ensure stable cable burial along the New Jersey's dynamic coast and to avoid nearshore and shoreline impacts

This appendix to the COP documents the sediment transport modeling assessment of the sediment-disturbing offshore cable installation activities associated with the development of the Projects. The cable installation methods may vary along the route depending on subsurface conditions. The installation methods are described

[1] Project 1 will consist of a minimum of 105 WTGs and up to a maximum of 136 WTGs. Project 2 will consist of a minimum of 64 WTGs and up to a maximum of 95 WTGs.

in detail in the COP and the details of the assumed modeling parameters are documented within this report. Consistent with the PDE, this study simulated multiple scenarios to capture a conservative design and range of effects associated with the installation of IACs in the WTA, offshore export cables in the two ECCs, and landfall approaches. The representative scenarios include:

- IAC installation with jet trenching installation parameters
- IAC installation with mechanical trenching installation parameters
- Monmouth ECC cable installation (Branch 1) with jet trenching installation parameters
- Monmouth ECC cable installation (Branch 2) with jet trenching installation parameters
- Atlantic ECC cable installation (Branch 1) with jet trenching installation parameters
- Atlantic ECC cable installation (Branch 2) with jet trenching installation parameters
- Monmouth ECC landfall approach with HDD pit activities
- Atlantic ECC landfall approach with HDD pit activities

Additional modeling of sandwave clearance was performed to bound the potential effects of seabed preparation, prior to cable installation, assuming conservative installation parameters associated with the anticipated equipment. It is expected that there will be sufficient time between sandwave clearance and cable installation such that the effects from sandwave clearance do not compound or influence effects from cable installation activities. For the sandwave clearance model inputs and modeling results refer to Attachment A as this information was not included in the main body of this report. The environmental data, sediment characteristics, and general sediment dispersion modeling approach described in the body of this report apply to the sandwave modeling and as such are not discussed in Attachment A.

The sediment transport modeling assessment was carried out through two interconnected modeling tasks:

1. Development of a three-dimensional hydrodynamic model application of a domain encompassing the Projects' activities using the BFHYDRO modeling system; and
2. Simulations of the suspended sediment fate and transport, including evaluation of seabed deposition and suspended sediment plumes, using the SSFATE (Suspended Sediment FATE) modeling system to simulate installation activities. Velocity fields developed using the BFHYDRO model are used as the primary forcing for SSFATE.

This study was carried out to characterize the effects associated with the offshore cable installation activities. The effects of cable installation activities were quantified using two parameters: 1) water column concentrations of total suspended sediment (TSS), and 2) sediment thickness on the seabed resulting from the deposition of the suspended sediments over time. These thresholds were selected either because they are thresholds of biological significance or because they provide an effective means of demonstrating the physical effects. The results are presented with respect to the following thresholds:

- Water column concentrations thresholds: 10, 25, 50, 100, 200, and 650 milligrams per liter (mg/L)
- Water column exposure durations: 2, 4, 6, and 12 hours
- Seabed deposition: 1, 5, 10, 20, and 100 millimeters (mm)

Simulations of several possible IAC or offshore export cable installation methods using either jet trenching installation parameters (for IAC and export cable installation) or mechanical trenching installation parameters (for IAC installation only) predicted above-ambient TSS ≥10 mg/L and deposition over 1 mm stayed relatively close to the route centerline. This is due to sediments being introduced to the water column closer to the seabed. TSS concentrations ≥10 mg/L traveled a maximum distance of approximately 2.9 km, 2.6 km, and 1.7 km for inter-array, Monmouth ECC, and Atlantic ECC cable installation, respectively. For the landfall approach scenarios, results were conservative as it assumes no cofferdam was deployed during construction activities. Additionally, use of an excavator was assumed and sediment was introduced at the surface. This resulted in a maximum distance for the predicted above-ambient TSS concentrations ≥10 mg/L of approximately 3.3 km and 1.9 km for the Monmouth and Atlantic HDD pits, respectively.

Above-ambient TSS concentrations stemming from cable installation for the IAC, Monmouth ECC, and Atlantic ECC model scenarios remained relatively close to the route centerline, were constrained to the bottom of the water column, and were short-lived. For the IAC and Atlantic ECC model scenarios, above-ambient TSS concentrations substantially dissipated within 2 to 4 hours and fully dissipated in less than 6 hours. For the Monmouth ECC model scenarios, above-ambient TSS concentrations substantially dissipated within 2 to 6 hours but required between 12 and 24 hours to fully dissipate, likely due to the relatively longer route (i.e., larger volume of suspended sediment), route orientation in relation to currents, and more frequent occurrence of fine sediment. For the landfall approach scenarios, the tails of the plumes, with concentrations ≥10 mg/L, were transported away from the source and were short-lived, while concentrations around the HDD pits dissipated within 6 to 24 hours for the Monmouth HDD pit and 6 to 12 hours for the Atlantic HDD pit. The larger areas of TSS concentrations above thresholds and the longer time for the plume to diminish to ambient conditions for the Monmouth HDD pit may be attributed to sediments being released in deeper water, the higher fraction of fine sediments taking longer to settle, and slightly stronger currents transporting the sediments parallel with the shore.

Deposition ≥1 mm was limited to 110 m from the IAC centerline for jet trenching installation parameters and to 50 m for mechanical trenching installation parameters. Variations in plume extent and duration for IAC installation can be attributed to differences in cross-sectional area and advance rates, which impacted the timing of the currents. Deposition ≥1 mm was limited to 200 m from the Monmouth ECC centerline and to 50 m of the Atlantic ECC centerline. The maximum deposition associated with IAC, Atlantic ECC, and Monmouth ECC model scenarios was less than 5 mm, between 5-10 mm, and between 10-20 mm, respectively, with all the maximum deposition thicknesses predicted to remain within 15 m from each route's centerline. For the Monmouth and Atlantic HDD pit excavations, deposition ≥1 mm was predicted to extend a maximum distance of 479 m and 200 m, respectively. The Atlantic landfall approach scenario was predicted to have higher areas of deposition for the 10 mm and 20 mm thresholds due to a higher fraction of coarse sediment. In combination with the sediment type and the relatively more shore-perpendicular nature of the currents at the Atlantic HDD pit, more sediment remained close to the pit and settled to the bottom rather than lingering in the water column or being transported as a suspended sediment plume.

While the plume patterns for the respective representative IAC scenarios, offshore export cable scenarios, and landfall approach scenarios were generally similar, differences in the extent and persistence of the plumes and the extent and thickness of deposition may be attributed to route orientation relative to currents, timing of currents, installation parameters, volume suspended, and sediment grain size distribution.

1 INTRODUCTION

Atlantic Shores Offshore Wind, LLC (Atlantic Shores), a 50/50 joint venture between EDF-RE Offshore Development, LLC, a wholly owned subsidiary of EDF Renewables, Inc. (EDF Renewables) and Shell New Energies US LLC (Shell), are proposing to develop offshore wind energy generation projects (the Projects) within the southern portion of Lease Area OCS-A 0499 (the Lease Area). The Lease Area is approximately 183,253 acres (742 km^2) in size and is located on the Outer Continental Shelf (OCS) within the New Jersey Wind Energy Area (WEA). The New Jersey WEA was identified as suitable for offshore renewable energy development by the Bureau of Ocean Energy Management (BOEM) through a multi-year, public environmental review process. Through this review process, the New Jersey WEA was sited to exclude areas of high value habitat and conflicting water and air space uses.

The Construction and Operations Plan (COP) has been developed in accordance with 30 CFR § 585 and the stipulations in Atlantic Shores' Lease Agreement OCS-A 0499. Atlantic Shores is requesting BOEM's review and authorization of the Projects in accordance with BOEM's (2018) Project Design Envelope (PDE) guidance. A PDE provides a reasonable range of designs for proposed components and installation techniques to deliver the Projects, which provides Atlantic Shores with the flexibility to optimize the Project and take advantage of anticipated improvements in rapidly-evolving offshore wind technology while providing BOEM with the information required to fulfill its expected role as the lead federal agency under the National Environmental Policy Act (NEPA). The COP will also inform the state and local regulatory processes.

Atlantic Shores' proposed offshore wind energy generation facilities will be located in an approximately 102,124-acre (413-km^2) Wind Turbine Area (WTA) located in the southern portion of the Lease Area. The WTA consists of two areas, Project 1 and Project 2. Project 1 is located in the western 54,175 acres (219.2 km2) of the WTA and Project 2 is located in the eastern 31,847 acres (128.9 km2) of the WTA, with a 16,102-acre (65.2-km2) Overlap Area that could be used by either Project 1 or Project 2. In addition to the WTA, both the PDE includes two offshore Export Cable Corridors (ECCs) within federal and New Jersey state waters as well as two onshore interconnection cable routes, onshore substation sites, and a proposed operations and maintenance (O&M) facility in New Jersey, each of which could be used by Project 1, Project 2, or both.

At its closest point, the WTA is approximately 8.7 miles (mi) (14 km) from the New Jersey shoreline. Within the WTA, the Projects will include up to 200 wind turbine generators[2] (WTGs) and up to 10 offshore substations (OSSs). The WTGs and OSSs will be connected by a system of 66 kV to 150 kV inter-array cables (IACs). OSSs within the WTA may be connected to each other by 66 kV to 275 kV inter-link cables.

Energy from the OSSs will be delivered to shore via 230 kV to 525 kV high voltage alternating current (HVAC) or high voltage direct current (HVDC) export cables. Up to five export cables could be installed within either ECC (the Atlantic ECC and the Monmouth ECC); however, the total number of cables for both ECCs combined will be up to eight export cables. The export cables will traverse federal and state waters to deliver energy from the OSSs to landfall sites in New Jersey. The Atlantic ECC travels from the western tip of the WTA westward to the Atlantic Landfall Site in Atlantic City, NJ and has a total length of approximately 12 mi (19 km). The approximately 61 mi (98 km) long Monmouth ECC travels from the eastern corner of the WTA along the eastern edge of Lease Area OCS-A 0499 to the Monmouth Landfall Site in Sea Girt, NJ.

At the Monmouth and Atlantic ECC Landfall Sites, horizontal directional drilling (HDD) will be employed to support each export cables' offshore-to-onshore transition. The HDD landfall technique has been selected both to ensure stable cable burial along the New Jersey's dynamic coast and to avoid nearshore and shoreline impacts.

This appendix to the COP documents the sediment transport modeling assessment of the sediment-disturbing offshore cable installation activities associated with the development of the Projects. The cable installation

[2] Project 1 will consist of a minimum of 105 WTGs and up to a maximum of 136 WTGs. Project 2 will consist of a minimum of 64 WTGs and up to a maximum of 95 WTGs.

methods may vary along the route depending on subsurface conditions. The installation methods are described in detail in the COP and the details of the assumed modeling parameters are documented within this report. Consistent with the PDE, this study simulated multiple scenarios to capture a conservative design and range of effects associated with the installation of IACs in the WTA, offshore export cables in the two ECCs, and landfall approaches. An illustration of the Atlantic Shores Offshore Project Region (Offshore Project Region) and relevant study components is presented in Figure 1.

Additional modeling of sandwave clearance was performed to bound the potential effects of seabed preparation, prior to cable installation, assuming conservative installation parameters associated with the anticipated equipment. It is expected that there will be sufficient time between sandwave clearance and cable installation such that the effects from sandwave clearance do not compound or influence effects from cable installation activities. For the sandwave clearance model inputs and modeling results refer to Attachment A as this information was not included in the main body of this report. The environmental data, sediment characteristics, and general sediment dispersion modeling approach described in the body of this report apply to the sandwave modeling and as such are not discussed in Attachment A.

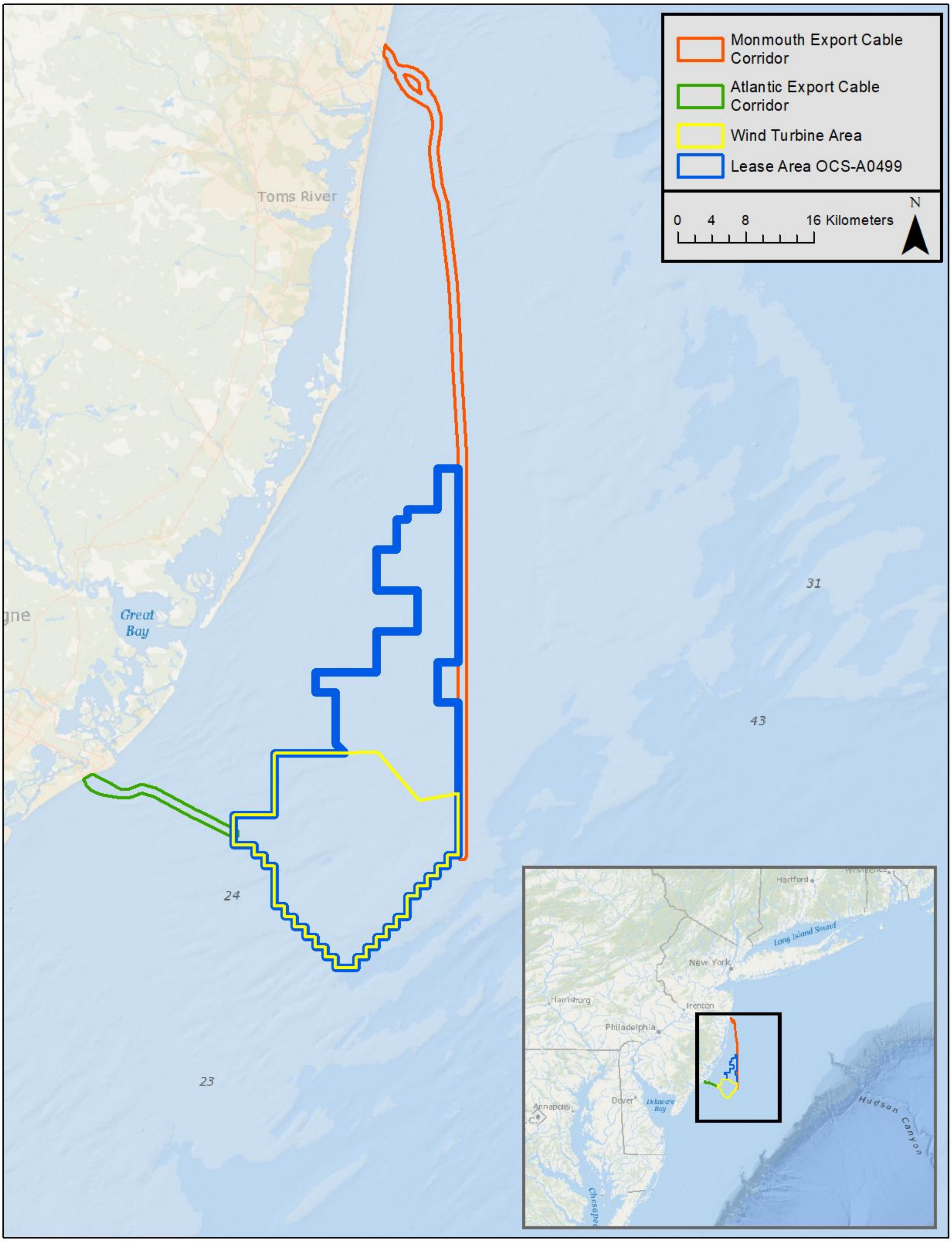

Figure 1. Map of Atlantic Shores Offshore Project Region with Offshore Components.

1.1 Study Scope and Objectives

RPS applied customized hydrodynamic and sediment transport and dispersion models to assess potential effects from sediment suspension during cable installation activities. This approach is consistent to the modeling approach used for many similar studies that have been accepted by state and federal regulatory agencies for pipeline and cable installation as well as harbor dredging and land reclamation activities. Specifically, the analysis included two interconnected modeling tasks:

1. Development of a three-dimensional hydrodynamic model application of a domain encompassing the Project activities using the BFHYDRO modeling system; and
2. Simulations of the suspended sediment fate and transport (including evaluation of seabed deposition and suspended sediment plumes) using the SSFATE (Suspended Sediment FATE) modeling system to simulate installation activities. Velocity fields developed using the BFHYDRO model are used as the primary forcing for SSFATE.

This study simulated multiple scenarios to capture a conservative design and an encompassing range of effects associated with the installation of IACs in the WTA, offshore export cables in the two ECCs, and landfall approaches. While it is proposed that up to five cables will be installed within each ECC, each cable will be installed in a separate trench at different timeframes. Therefore, the modeled scenarios can be considered as a single representative cable per ECC. Because each export cable route diverges nearshore, resulting in two “branches” per ECC, two scenarios were modeled within the Atlantic ECC and Monmouth ECC so that the environmental forcing conditions could be accounted for. While multiple landfall approaches are proposed, one landfall approach per ECC was simulated and can be considered representative of other landfall approaches in proximity to the ECC landfall locations.

This study was carried out to characterize the effects associated with the offshore cable installation activities. The effects of cable installation activities were quantified using two parameters: 1) water column concentrations of total suspended sediment (TSS), and 2) sediment thickness on the seabed resulting from the deposition of the suspended sediments over time. The results are presented with respect to the following thresholds:

- Water column concentrations thresholds: 10, 25, 50, 100, 200, and 650 milligrams per liter (mg/L)
- Water column exposure durations: 2, 4, 6, and 12 hours
- Seabed deposition: 1, 5, 10, 20, and 100 millimeters (mm)

These thresholds were selected either because they are thresholds of biological significance (Anderson and Mackas, 1986; Berry et al., 2011; Cake, 1983; Essink, 1999; Fabricius, 2005; Gilmour, 1999; Hendrick et al., 2016; Murphy, 1985; Rayment, 2002; Read et al., 1982, 1983; Rogers, 1990; Turner and Miller, 1991; Wilber and Clarke, 2001) or because they provide an effective means of demonstrating the physical effects. Thresholds associated with biological significance are documented in Sections 4.5.2.1 and 4.6.2.1 of the COP, which are the benthic and finfish and invertebrate sections, respectively.

This report describes the models used, modeling approach, and results of the study. A description of the environmental data sources used is provided in Section 2. The BFHYDRO hydrodynamic model and its application to the Offshore Project Region are presented in Section 3, Section 4 provides an overview of the SSFATE sediment dispersion model and results from the application of SSFATE for each scenario, and references are provided in Section 5.

2 STUDY ENVIRONMENTAL DATA

The inputs for hydrodynamic and sediment dispersion modeling used environmental data gathered from public sources or provided by Atlantic Shores (Figure 2). An overview of the data types and sources is provided below while more detailed discussions of the data are presented in the hydrodynamic and sediment transport modeling sections. This study utilized sediment data from field campaigns focused on the WTA and the ECCs. Sample sites and detailed grain size results are documented in Section 4.5.1.1 in Volume II, Appendix II-A3 of the COP. These field campaigns produced vibracores, which underwent varying degrees of analysis including sieve analysis, hydrometer analysis, and moisture testing. Detailed information about samples, as they were used to develop inputs to the sediment transport model, is provided in Section 4.2.3.

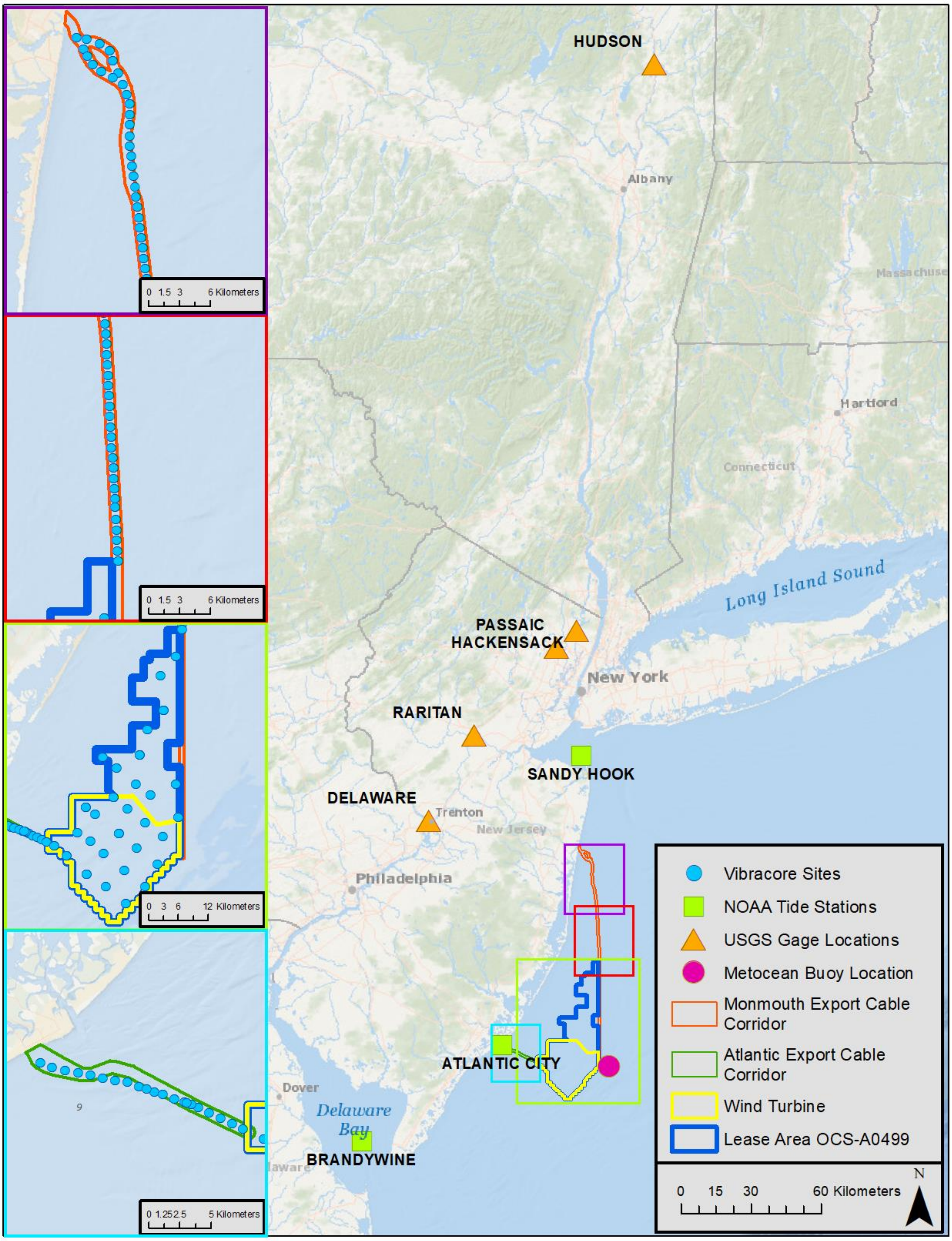

Figure 2. Locations of Environmental Data Sources.

2.1 Shoreline Data

The BFHYDRO hydrodynamic model domain extended from approximately Montauk, New York at the western end of Long Island, west to Newark, New Jersey and south to Assateague Island, Maryland. To best locate and define open boundary conditions, the modeling domain is significantly larger than the Lease Area footprint. The majority of the shoreline for the domain was developed by merging shoreline data from New Jersey and New York, which were obtained from their respective Geographic Information System (GIS) clearinghouses (NJDEP, 2015; NYSDOS, 2003). The Delaware and Maryland shorelines were taken from a high resolution world basemap. The shoreline data were used as a guide for developing the hydrodynamic model grid and to develop the land/water boundaries in the concentration and deposition grid used in the sediment transport modeling.

2.2 Bathymetry Data

Bathymetric data were gathered both from the National Oceanic and Atmospheric Administration (NOAA) datasets for coastal and offshore waters, as well as from the General Bathymetric Chart of the Oceans (GEBCO). NOAA National Ocean Service (NOS) hydrographic survey data were downloaded from the NOAA Bathymetric Data Viewer (NOAA, 2020a). GEBCO’s gridded data were obtained for the domain (GEBCO, 2020) and combined with the NOAA data for a complete dataset within the model domain. The combined bathymetric dataset was used to develop depths for the hydrodynamic model grid as well as the depth grid used for sediment transport modeling.

2.3 Meteorological Observations

Meteorological (i.e., wind) data used as inputs to the hydrodynamic model were obtained from Atlantic Shores and the NOAA National Data Buoy Center (NDBC) LLNR 830 Long Island station (NOAA, 2020c), the locations of which are shown on Figure 2. The client-provided data were used as hydrodynamic model inputs, while the NDBC data were used to compare the client-provided data to long-term averages. Wind speed and direction at the NDBC station were obtained from an anemometer located approximately 4.1 m above mean sea level, where measurements were recorded hourly. LiDAR data from the Atlantic Shores buoy were obtained at various elevations. However, 10-minute speeds at 10 m above mean sea level were extracted and hourly-averaged for modeling efforts.

Monthly average wind speeds at the Atlantic Shores buoy from April to September 2020 (timeframe of available data during time of data collection) are presented in Table 1, along with an average of those months. Monthly average wind speeds for the NDBC station from 2006 to 2016 are presented in Table 2, along with annual averages. Wind roses for the same periods are provided in Figure 3 and Figure 4 for the Atlantic Shores buoy and NDBC station, respectively. The currents in the region are dominated by the tides, which repeat periodically. Therefore, wind speed does not have a major influence on the currents, particularly near the seabed. While any time period would capture the variability of tidal currents, modeling was conducted during the month of May. This was selected from the client-provided data because the average wind speeds in May (6.56 m/s) are broadly representative of the wind conditions at the site when compared to the NDBC station annual average wind speed of 6.75 m/s. Although the September average wind speed is closer to the NDBC station annual average wind speed, May was selected because the dataset is more complete.

Table 1. Monthly Average Wind Speeds at Atlantic Shores Buoy Available at Time of Data Collection.

Timeframe	Monthly Average Wind Speed (m/s)
	2020
Apr	7.24
May	6.56
Jun	5.41
Jul	4.94
Aug	5.14
Sep	6.82
Annual	6.02

Table 2. Monthly Average Wind Speeds from LLNR 830. Incomplete datasets denoted using a "-".

Timeframe	Monthly Average Wind Speed (m/s)															Average
	2006	2007	2008	2009	2010	2011	2012	2013	2014	2015	2016	2017	2018	2019	2020	
Jan	8.21	8.18	8.26	-	8.62	7.74	8.64	7.81	-	-	8.84	8.14	8.50	8.50	7.86	8.28
Feb	8.72	9.35	7.50	8.68	9.32	8.29	7.67	9.10	-	-	8.44	7.45	6.76	7.14	6.65	8.08
Mar	7.21	7.67	7.66	6.47	6.81	7.15	6.75	8.36	-	-	6.91	8.69	9.10	6.83	6.66	7.41
Apr	5.93	-	5.99	6.47	5.47	6.66	6.29	6.39	-	6.38	6.52	5.68	6.86	6.12	7.23	6.31
May	5.21	6.77	6.28	5.23	5.49	4.85	4.97	5.84	-	5.11	5.38	6.12	5.06	5.65	6.26	5.58
Jun	5.68	8.41	4.80	4.60	5.11	4.53	5.47	5.80	-	5.33	5.03	5.84	4.81	5.10	4.74	5.38
Jul	5.20	-	4.60	5.06	5.00	4.74	5.15	5.88	-	4.51	4.71	4.86	5.02	4.59	5.10	4.95
Aug	5.08	-	4.46	4.70	5.59	-	4.86	5.10	-	4.90	5.37	5.06	5.76	5.12	5.61	5.13
Sep	5.84	-	5.72	6.14	6.89	-	5.99	5.94	4.47	5.84	6.76	6.07	6.22	6.20	5.91	6.00
Oct	7.94	-	7.36	7.89	8.10	-	7.43	7.25	7.80	8.13	7.25	6.95	7.64	8.13	-	7.66
Nov	6.63	-	8.00	8.21	7.86	7.31	8.11	-	8.77	7.08	7.92	7.99	8.63	8.41	-	7.91
Dec	8.07	-	9.18	9.94	9.75	7.35	7.58	-	7.90	7.07	8.88	8.05	7.77	8.47	-	8.33
Annual	6.64	8.08	6.65	6.67	7.00	6.51	6.58	6.75	7.24	6.04	6.83	6.74	6.84	6.69	6.22	**6.75**

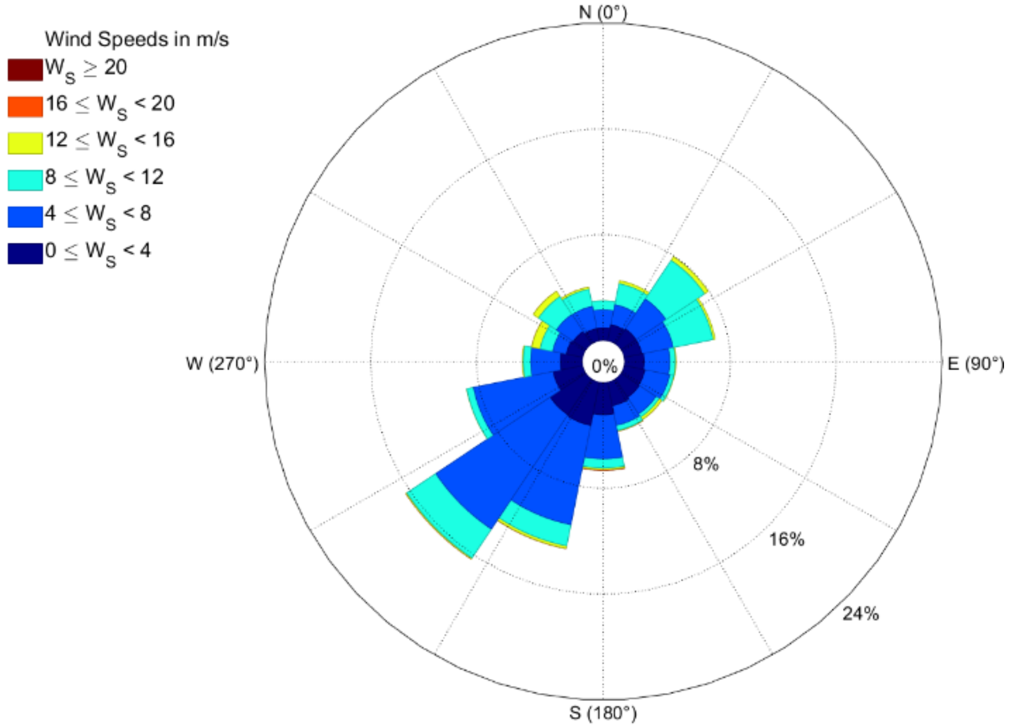

Figure 3. Wind Rose for April-September 2020 at Atlantic Shores Buoy.

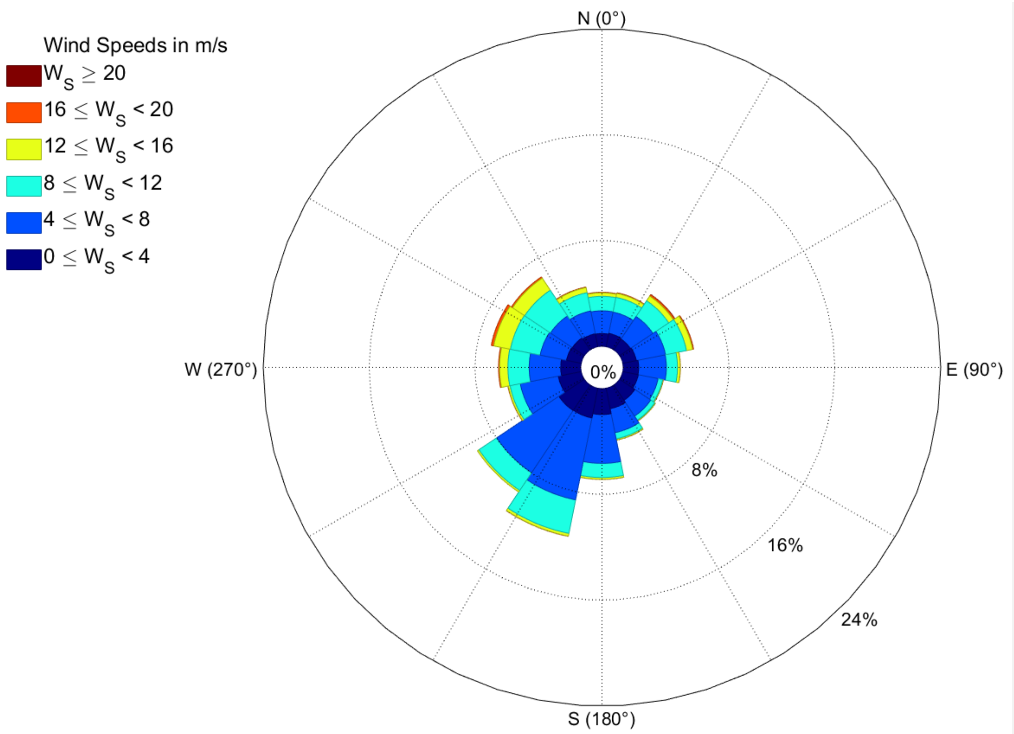

Figure 4. Wind Rose for 2006–2020 at NDBC LLNR 830 Long Island Station.

2.4 Sea Surface Height (Tides) Observations

Sea surface height characteristics were used to develop model forcing and verify hydrodynamic model predictions. Data used for this study included data from the publicly-available TPXO7 global tidal model, developed by Oregon State University and available in the form of tidal harmonic constituents, and from NOAA Tides and Currents as time histories of observed water surface elevations. Tidal harmonic constituents are the amplitude and phase of known periodic constituents of the tidal signal, where the tidal signal is the sum of all constituents added together by superposition. The amplitude describes the difference between a mean sea level datum and the peak water level for a constituent, and the phase describes the timing of the signal relative to a time datum. The constituent period determines the time for one full oscillation of the signal. The names of tidal harmonic constituents indicate the approximate period (e.g., M2 is twice daily and O1 is once daily).

The TPXO7 output was used to characterize the tides in the hydrodynamic model boundary forcing. This model output contains tidal harmonic constituent data on a one-quarter degree resolution across the globe. The model was based on data from the TOPEX/Poseidon and Jason satellites, and the model methodology is documented in Egbert et al. (1994) and Egbert and Erofeeva (2002). The constituents obtained and their periods are provided in Table 3.

Observation-based water surface elevation data spanning the model verification period were obtained from NOAA Tides and Currents for stations within the Offshore Projects' Region (Figure 2). These time series were used to verify model predictions at both the NOAA station locations and at the Atlantic Shores buoy location. Details on the verification process are provided in Section 3.2.2.1.

Table 3. Tidal Harmonic Constituents used as Hydrodynamic Model Boundary Forcing.

Name	Constituent	Speed (degrees/hour)	Period (hours)
M2	Principal lunar semidiurnal constituent	28.98	12.42
S2	Principal solar semidiurnal constituent	30.00	12.00
N2	Larger lunar elliptic semidiurnal constituent	28.44	12.66
K1	Lunar diurnal constituent	15.04	23.93
O1	Lunar diurnal constituent	13.94	25.82
M4	Shallow water overtides of principal lunar constituent	57.97	6.21
M6	Shallow water overtides of principal lunar constituent	86.95	4.14

2.5 Riverine Observations

Daily flow rates for five rivers within the model domain were obtained for use as input for the hydrodynamic model. Data from the United States Geological Survey (USGS) for the Delaware, Hackensack, Hudson, Passaic, and Raritan Rivers were obtained for 2018-2020 to develop the river boundary conditions (Table 4 [USGS, 2020]). Daily river flows were used in both the hydrodynamic model verification process and final hydrodynamic model runs.

Table 4. Riverine Observations.

River	Start Day Obtained	End Day Obtained	Flow Resolution
Delaware	1/1/2018	10/14/2020	Daily
Hackensack	1/1/2018	10/14/2020	Daily
Hudson	1/1/2018	10/14/2020	Daily
Passaic	1/1/2018	10/14/2020	Daily
Raritan	1/1/2018	10/14/2020	Daily

2.6 Ocean Current Observations

This study used observations of ocean currents from the Atlantic Shores buoy. Among other metocean data, the buoy has been collecting current speeds and directions since February 2020 at multiple ‘bins’ in the water column to provide observations of the currents as a function of depth, as detailed in Table 5. The current observations were used to verify model predictions directly through comparison of the observed data to model predictions for times within the buoy deployment period.

Table 5. Atlantic Shores Buoy Metrics and Current Observations.

Time Step (min)	Start Day Obtained	End Day Obtained	Bin Resolution (m)	Bin Range (m)
10	2/26/2020	10/6/2020	1	3-36

3 HYDRODYNAMIC MODELING

The first modeling task was the development, verification, and application of a three-dimensional hydrodynamic model with a domain that includes all of the Projects' activities. Developed by RPS, the WQMAP model system contains the BFHYDRO hydrodynamic model (Muin and Spaulding, 1997), which was used to simulate the tidal and river forcing to predict the circulation pattern throughout the domain, and to provide hydrodynamic conditions (spatially- and temporally-varying currents) for input to the sediment dispersion model. The hydrodynamic modeling task included gathering and analyzing environmental data as detailed in Section 2, developing a hydrodynamic model grid and boundary conditions, verifying model performance for a period of time with observation data, and developing currents for a timeframe characterized by typical wind conditions to be used in sediment transport simulations.

As described in Section 2.2 in Volume II of the COP, circulation (currents) in the domain is influenced by two main current systems: the southward flowing cool water temperatures from New England and the northward flowing warm water of the Gulf Stream (MAROA, 2020). Tidal currents in the domain are rotary currents and are predominately semidiurnal (two nearly equal high tides and low tides every day) (USDOI, 1982). Depending on wind speed and water depth, wind can influence surface currents and, at times, bottom currents, playing a minor role in sediment transport through most of the domain. As previously described, tidal currents exhibit cyclical, repeating patterns, and are not characterized by season. Therefore, wind was chosen as the metric when identifying an environmental timeframe used in the sediment transport and dispersion modeling. A comprehensive description of local tides and currents is documented in Section 2.2 of the COP.

3.1 BFHYDRO Model Description

The WQMAP system contains multiple models and a graphical user interface for handling input and output. The computational engine is a family of general curvilinear coordinate system computer models, including a boundary conforming gridding model (BFGRID), a hydrodynamic model (BFHYDRO), a single constituent mass transport model (BFMASS), and an eight-state variable water quality, eutrophication model (BFWASP).

The BFHYDRO model is a boundary-fitted hydrodynamic model (Muin and Spaulding, 1997; Mendelsohn et al., 1995; Huang and Spaulding, 1995; Swanson et al., 1989) that can be used to generate tidal or river elevations, velocities, and salinity and temperature distributions. The model utilizes a boundary-fitting technique, which matches the grid coordinates with shoreline and bathymetric feature boundaries for highly accurate representations of areas with complex coastal or riverine geometries. This system also allows the modeling team to adjust the model grid resolution as desired and introduce lower mesh resolution (larger cells) at locations several miles from the proposed route for computational efficiency. BFHYDRO may be applied in either two or three dimensions depending on the nature of the problem and the complexity of the study. A detailed description of the model with associated test cases is described in Muin and Spaulding (1997), and Muin (1993). The model has undergone extensive testing against analytical solutions and has been found to perform accurately and quickly. Specific model comparisons are found in Swanson et al. (2012), Mendelsohn et al. (2003), Muin and Spaulding (1997), Mendelsohn et al. (1995) and Huang and Spaulding, (1995). A brief description of the model follows.

3.1.1 Model Theory

The boundary-fitted method uses a set of coupled, quasi-linear, elliptic transformation equations to map an arbitrary horizontal multi-connected region from physical space to a rectangular mesh structure in the transformed horizontal plane (Spaulding, 1984). The three-dimensional conservation of mass and momentum equations, with approximations suitable for lakes, rivers, estuaries, and coastal oceans (Swanson, 1986; Muin, 1993) that form the basis of the model, are then solved in this transformed space. A sigma stretching system is used in the vertical to map the free surface and bottom onto coordinate surfaces to resolve bathymetric variations. The vertical mesh stretches and shrinks with the changing tidal elevation or river stage, maintaining a constant number of layers, so that no interpolation is required to simulate the surface slope or the bathymetry (Figure 5).

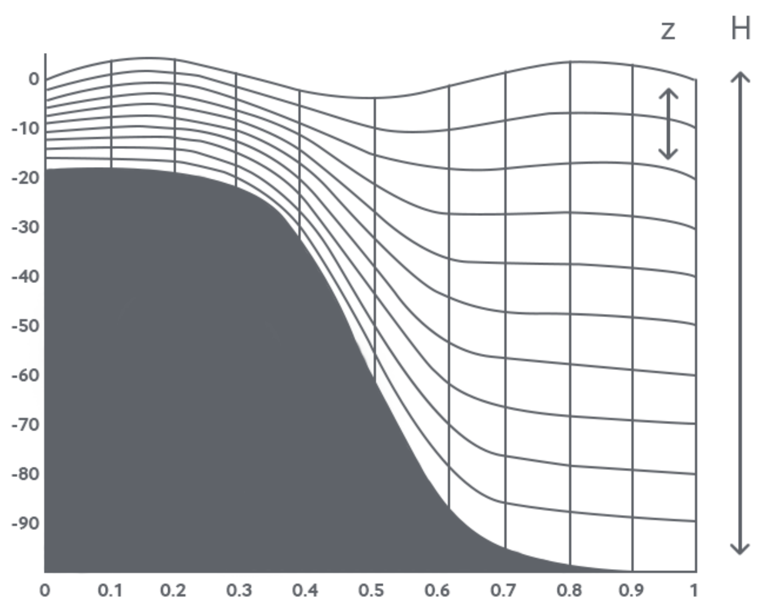

Figure 5. Schematic of the BFHYDRO Vertical Sigma Coordinate System.

The basic equations are written in spherical coordinates to allow for accurate representation of large modeled areas without distortion. The conservation equations for water mass, momentum (in three dimensions) and constituent mass (temperature [heat] and salinity) form the basis of the model and are well established. It is assumed that the discharge is incompressible, that the fluid is in hydrostatic balance, the horizontal friction is not significant, and the Boussinesq approximation applies; all customary assumptions.

The boundary conditions are as follows:

- At land, the normal component of velocity is zero.
- At open boundaries, the free surface elevation and temperature (and salinity for estuarine and coastal applications) must be specified.
- On outflow, temperature (heat) and salinity is advected out of the model domain.
- At river boundaries, the volume flux, with positive discharge into the model domain, and temperature (and occasionally salinity) must be specified.
- A bottom stress or a no slip condition can be applied at the bottom. No temperature (heat) is assumed to transfer to or from the bottom, a conservative assumption as some transfer of heat to the bottom is expected to occur.
- A wind stress, and appropriate heat transfer terms, are applied at the water surface. The surface heat balance includes all the primary heat transfer mechanisms for environmental interaction.

There are various options for specification of vertical eddy viscosity, (for momentum) and vertical eddy diffusivity, (for constituent mass [temperature and salinity]). The simplest formulation is that both are constant throughout the water column. They can also be functions of the local Richardson number, which, in turn, is a function of the vertical density gradient and vertical gradient of horizontal velocity. A one-equation or two-equation turbulence closure model may also be used.

The set of governing equations with dependent and independent variables transformed from spherical to curvilinear coordinates, in concert with the boundary conditions, is solved by a semi-implicit, split mode finite difference procedure (Swanson, 1986). The equations of motion are vertically integrated and, through simple algebraic manipulation, are recast in terms of a single Helmholtz equation in surface elevation. This equation is solved using a sparse matrix solution technique to predict the spatial distribution of surface elevation for each grid.

The vertically-averaged velocity is then determined explicitly using the momentum equation. This step constitutes the external or vertically-averaged mode. Vertical deviations of the velocity field from this vertically-averaged value are then calculated, using a tridiagonal matrix technique. The deviations are added to the vertically-averaged values to obtain the vertical profile of velocity at each grid cell, thereby generating the complete current patterns (internal mode). The methodology allows time steps based on the advective, rather than the gravity, wave speed as in conventional explicit finite difference methods, and therefore results in a computationally efficient solution procedure (Swanson, 1986; Muin, 1993).

3.2 BFHYDRO Model Application

The model application was developed for simulations in the three-dimensional mode. First, an application was developed for a period with available in-situ current observations to verify model performance. Subsequent to model verification, the output from a different period within this timeframe that reflected typical wind conditions was used in the sediment transport modeling. The main model application features are the model grid, boundary forcing, and bathymetry. These features are described in more detail below.

3.2.1 Model Grid

As described in Section 2.1, the shoreline for the model domain was developed based on merging shoreline data from each of the relevant states. The grid was mapped to the shoreline, with a coarse resolution at distances farther away from the immediate domain and fine resolution in areas closest to the Projects' components or where necessary to capture the physical characteristics of the domain. Figure 6 shows the computational model grid cells for the entire domain, which consists of 9,465 active water cells. The vertical grid is represented by 11 layers to represent vertical variability in currents from tidal and wind forcing. Model boundary conditions included specification of tidal harmonic characteristics at open boundary water cells at the edge of the domain, surface winds applied to all cell surfaces, and daily river flow applied at riverine boundaries.

Model grid bathymetry was assigned by interpolating from a set of individual data points (developed as described in Section 2.2) onto the model grid. For grid cells with multiple soundings, values were averaged. For grid cells without soundings, the values were interpolated based on the closest soundings. Figure 7 is focused on the bathymetry in the region of the Offshore Projects, depicting the WTA and both ECCs.

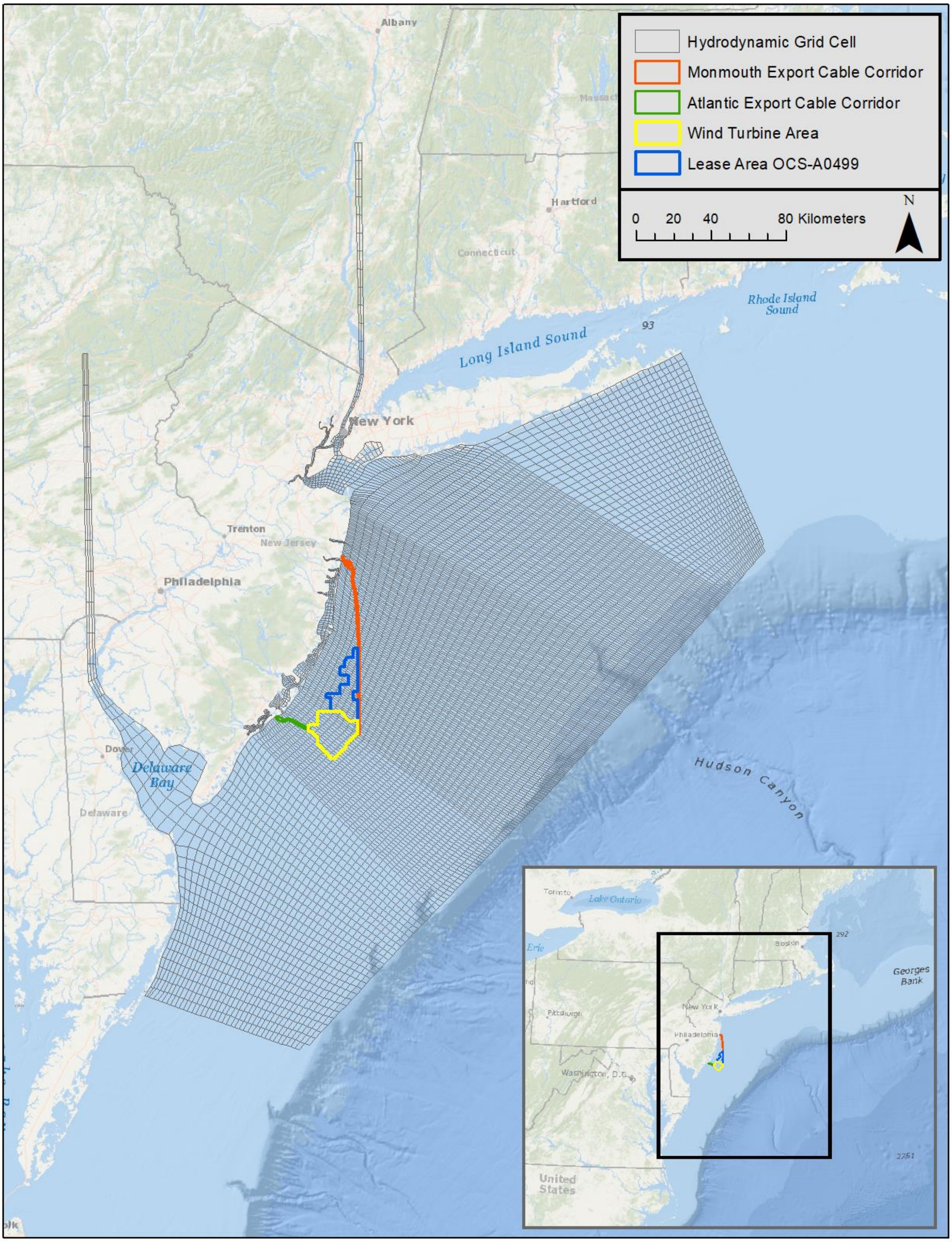

Figure 6. Hydrodynamic Model Grid.

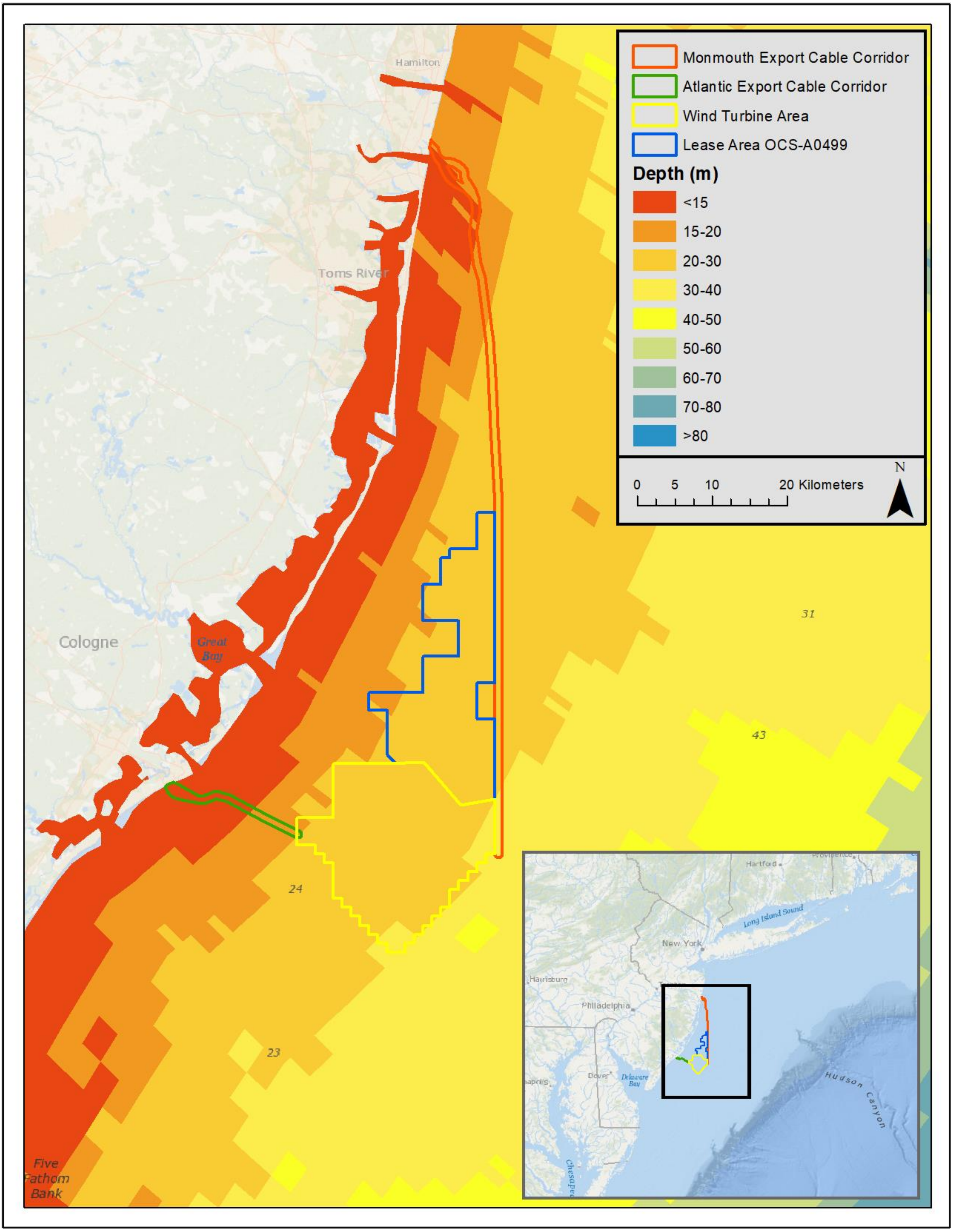

Figure 7. Model Grid Bathymetry Focused on the Region of the Projects' Offshore Components.

3.2.2 Model Results

The model was run to include two different periods: the verification period and a scenario period. The verification period is a period with available observations such that the model predictions can be verified and the scenario period is the period of time simulated to produce a data set for the sediment transport modeling.

3.2.2.1 Model Application for Verification Period

Model-predicted water surface elevations and current speeds at multiple water depths were compared to available observations to ensure the model was adequately reproducing tidal amplitude, current velocity, and current direction. The period used for model verification was April 1 to September 30, 2020. This date range was chosen because it had oceanographic (current) observations available from the Atlantic Shores buoy.

Model-predicted water surface elevations were compared to water surface elevations at the Atlantic Shores buoy and NOAA Tides and Currents stations Brandywine Shoal Light, DE and Atlantic City, NJ (Figure 8). A subset was selected for ease of viewing, as the verification period spans several months. This figure shows that the model was able to recreate the amplitude and phase throughout the domain.

Comparisons of current direction and speed at the surface and bottom of the water column between model results and observed data are presented in Figure 9 and Figure 10, respectively. Current roses show the frequency and intensity of current speed and direction. The rose petals reflect the direction the current flows towards and the color of the petals reflects the frequency of different speed intervals in each respective direction. The model was able to recreate the range of speeds and general trends of directions. Both the observed and modeled show that bottom speeds at the locations with observations are between approximately 0.1–0.2 m/s on average. The ability of the model to recreate the currents across the large domain and to recreate the predominate circulation features at these discrete points within the domain provides confidence that the model can be used to simulate actual conditions.

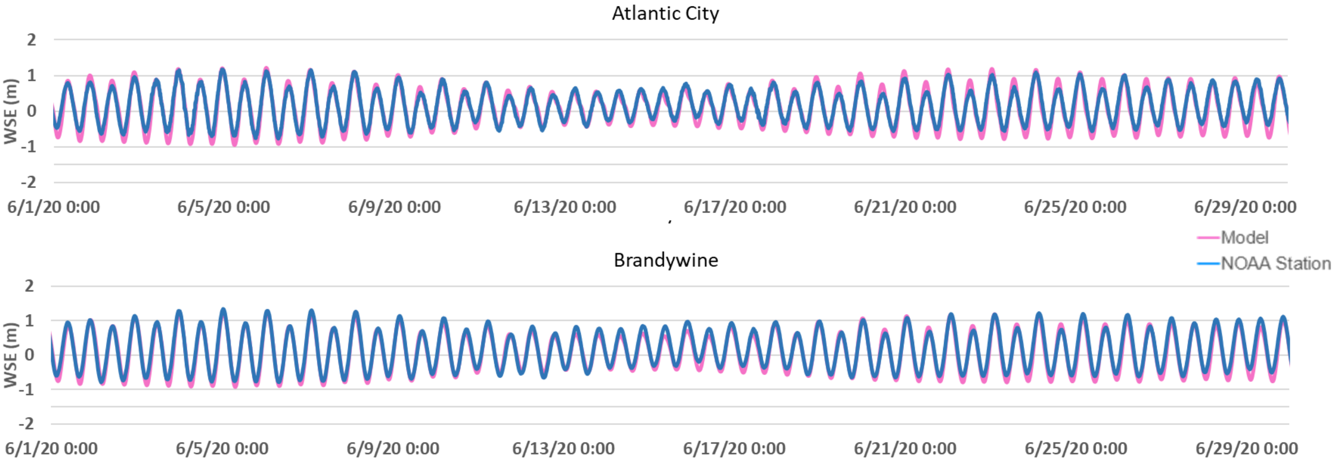

Figure 8. Comparison of Model-Predicted Water Surface Elevations to Water Surface Elevations at Two NOAA Stations for a Subset of Verification Period.

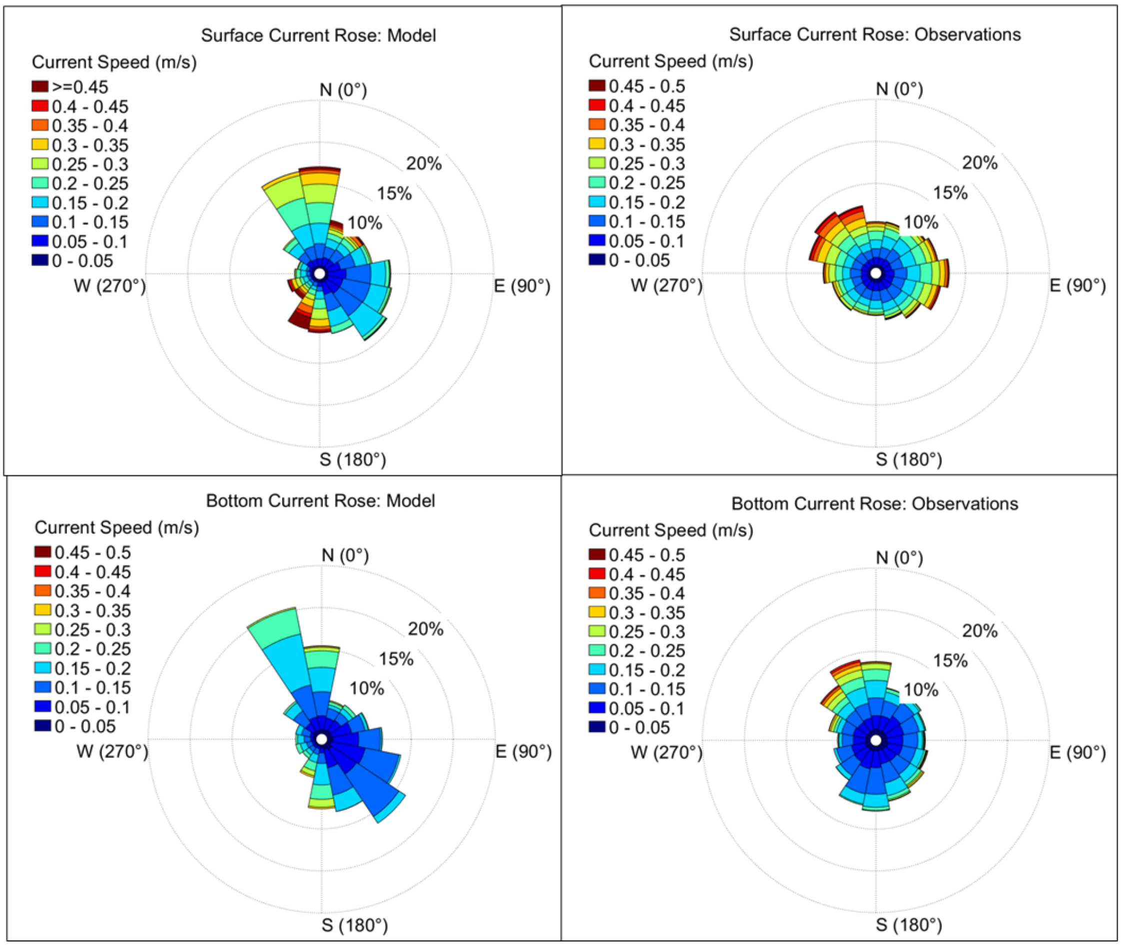

Figure 9. Current Rose Comparison of Modeled (Left) to Observed (Right) Currents at the Surface (Top) and Bottom (Bottom) at Atlantic Shores Buoy for Duration of Verification Period.

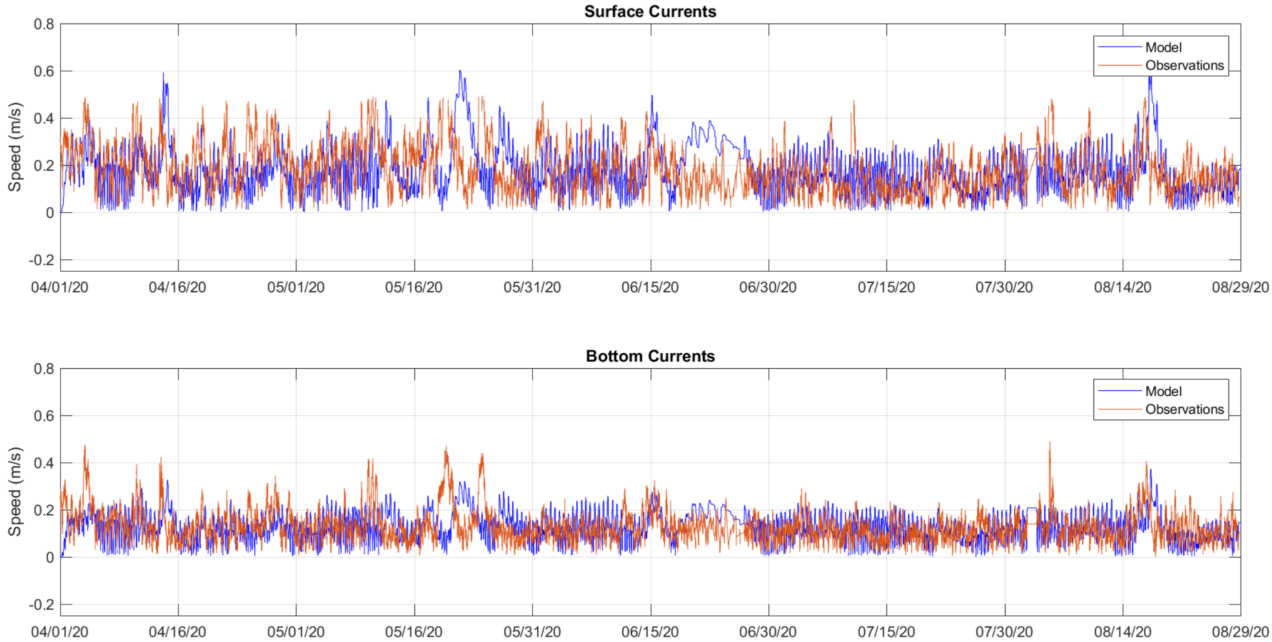

Figure 10. Comparison of Model-Predicted and Observed Surface and Bottom Currents at Atlantic Shores Buoy for Duration of Verification Period.

3.2.2.2 Model Application for Scenario Period

Once the model performance was verified, an analysis of wind speeds, as described in Section 2.3, was conducted to determine a representative time period for model scenarios. May 2020 was determined to be a period with typical winds, which were applied to all cell surfaces, while tidal harmonics and river flows were applied to open boundary water cells and riverine boundary cells, respectively. Snapshots of typical modeled flood and ebb bottom current speeds and patterns are shown in Figure 11 and Figure 12, respectively. Surface speeds are of a similar pattern with slightly stronger magnitudes.

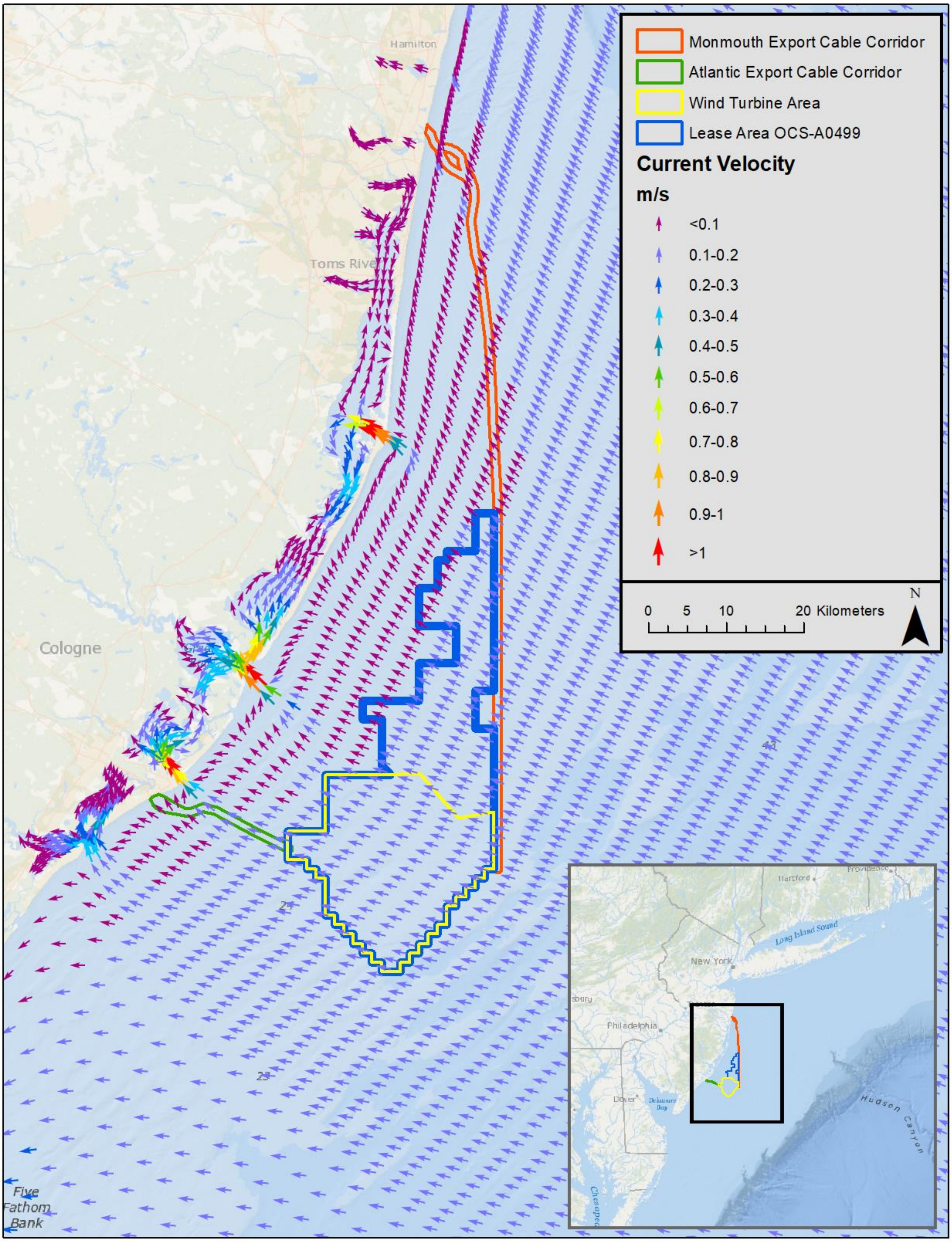

Figure 11. Snapshot Showing Peak Flood Bottom Currents.

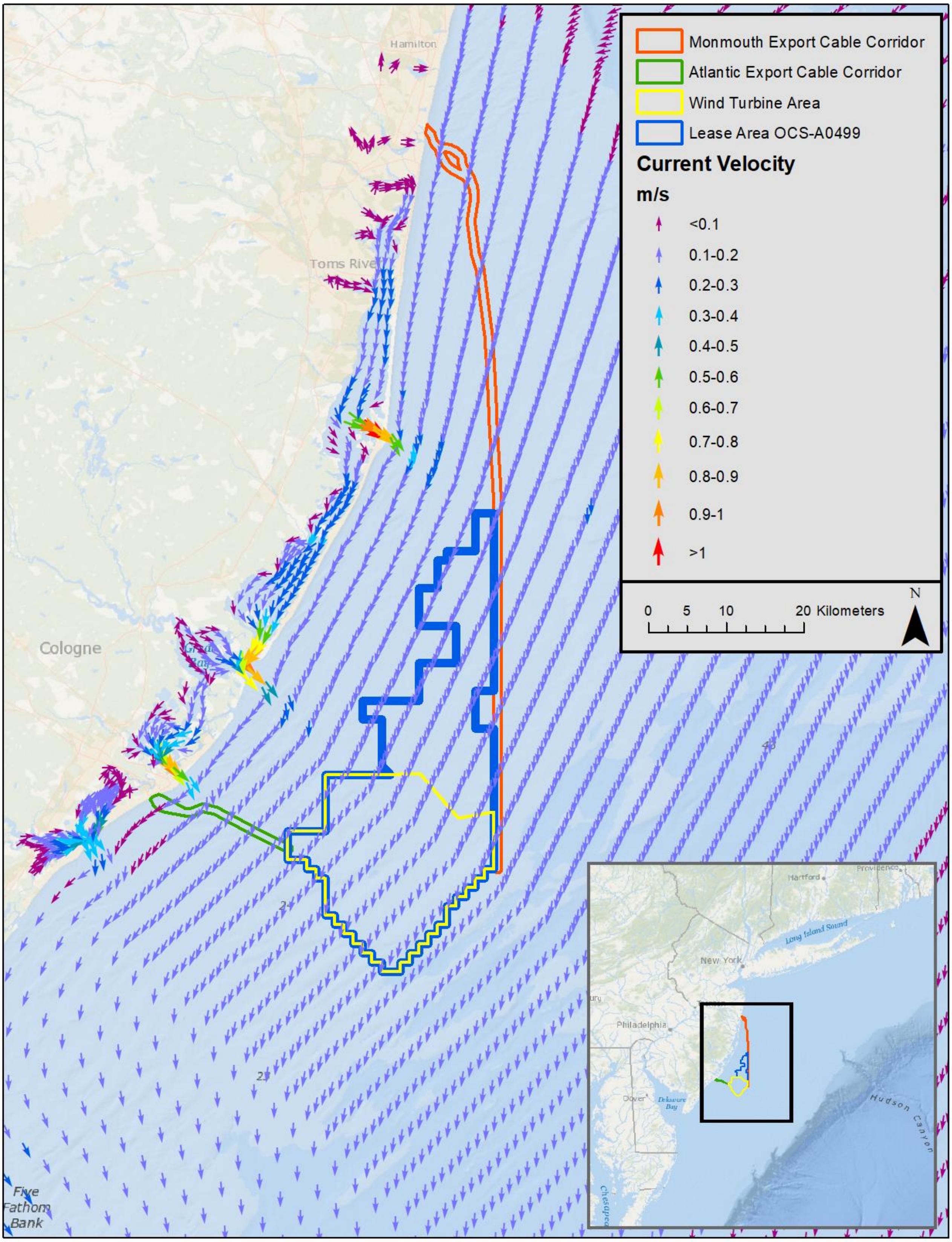

Figure 12. Snapshot Showing Peak Ebb Bottom Currents.

4 SEDIMENT MODELING

The sediment transport modeling was conducted using SSFATE, an in-house model co-developed and maintained by RPS. Descriptions of the model, model application, and the modeling results are presented in the following sections.

4.1 SSFATE Model Description

SSFATE is a three-dimensional Lagrangian (particle) model developed jointly by the United States Army Corps of Engineers' Environmental Research and Development Center (USACE ERDC) and Applied Science Associates (now part of RPS) to simulate sediment resuspension and deposition originally from marine dredging operations. Model development was documented in a series of USACE's Dredging Operations and Environmental Research Program technical notes (Johnson et al. 2000; Swanson et al. 2000), at previous World Dredging Conferences (Anderson et al. 2001), and at a series of Western Dredging Association Conferences (Swanson et al. 2006; Swanson and Isaji 2004). Following dozens of technical studies, which demonstrated successful application to dredging, SSFATE was further developed to include simulation of cable and pipeline burial operations using water jet trenchers (Swanson et al. 2006) and mechanical ploughs as well as sediment dumping and dewatering operations. The current modeling system includes a GIS-based interface for visualization and analysis of model output.

SSFATE computes the excess TSS concentrations (i.e., above background levels) in the water column and sediment depositional patterns on the seabed resulting from sediment-disturbing construction activities. The model uses specifications for the suspended sediment source strengths (i.e., mass flux), vertical distributions of sediments, and sediment grain-size distributions to represent loads to the water column from different construction activities such as dredging, dumping, cable and pipeline line installation, pile driving, dam installation and removal, and land reclamation. Multiple sediment types or fractions can be simulated simultaneously, as can discharges from moving sources. The focus of the model is on the far-field processes (i.e., meters or kilometers beyond the initial disturbance) affecting the dispersion of suspended sediment, and is used to predict the transport, dispersion, and settling of suspended sediment released to the water column.

4.1.1 Model Theory

SSFATE predicts the three-dimensional path and fate of sediment particles based on sediment properties, sediment loading characteristics, and environmental conditions (e.g., bathymetry and currents). The computational model uses a Lagrangian, or particle-based scheme to represent the total mass of suspended sediments over time, which provides a method to track suspended sediment without any loss of mass. This is a better approach as compared to Eulerian (continuous) models, which may lose mass due to the nature of the numerical approximations used for the conservation equations. Thus, the Lagrangian method is not subject to artificial diffusion near sharp concentration gradients and can easily simulate all types of sediment sources.

Sediment particles in SSFATE are divided into five size classes, each having unique behaviors for transport, dispersion, and settling (Table 6). For any given location (segment of the route), the sediment characterization is defined using the five classes, with each class representing a percent of the distribution and all five classes summing to 100%. The model determines the number of particles used per time step depending on the model time step and overall duration thereby ensuring an equal number of particles is used to define the source throughout the simulation. While a minimum of one particle per sediment size class per time step is enforced, typically multiple particles are used. The mass per particle varies depending on the total number of particles released, the grain size distribution, and the mass flux per time step.

Table 6. Sediment Size Classes used in SSFATE.

Description	Class	Type	Size Range (microns)
Fine	1	Clay	0-7
	2	Fine silt	8-35
	3	Coarse silt	36-74
	4	Fine sand	75-130
Coarse	5	Coarse sand	>130

Horizontal transport, settling, and turbulence-induced suspension of each particle are computed independently by the model for each time step. Particle advection is based on the relationship that a particle moves linearly, in three-dimensions, with a local velocity obtained from the hydrodynamic field, for a specified model time step. Diffusion is assumed to follow a simple random walk process, with the diffusion distance defined as the square root of the product of an input diffusion coefficient, and at each time step is decomposed into X and Y displacements via a random direction function. The vertical Z diffusion distance is scaled by a random positive or negative direction.

Particle settling rates are calculated using Stokes equations and are based on the size and density of each particle class. Settling of mixtures of particles is a complex process due to interaction of the different size classes, some of which tend to be cohesive and thus clump together to form larger particles that have different settling rates than would be expected based on their individual sizes. Enhanced settlement rates due to flocculation and scavenging are particularly important for clay and fine-silt sized particles (Swanson 2004; Teeter 1998), and these processes have been implemented in SSFATE. These processes are bound by upper and lower concentration limits, defined through empirical studies, which contribute to flocculation for each size class of particles. Above and below these limits, particle collisions are either too infrequent to promote aggregation or so numerous that the interactions hinder settling.

Deposition is calculated as a probability function of the prevailing bottom stress and local sediment concentration and size class. The bottom shear stress is based on the combined velocity due to waves (if used) and currents using the parametric approximation by Soulsby (1998). Sediment particles that are deposited may be subsequently resuspended into the lower water column if critical levels of bottom stress are exceeded, and the model employs two different resuspension algorithms. The first applies to material deposited in the last tidal cycle (Lin et al. 2003). This accounts for the fact that newly-deposited material will not have had time to consolidate and will be resuspended with less effort (lower shear force) than consolidated bottom material. The second algorithm is the established Van Rijn (1989) method and applies to all other material that has been deposited prior to the start of the last tidal cycle. Swanson et al. (2007) summarize the justifications and tests for each of these resuspension schemes. Particles initially released by operations are continuously tracked for the length of the simulation, whether in suspension or deposited.

For each model time step, the suspended concentration of each sediment class as well as the total concentration is computed on a concentration grid. The concentration grid is a uniform rectangular grid in the horizontal dimension with user-specified cell size and a uniform thickness in the vertical dimension (z-grid). The concentration grid is independent of the resolution of the hydrodynamic data used to calculate transport, thus supporting finer spatial differentiation of plume concentrations and avoiding underestimation of concentrations caused by spatial averaging over larger volumes/areas. Model outputs include water-column concentrations in both horizontal and vertical dimensions, time-series plots of suspended sediment concentrations at points of interest, and thickness contours of sediment deposited on the seafloor. Deposition is calculated as the mass of sediment particles that accumulate over a unit area and is calculated on the same grid as concentration. Because the amount of water in the deposited sediment is unknown, by default, SSFATE converts mass to thickness using the sediment density and assuming no water content.

For a detailed description of the SSFATE model equations governing sediment transport, settling, deposition, and resuspension, the interested reader is directed to Swanson et al. (2007).

4.1.2 General Description of SSFATE Model Set-Up

Setup of an SSFATE model scenario consists of defining how each sediment disturbance activity will be parameterized, establishing the sediment source terms, and defining environmental and numerical calculation parameters. For each scenario, the source definition includes:

- Geographic extent of construction activity (point release versus line source [route]);
- Spatially-varying sediment characteristics including sediment grain size and moisture content;
- Timing and duration of activity;
- Sediment volumes, cross-sectional areas, and depths associated with activity;
- Production rate of activity;
- Loss (resuspension) rates of activity; and
- Vertical distribution of sediments as they are initially released to the water column.

The sediment source for cable installation simulations is defined through a load source file, which defines the location of the sources, mass flux of sediment disturbed through operations, loss rate of the disturbed flux resuspended into the water column, vertical position of the mass introduced to the water column, and grain size distribution of the mass introduced to the water column along the route of installation. A component of the sediment grain size distribution is a definition of the percent solids, which is used in the mass flux calculation. Bed sediments contain some water within interstitial pore spaces, and therefore the trench volume consists of both sediment and interstitial water. Therefore, the percent solid of the sediment samples, based on laboratory measurements of moisture content, are used in the calculation of total mass flux. The sediment source can vary spatially, and therefore the line source file is broken into multiple discrete entries, each representing a segment of the route with uniform characteristics. The segments are defined to capture curved route geometry and provide a continuous route aligned with the installation plan.

A model scenario also requires characterization of the environment, including a definition of the domain's spatially- and time-varying currents (BFHYDRO output) and waterbody bathymetry (depth grid). Model setup also requires specification of the concentration and deposition grid, which is the grid at which concentration and deposition calculations are made. The concentration and deposition grid in SSFATE is independent of the resolution of the hydrodynamic or bathymetric data used as inputs. This allows finer resolution which better captures water column concentrations without being biased by numerical diffusion. The concentration and deposition gridding is based on a prescribed square grid resolution in the horizontal plan view and a constant thickness in the vertical. The extent of the concentration is determined dynamically, fit to the extent the sediments travel.

4.2 Study Model Application

A number of SSFATE model scenarios were run to encompass the potential cable routes and construction approaches. The following sections describe the routes and associated sediment-suspending activities as they pertain to defining modeling inputs.

4.2.1 Scenario Components: Routes and Approaches

The model scenarios have been separated into three components: (1) the representative IAC located within the WTA, (2) the representative offshore export cables located within the Monmouth and Atlantic ECCs, and (3) the representative landfall approaches for each ECC. A key component of the modeling is the delineated geographical extent of the source. Therefore, the cable routes modeled and corresponding burial equipment types are presented in Table 7.

Table 7. Construction Activities Modeled.

Component	Equipment Type	Total Route Length (km)
Representative IAC	Jet Trencher	10.1
Representative IAC	Mechanical Trencher	10.1
Monmouth ECC – Branch 1	Jet Trencher	96.9
Monmouth ECC – Branch 2	Jet Trencher	97.5
Atlantic ECC – Branch 1	Jet Trencher	18.6
Atlantic ECC – Branch 2	Jet Trencher	18.3
Monmouth ECC Landfall Approach, Representative HDD Pit	Excavator	N/A
Atlantic ECC Landfall Approach, Representative HDD Pit	Excavator	N/A

An individual representative IAC route (Figure 13) that passed through a region of finer sediment was modeled as a conservative assessment of potential impacts from cable installation within the WTA. Fine sediments (e.g., clays, silts) tend to last longer in the water column, whereas coarse sediment (e.g., fine sand, coarse sand) will settle at a faster rate. To evaluate the influence of equipment type on sediment dispersion, two possible equipment types were assessed for IAC installation: jet trencher and mechanical trencher.

The modeled offshore export cable scenarios included representative routes along the full length of the Monmouth (Figure 14) and Atlantic (Figure 15) ECCs. As described in Section 1.1, both ECCs diverge nearshore then converge to reach their respective landfall site. To account for each divergence (“branch”), a total of four ECC scenarios were modeled. The Atlantic ECC begins on the western edge of the WTA, while the Monmouth ECC begins on the eastern edge.

The modeled landfall approaches included representative HDD pits along both the Monmouth (Figure 16) and Atlantic (Figure 17) ECCs. Only the excavation of the HDD pits was modeled but can be considered representative of backfill as this operation would take place on the order of hours to days after excavation. Additionally, only one HDD pit location was modeled within each ECC but can be considered representative of both landfall locations due to the proximity of the landfall locations, similar sediment characteristics, and similar hydrodynamic forcing conditions.

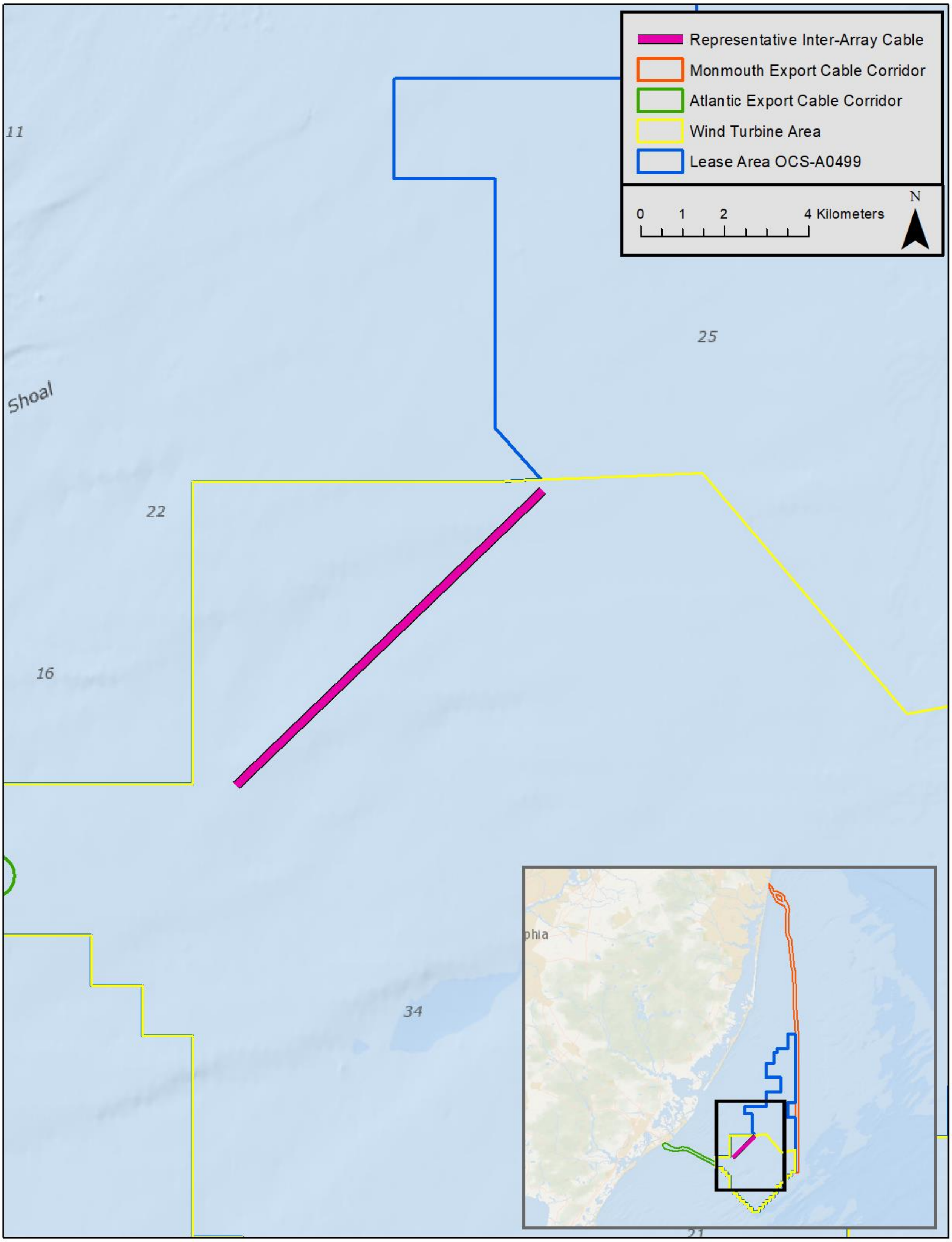

Figure 13. Modeled Representative Inter-Array Cable Route.

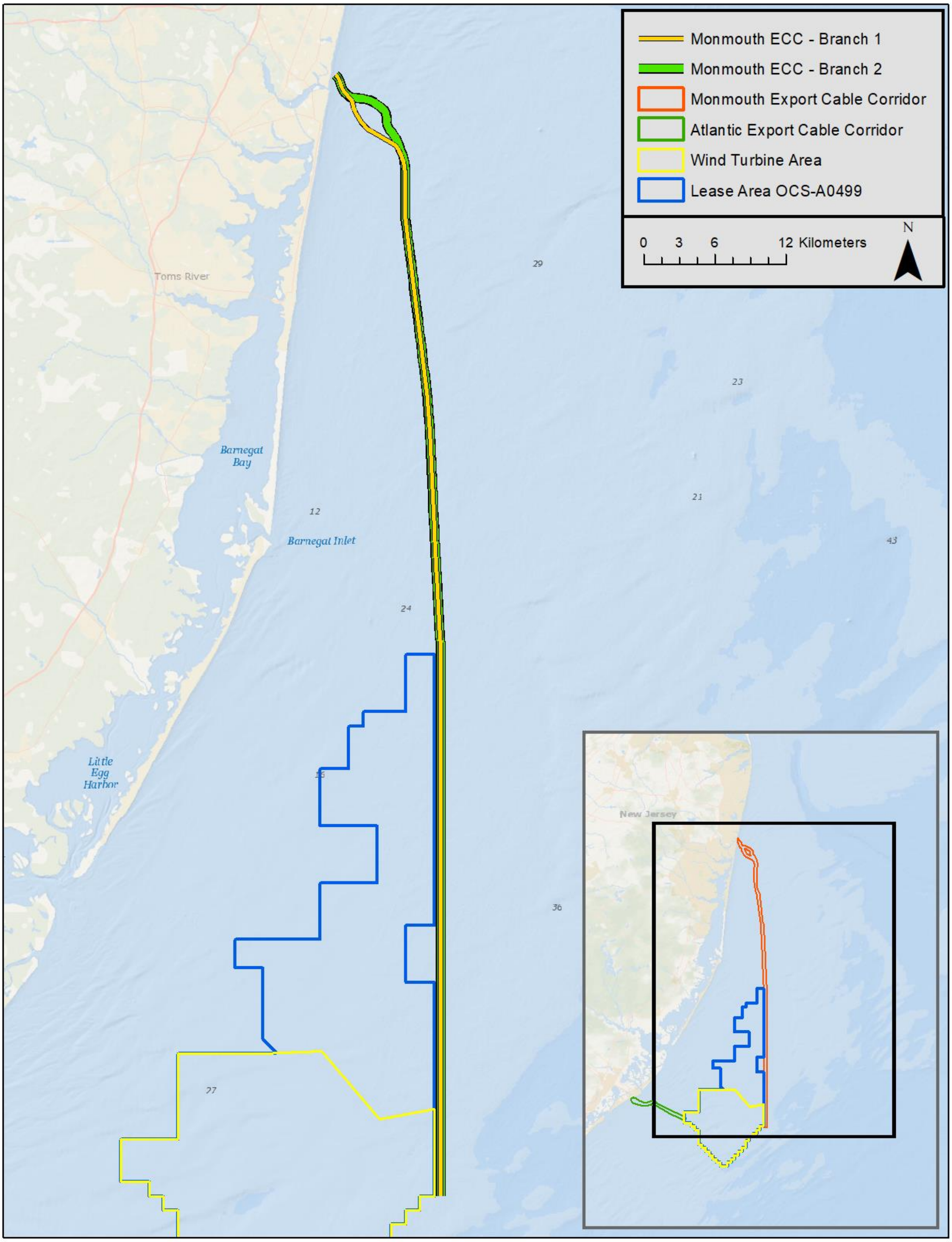

Figure 14. Modeled Monmouth Export Cable, Branch 1 and Branch 2.

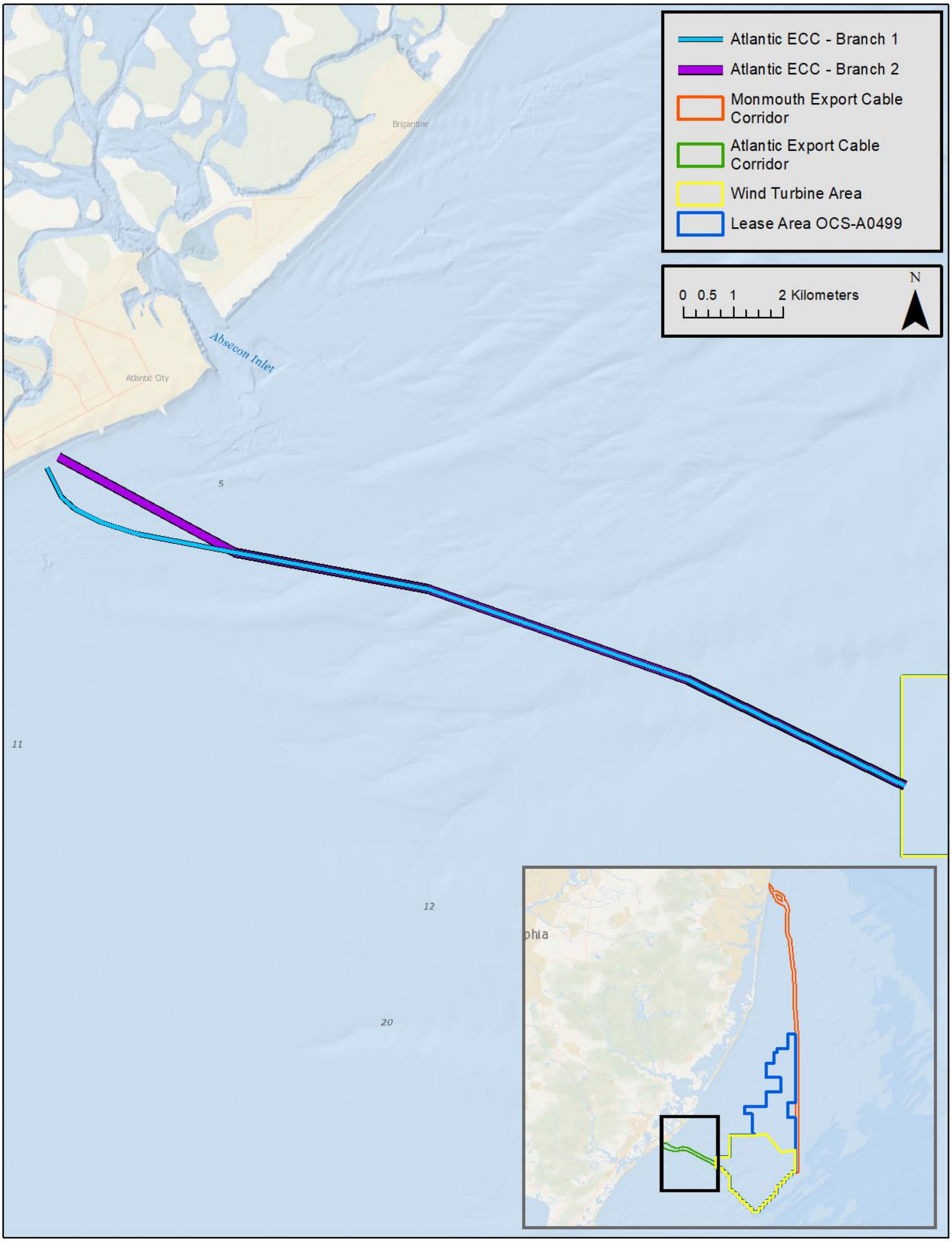

Figure 15. Modeled Atlantic Export Cable, Branch 1 and Branch 2.

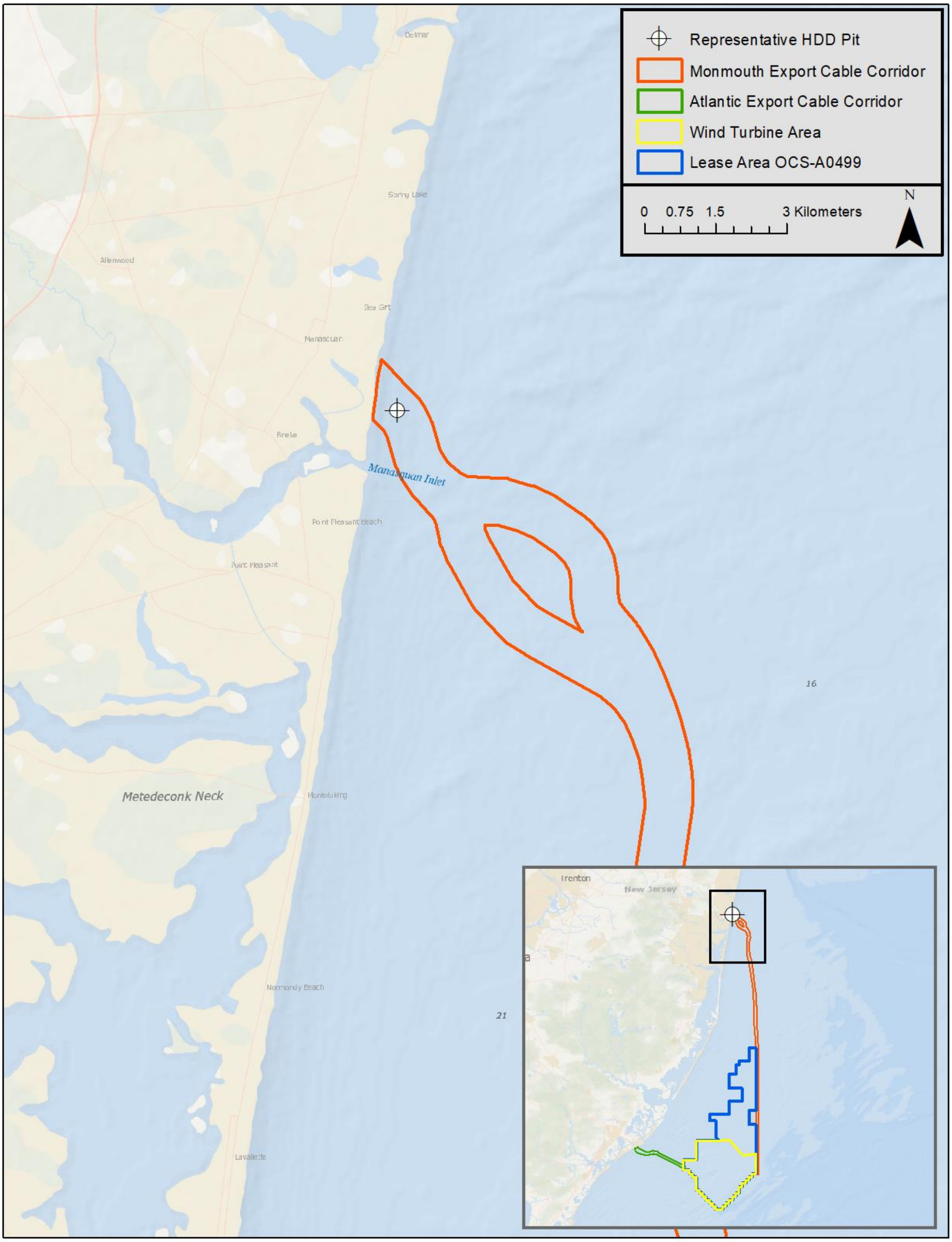

Figure 16. Modeled Monmouth ECC Representative Landfall Approach.

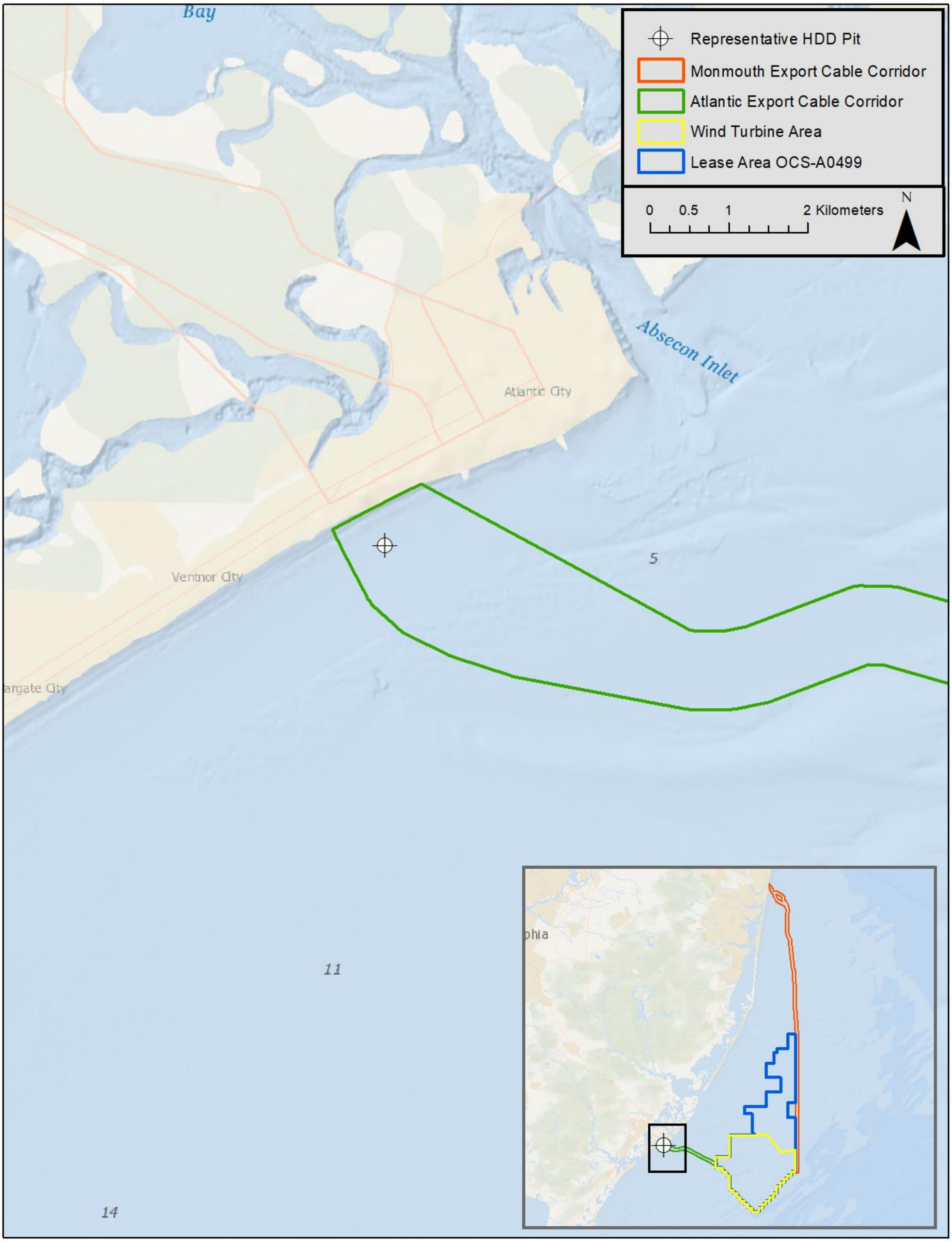

Figure 17. Modeled Atlantic ECC Representative Landfall Approach.

4.2.2 Project Components: Construction Activities

Cable installation activities that will suspend sediments in the water column include IAC burial within the WTA, cable burial along the ECCs, and HDD pit activity for the landfall approaches. Inter-array and offshore export cable installation may be achieved through various methods, which may be combined interchangeably. A preliminary analysis was performed to evaluate the sensitivity of equipment type and the rate of installation on the fate and transport of suspended sediments. Three burial techniques (jet trenching, jet ploughing, and mechanical trenching) and two installation rates (fast and slow) were used in this sensitivity analysis. Jet trenching and mechanical trenching were selected for use in the final modeling because the results predicted higher impacts associated with those equipment types when compared to jet ploughing. For example, simulations with jet trenching and mechanical trenching were predicted to have: 1) larger areas exceeding TSS concentration thresholds (25, 50, 100, 200 mg/L), 2) deposition above thresholds (1, 5 mm) extending further away from the route centerline, 3) larger areas exceeding depositional thickness thresholds (1, 5, 20, 100 mm), 4) higher maximum TSS concentrations, and 5) larger maximum depositional thicknesses. For the jet trenching and mechanical trenching simulations, a slower installation rate resulted in larger areas exposed to TSS concentrations for longer durations when compared with the faster installation rate. To reflect the maximum design cases (i.e., largest impacts associated with TSS concentrations and deposition for installation equipment and parameters), jet trenching and mechanical trenching techniques were selected for use in final modeling and the slow installation rates were assumed to bound the potential effects associated with cable installation activities.

The jet trenching scenario, using the slower installation rate, was determined to be the maximum design case and was used for final modeling efforts for the ECCs. Assuming the slower installation rate for both, jet trenching and mechanical trenching methods were used to model the representative IAC scenarios. The cable installation method was simulated using installation parameters that reflect a conservative estimate of typical installation speed and trench depth. Based on the equipment type, 25% of the sediment was mobilized into the water column near the seabed for inter-array and offshore export cable installation. Anticipated conservative HDD pit dimensions along each ECC were modeled using one equipment type (excavator). For HDD pit excavation, 100% of the sediment was mobilized and introduced at the water surface.

For all of these scenarios, a conservative approach was used by assuming no mitigation techniques (e.g., cofferdam, silt screen) would be deployed during construction activities. A summary of the IAC, offshore export cable, and HDD pit installation parameters is provided in Table 8.

Table 8. Construction Activity Modeling Parameters.

Component	Equipment Type	Trench Width (m)	Trench Depth (m)	Trench Cross-Sectional Area (m^2)	Pit Volume (m^3)	Advance Rate (m/hr)	Production Rate (m^3/hr)	Percent Mobilized (%)
Representative IAC	Jet Trencher	0.9	2	1.8	-	250	450	25
Representative IAC	Mechanical Trencher	0.65	2	1.3	-	150	195	25
Monmouth ECC – Branch 1	Jet Trencher	0.9	2	1.8	-	250	450	25
Monmouth ECC – Branch 2	Jet Trencher	0.9	2	1.8	-	250	450	25
Atlantic ECC – Branch 1	Jet Trencher	0.9	2	1.8	-	250	450	25
Atlantic ECC – Branch 2	Jet Trencher	0.9	2	1.8	-	250	450	25
Monmouth ECC Landfall Approach, Representative HDD Pit	Excavator	-	-	-	600	-	60	100
Atlantic ECC Landfall Approach, Representative HDD Pit	Excavator	-	-	-	600	-	60	100

4.2.3 Sediment Characteristics

The sediment characteristics are a key factor of the sediment load definition input to the SSFATE model. The spatially-varying sediment characteristics were developed based on analysis of the vibracore samples. The details of the sediment sampling and laboratory analysis are documented in Volume II, Appendix II-A3 of the COP and a description of the data manipulation process, as it pertains to modeling, is described below. The objective of the subsequent analysis of the sediment data was to develop the sediment characteristics that represent the upper two meters of the seabed, since that is the target depth of cable installation and represents the depth of sediments that may get resuspended during installation activities. Specifically, the sediment size distribution was delineated into five classes used in SSFATE (Table 6). Additionally, the water content measurement associated with each sediment sample was used to account for the percent of the upper seabed that is sediment.

The sampling included vibracores, which provide a vertical profile of sediments that are then analyzed at multiple depths from the profile. All samples were analyzed by a sieve. Sieve analyses are performed to determine a percent finer curve for the coarse sediment sizes (i.e., the fraction of coarse and fine sand as it pertains to the classes in SSFATE). To resolve the fine grain sediment classes, samples undergo a hydrometer analysis. For all stations without hydrometer data, the remaining fraction (percent finer than fine sand) was split evenly between the three classes of coarse silt, fine silt, and clay.

The resulting sediment grain size distributions and percent solids are shown in Figure 18, Figure 19, and Figure 20. Figure 18 shows the two-meter sediment characteristics in the lease area and Figure 19 and Figure 20 show the two-meter sediment characteristics in the Monmouth and Atlantic ECCs, respectively.

Most of the sediments are primarily fine and coarse sand. However, there are samples with noticeable fractions of fine sediments (i.e., clay, fine silt, and coarse silt). Samples along the ECCs are primarily coarse, with scattered sections of fine sediments. The Monmouth ECC, spanning a larger area, encompasses more fine sediment samples than the Atlantic ECC. The lease area has more coarse sediment samples, with fine sediment samples scattered throughout.

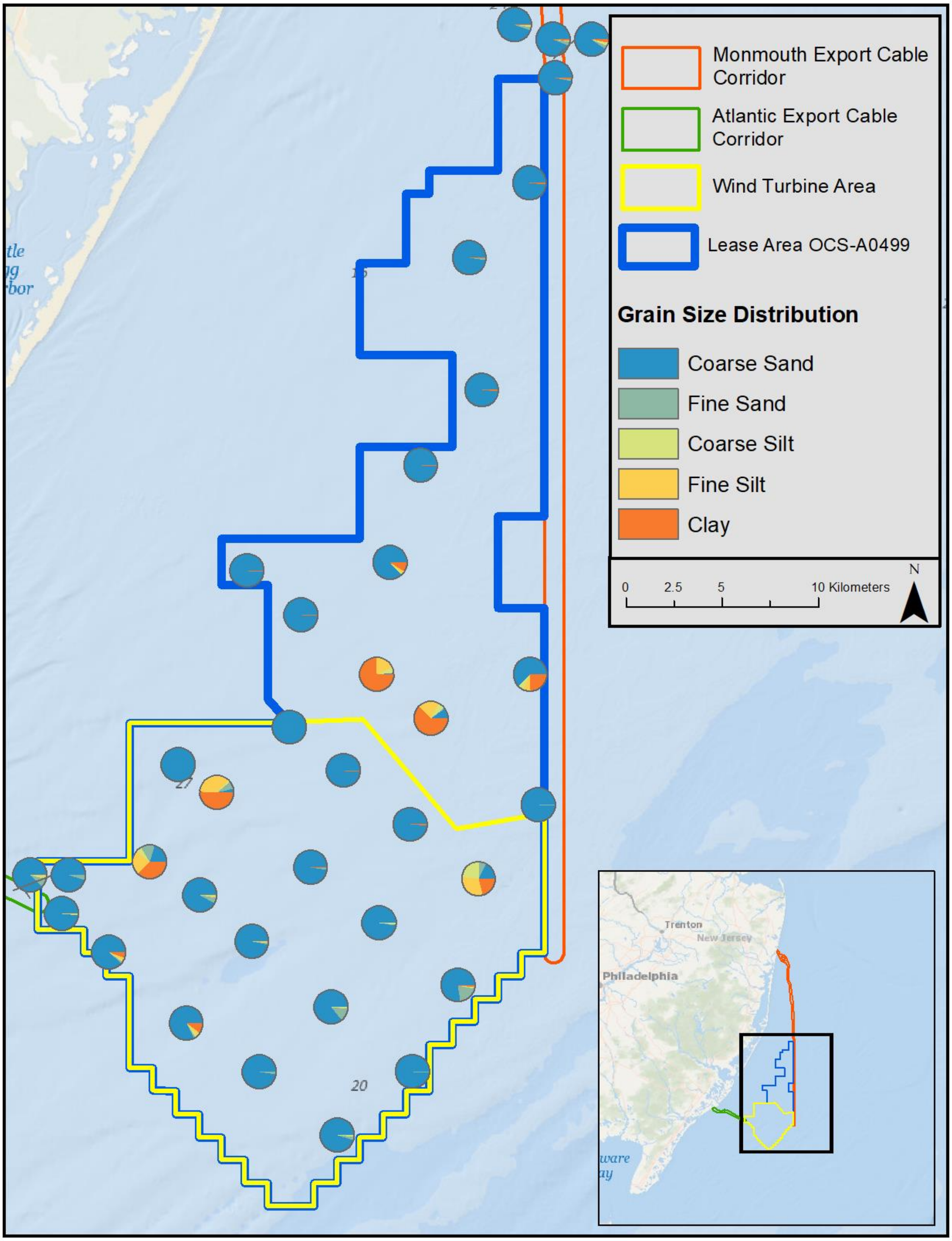

Figure 18. Sediment Grain Size Distributions for the Upper 2 m of the Seabed in the Lease Area.

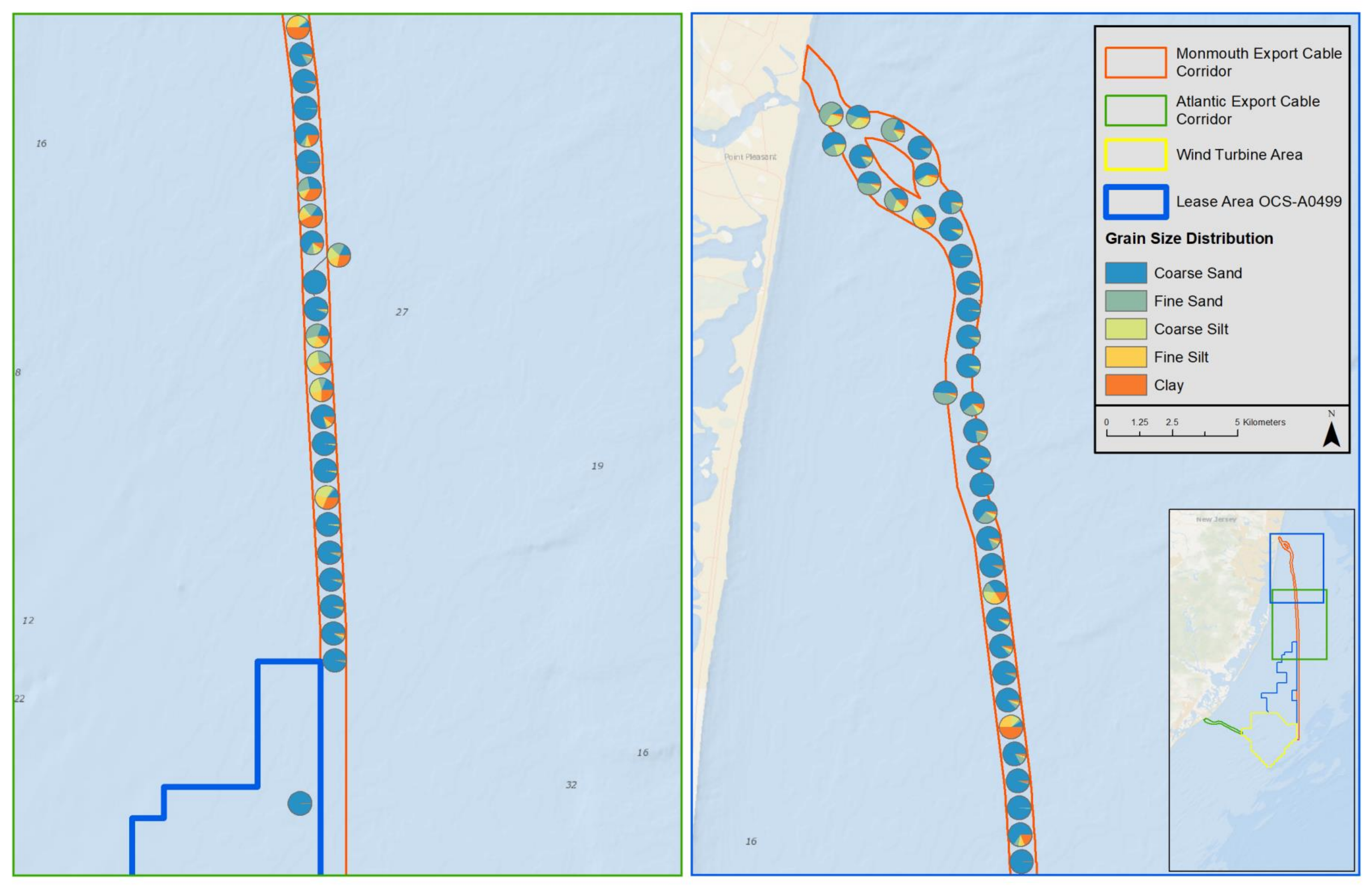

Figure 19. Sediment Grain Size Distributions for the Upper 2 m of the Seabed along the Monmouth ECC.

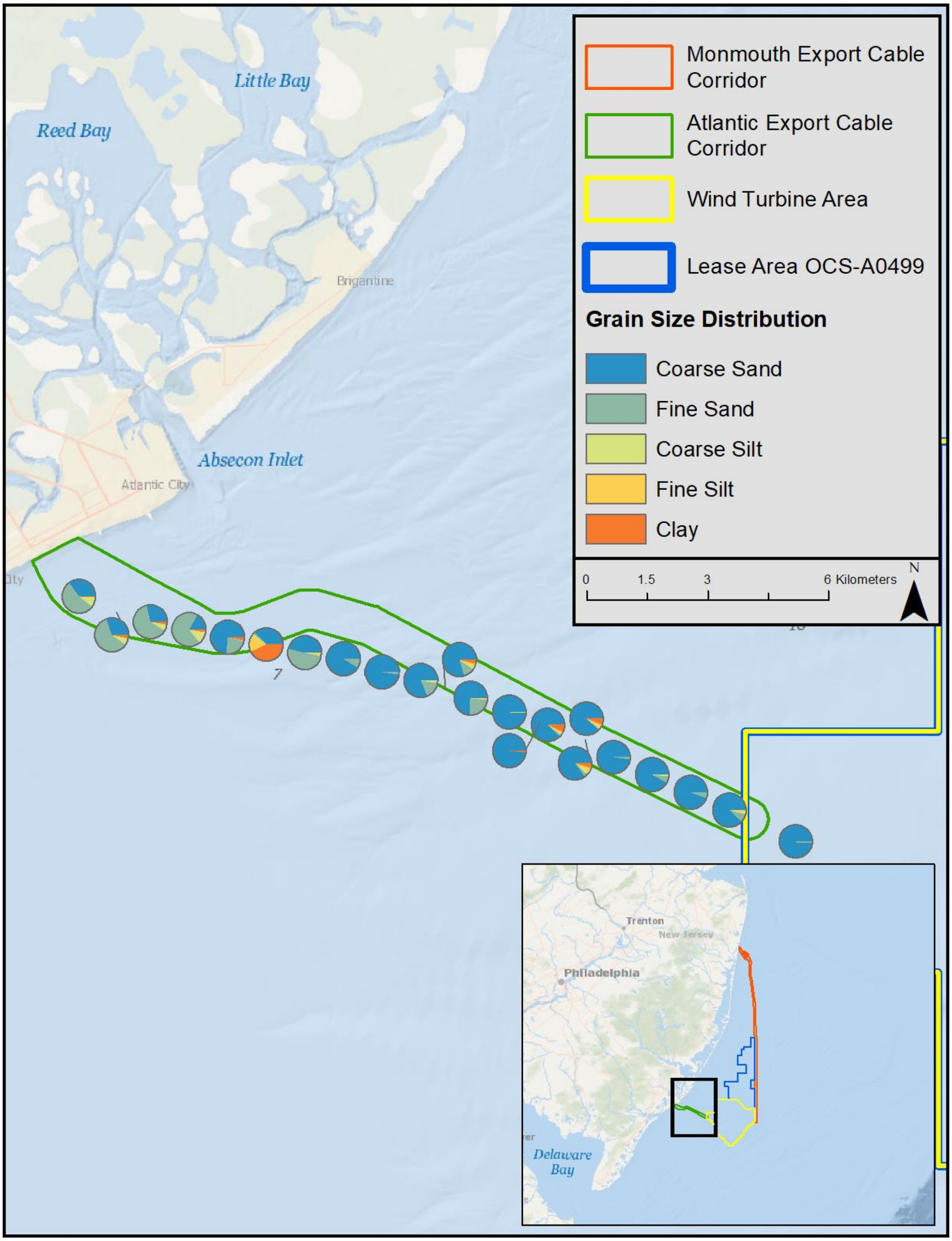

Figure 20. Sediment Grain Size Distributions for the Upper 2 m of the Seabed along the Atlantic ECC.

4.3 Sediment Modeling Results

SSFATE simulations were performed for each sediment disturbance activity. Sediment concentrations were computed on grids with varying resolutions in the horizontal and vertical dimensions to capture the unique results of each scenario. Model-predicted concentrations are considered above ambient or “excess” concentrations above background (i.e., a concentration of 0 mg/L is assumed for the ambient concentration).

The model results are presented in a series of figures and tables. Maps of the instantaneous TSS concentrations, maximum above-ambient TSS concentrations, duration of above-ambient TSS ≥10 mg/L, and seabed deposition are provided for each modeled scenario. The results tables quantify the area exceeding TSS thresholds for specific durations as well as areas of seabed deposition exceeding thickness thresholds for each scenario.

Additional information about standard graphical outputs for each scenario are provided below:

- **Maps of Instantaneous TSS Concentrations**: These figures show the instantaneous TSS concentrations at a moment in time. The concentrations are shown as contours using mg/L. The plan view shows the maximum concentration throughout the water column and the vertical cross-section shows the cross-sectional variability of concentrations along a transect.
- **Maps of Time-integrated Maximum TSS Concentrations**: These figures show the maximum time-integrated water column concentration from the entire water column in scaled plan view, including a vertical cross-sectional view of maximum TSS concentrations in the water column. The concentrations are shown as contours using mg/L. The entire area within the contour is at or above the concentration defined by the contour itself. Most importantly, it should be noted that these maps show the maximum TSS concentration that occurred throughout the entire simulation and that: (1) these concentrations do not persist throughout the entire simulation and may be just one time step; and (2) these concentrations do not occur concurrently throughout the entire modeled area but are the time-integrated spatial views of maximum predicted concentrations.
- **Maps of Duration of TSS Concentrations ≥10 mg/L:** These figures show the number of hours that the TSS concentrations are expected to be ≥10 mg/L.
- **Maps of Seabed Deposition**: These figures show the deposition on the seabed that would occur once the activity has been completed. The thickness levels are shown as contours (in mm) and the entire area within the contour is at or above the thickness defined by the contour itself.

4.3.1 Inter-array Cable

SSFATE modeling and results of a representative IAC using jet trenching and mechanical trenching are described below. A snapshot of the instantaneous concentrations from the cable installation using jet trenching parameters is presented in Figure 21. This figure illustrates that higher concentrations were contained around the route centerline, with lower concentrations biased towards the west/northwest due to bottom currents. The vertical cross-section shows that all concentrations were constrained to the bottom of the water column, with the highest concentrations closest to the bottom (i.e., localized to the source).

Side-by-side comparisons of the results of the IAC installation from jet trenching and mechanical trenching cable burial parameters are presented in Figure 22 through Figure 24. The map of time-integrated maximum concentrations is presented in Figure 22. In this figure, the cross-sectional view runs along the route centerline and shows that the plume was localized to the bottom of the water column. For both cases, the overall footprint shows how the plume oscillated with the tides, which is reflective in the oscillatory pattern of the TSS concentrations relative to the route centerline. Concentrations ≥10 mg/L contour had a maximum excursion of approximately 2.6 km and 2.9 km from the route centerline for jet and mechanical trenching cable burial parameters, respectively.

A map of hours with TSS concentrations ≥10 mg/L is presented in Figure 23. The results for both the jet and mechanical trenching parameters show that in any given location, the total exposure was typically 1 to 2 hours or 2 to 3 hours with small isolated patches of exposure between 3 to 6 hours for the jet trenching scenario and larger patches of exposure between 3 and 6 hours for the mechanical trenching scenario.

The map of deposition thickness for the inter-array scenarios is presented in Figure 24. This figure shows that deposition was mainly centered around the installation alignment with deposition ≥1 mm limited to approximately 50 m and 110 m for mechanical and jet trenching parameters, respectively. Deposition did not reach 5 mm in the simulation of mechanical trenching parameters, but small isolated patches ≥5 mm in the jet trenching simulation were predicted.

Figure 22 through Figure 24 indicate that most of the sediments settled out quickly and were not transported long distances by the currents. Relative to one another, the jet trenching simulation had a larger footprint for each threshold because of the larger cross-sectional area, but had less area of longer exposures to concentrations ≥10 mg/L due to the faster advance rate. Although these simulations were started at the same time using the same environmental conditions, different advance rates resulted in variable plume and depositional footprints. For example, the jet trenching plume would experience different currents 10 minutes into the simulation than the mechanical trenching plume. A faster advance rate means more of the trench has been excavated within 10 minutes so the forcing would no longer be the same due to temporal and spatial variability of the currents. Elevated TSS was confined to the bottom few meters of the water column, a small fraction of the water column, in the WTA. Maximum deposition in both simulations was typically less than 5 mm. Water quality impacts from IAC installation are therefore predicted to be short-term and localized.

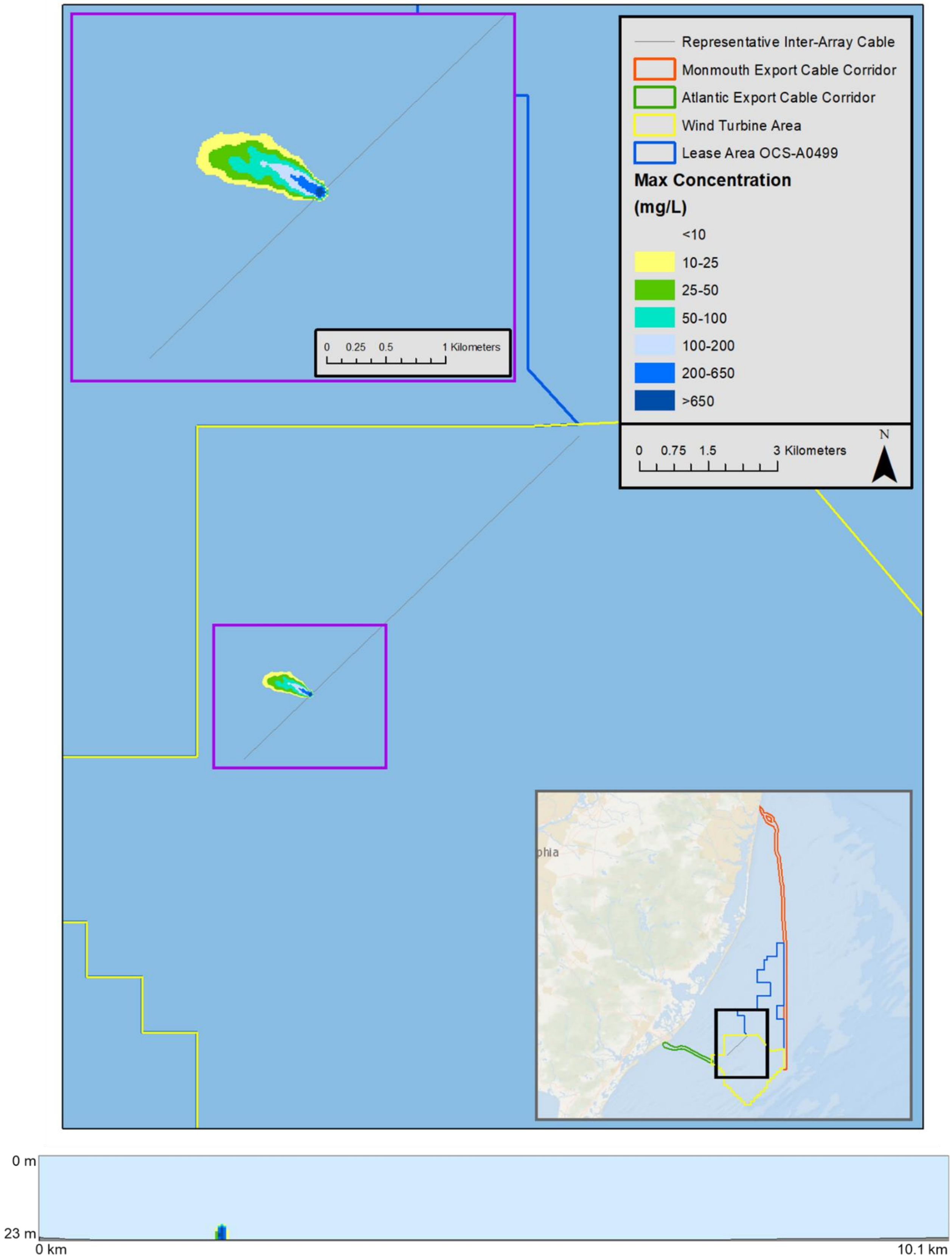

Figure 21. Snapshot of Instantaneous TSS Concentrations Associated with a Representative Inter-Array Cable Installation using Jet Trenching Parameters.

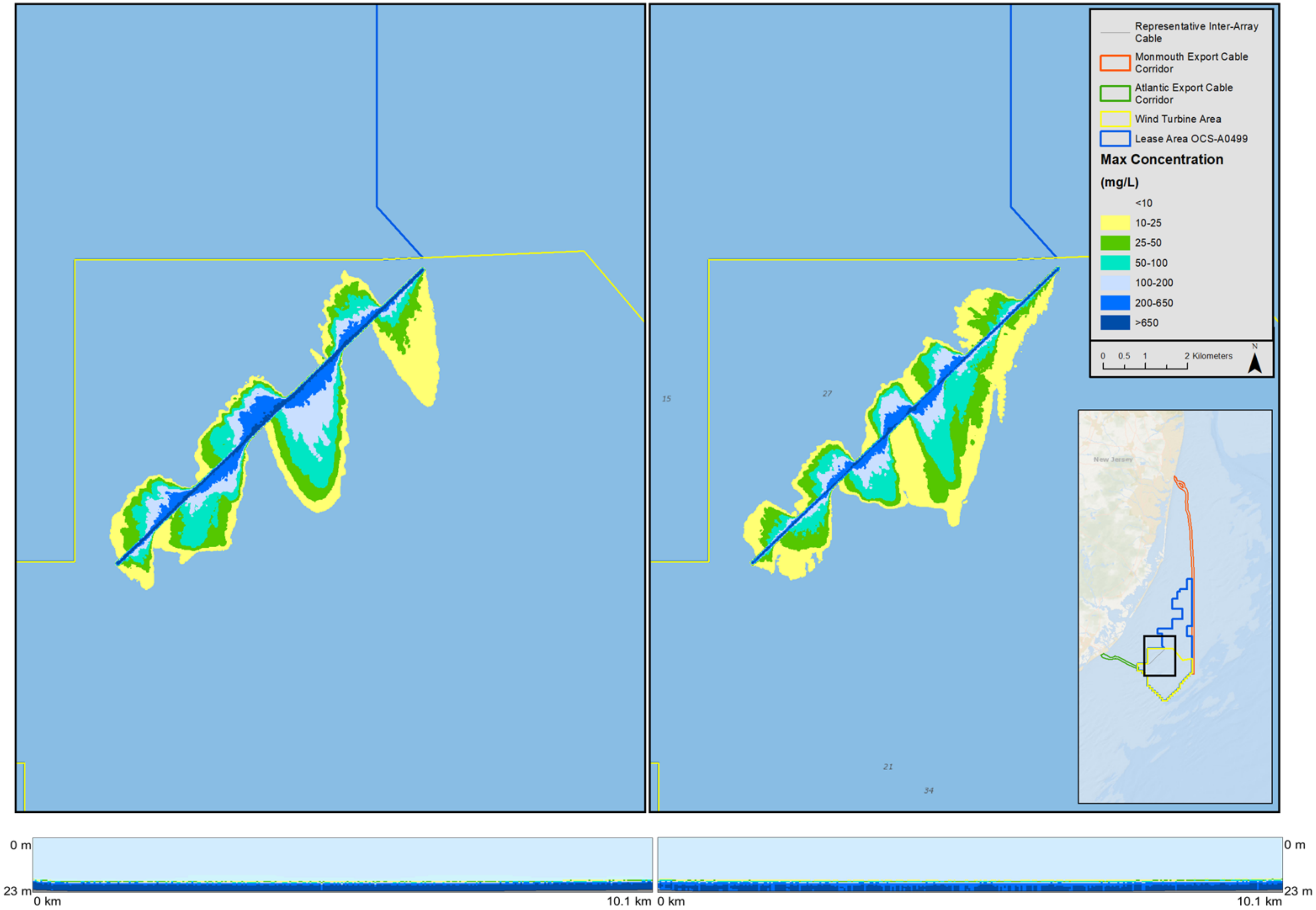

Figure 22. Map of Time-Integrated Maximum TSS Concentrations Associated with a Representative Inter-Array Cable Installation using Jet Trenching (Left) and Mechanical Trenching (Right) Cable Burial Parameters.

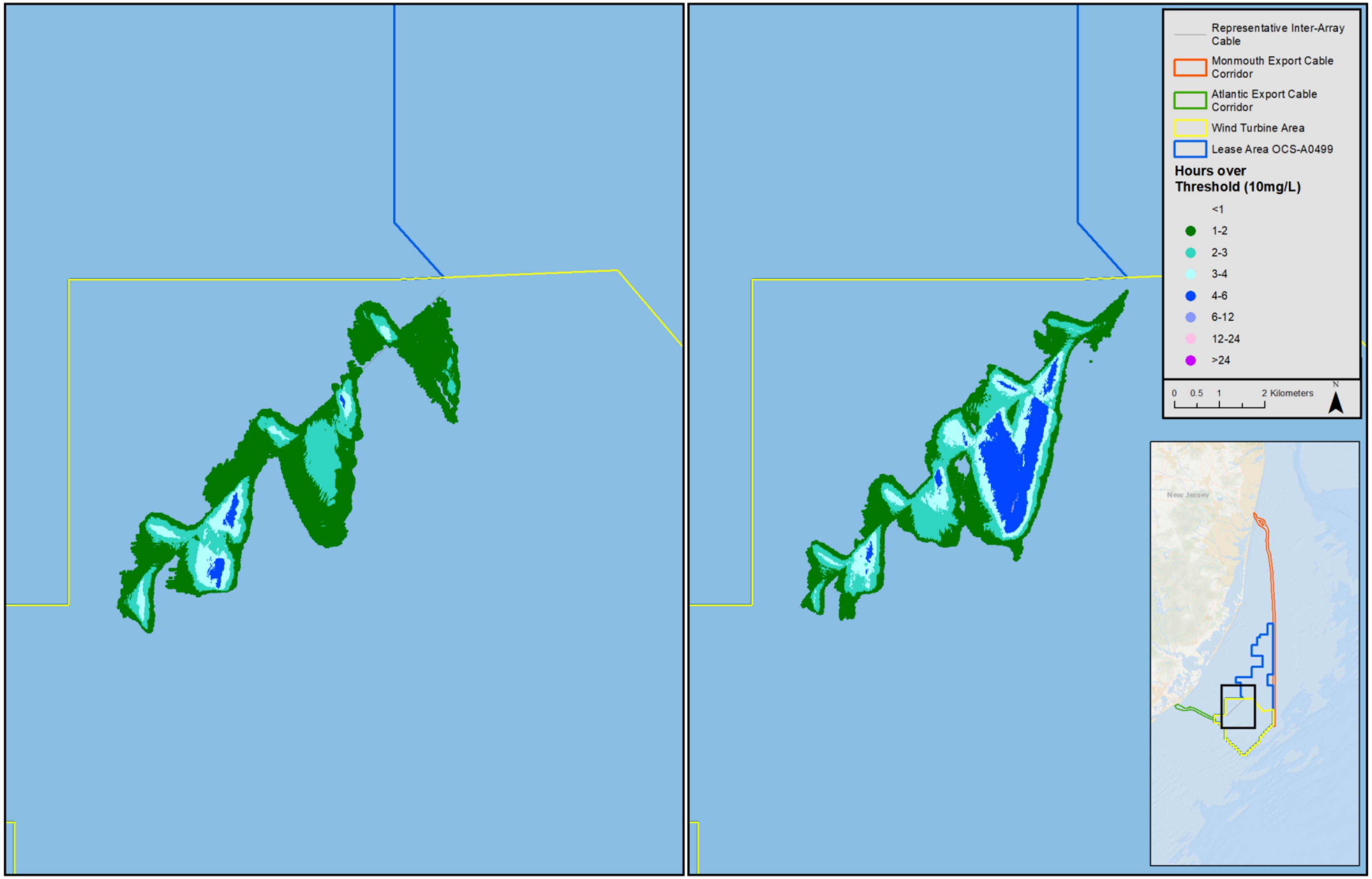

Figure 23. Map of Duration of TSS ≥10 mg/L Associated with a Representative Inter-Array Cable Installation using Jet Trenching (Left) and Mechanical Trenching (Right) Cable Burial Parameters.

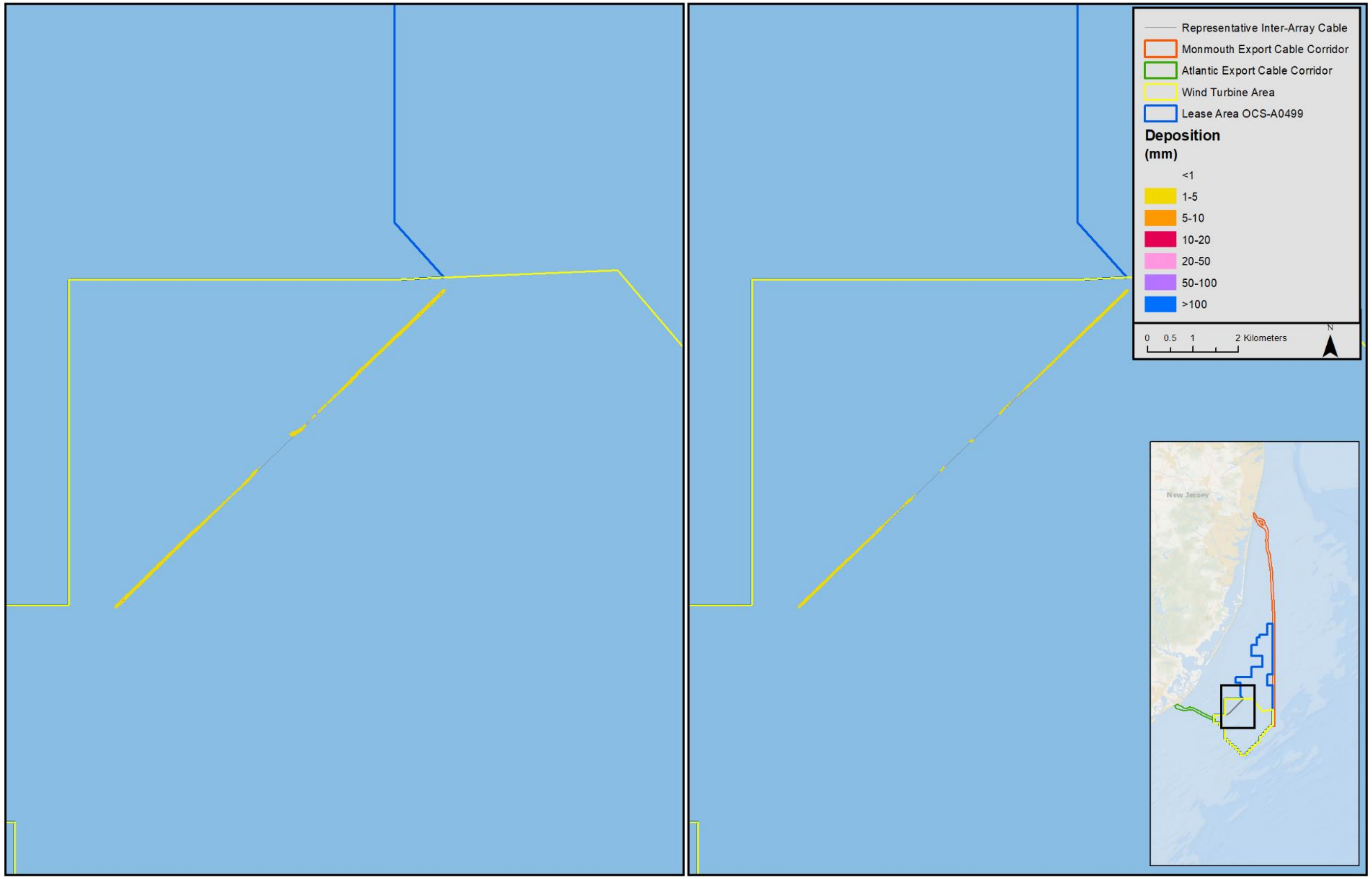

Figure 24. Map of Deposition Thickness Associated with a Representative Inter-Array Cable Installation Simulation using Jet Trenching (Left) and Mechanical Trenching (Right) Cable Burial Parameters.

4.3.2 ECCs

This section presents SSFATE modeling and results associated with TSS generation and sediment deposition from the simulations of cable installation activities in the Monmouth and Atlantic ECCs. The mapped result figures for the ECC scenarios are presented together because most of the modeled route was the same, with differences occurring after the route diverged to create Branches 1 and 2. Due to the similarity in results for each of the ECC branches, only one value was reported in the summary tables and discussed in the text for the Monmouth and Atlantic ECC modeling. The values reported and discussed reflect the scenario predicted to have the maximum effect (i.e., maximum effects scenario) for each of the respective ECC branches.

Monmouth Export Cable

A snapshot of the instantaneous concentrations from the Monmouth ECC – Branch 1 scenario is presented in Figure 25 along with the vertical cross-section across the plume. This figure was representative of both branches and illustrates that higher concentrations were contained around the route centerline, with lower concentrations biased towards the west due to bottom currents. The cross-section shows that the plume was localized to the bottom of the water column. The map of maximum time-integrated concentrations with the vertical cross-section across the plume (Figure 26), the duration of exposure to TSS above ≥10 mg/L (Figure 27), and the seabed deposition (Figure 28) show the entire Monmouth ECC route with zoomed-in extents highlighting results for Branches 1 and 2. Figure 26 illustrates how the plume moved from east to west with the tides, which is reflective in the oscillatory pattern of the concentrations relative to the route centerline. The oscillatory pattern was less evident in regions where the route is parallel to local currents and where the sediment is predominantly coarse because it tends to settle out of the water column relatively quickly and remain close to the route centerline. Concentrations ≥10 mg/L had a maximum excursion of approximately 2.6 km from the route centerline. The map of exposure of the water column to TSS concentrations ≥10 mg/L (Figure 27) shows a pattern similar to the maximum concentration, with most locations experiencing exposures of less than 4 hours, while some areas had exposures between 6 and a little over 12 hours. As presented in Figure 28, the deposition between 1 and 5 mm tended to stay central to the route centerline, with discontinuous patches between 5 and 10 mm.

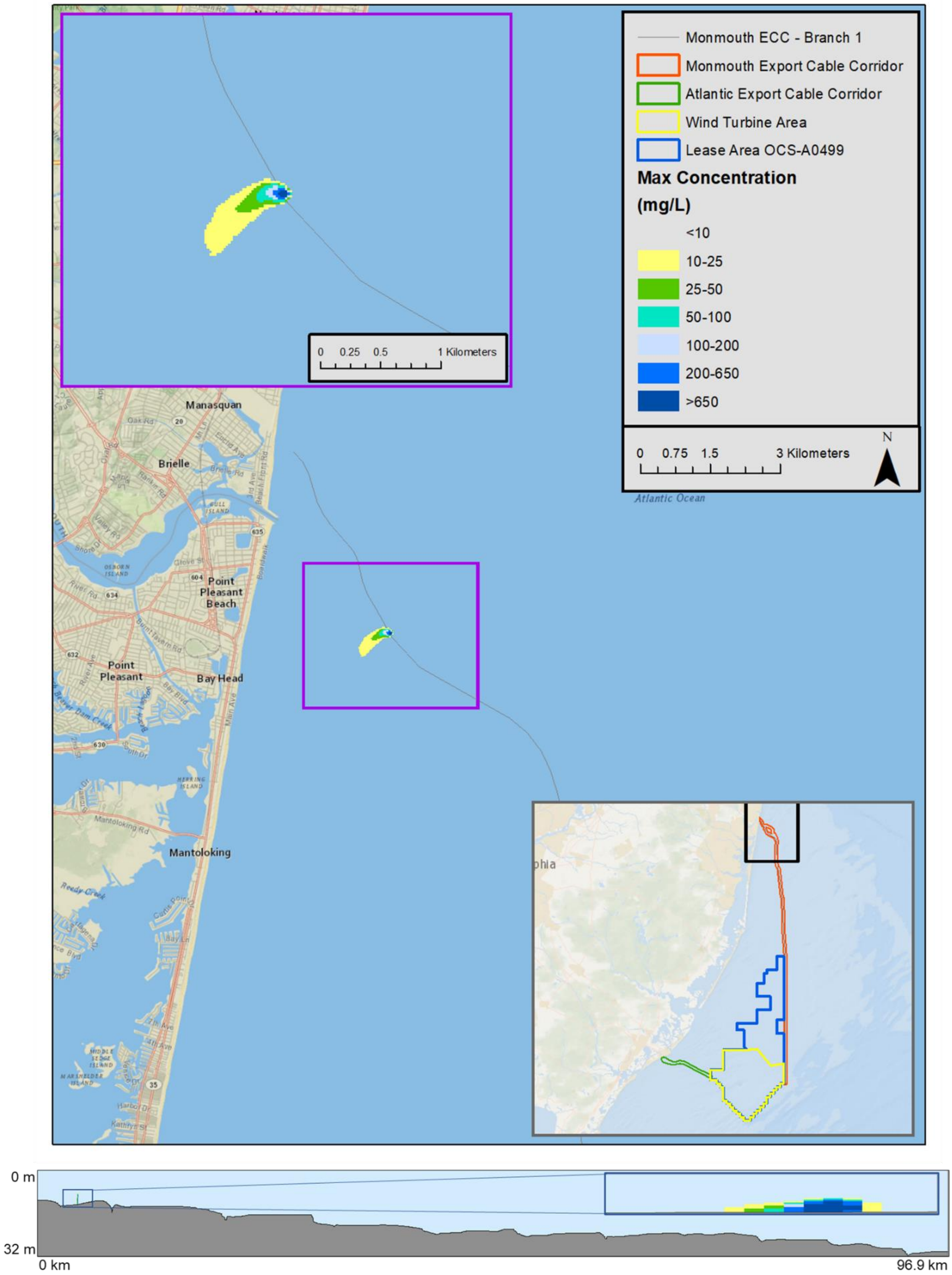

Figure 25. Snapshot of Instantaneous TSS Concentrations Associated with Cable Burial along the Monmouth ECC – Branch 1.

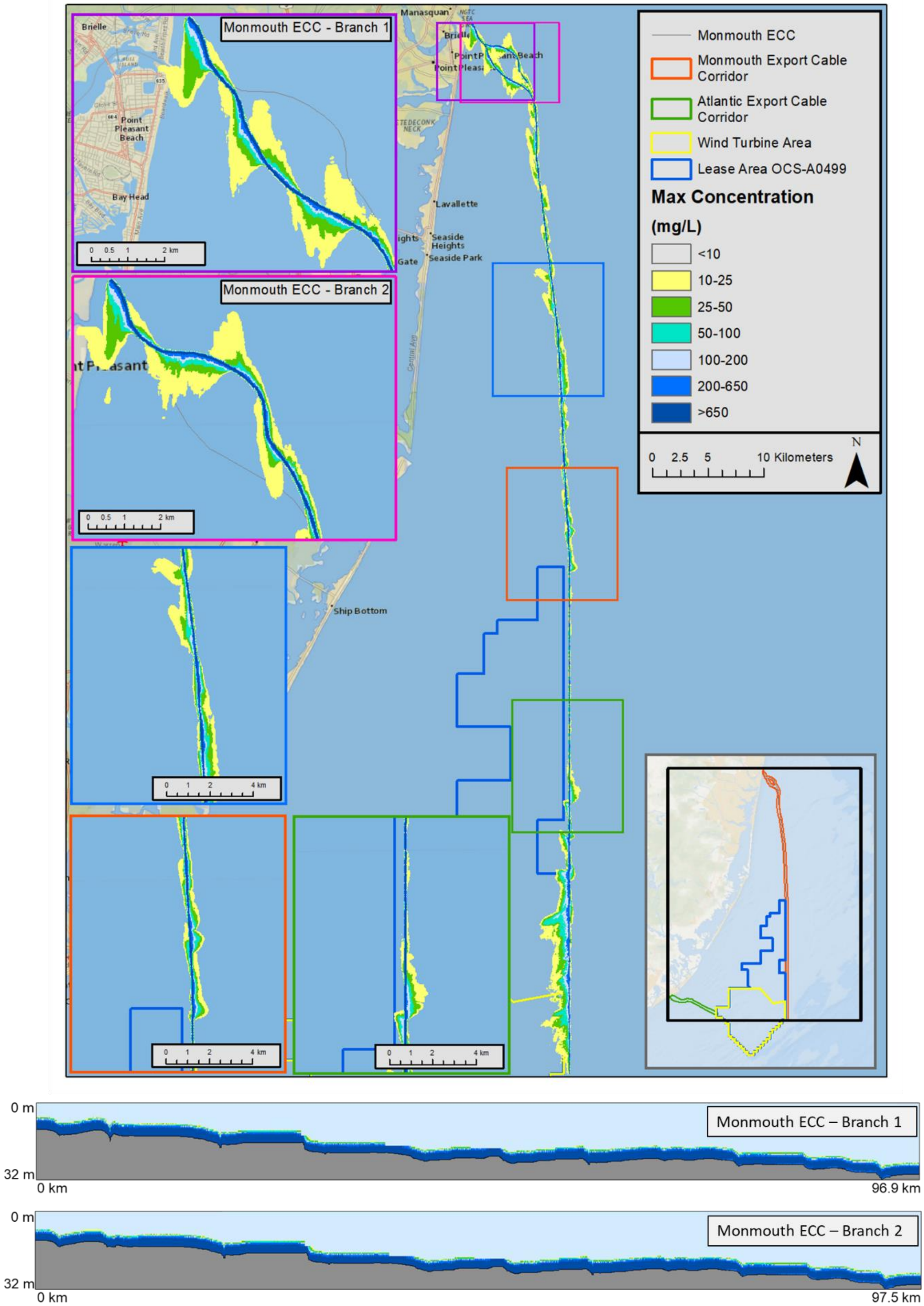

Figure 26. Map of Time-Integrated Maximum TSS Concentrations Associated with Cable Burial along the Monmouth ECC for Branch 1 and Branch 2.

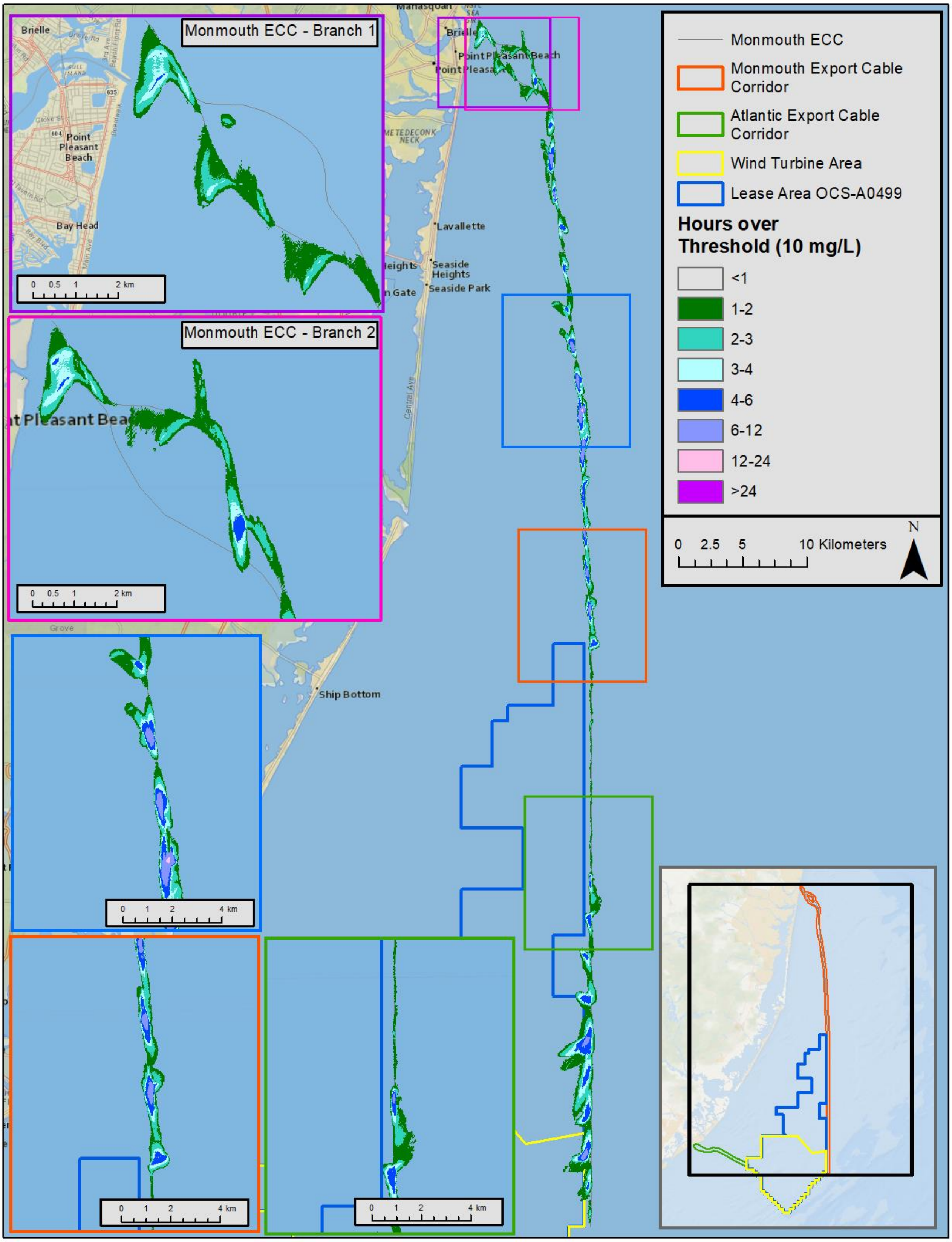

Figure 27. Map of Duration of TSS ≥10 mg/L Associated with Cable Burial along the Monmouth ECC for Branch 1 and Branch 2.

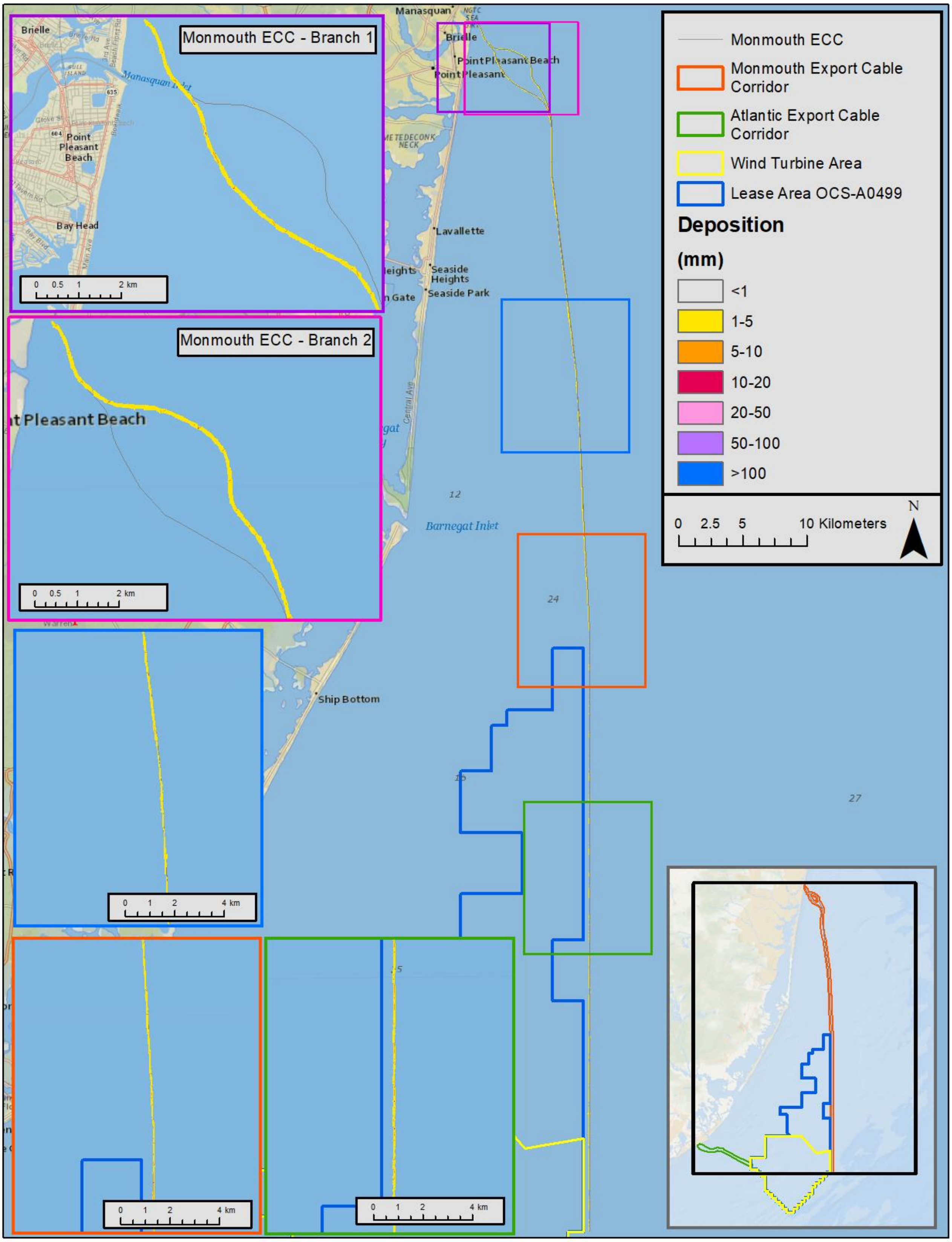

Figure 28. Map of Deposition Thickness Associated with Cable Burial along the Monmouth ECC for Branch 1 and Branch 2.

Atlantic Export Cable

A snapshot of the instantaneous concentrations from the Atlantic ECC – Branch 1 scenario is presented in Figure 29 along with the vertical cross-section across the plume. This figure is representative of both branches and illustrates that at this instance, TSS concentrations are contained around the route centerline, with lower concentrations biased towards the southwest due to bottom currents. The map of maximum time-integrated concentrations with the vertical cross-section across the plume (Figure 30), the duration of exposure to TSS ≥10 mg/L (Figure 31), and the seabed deposition (Figure 32) show the entire Atlantic ECC with zoomed-in extents highlighting results for Branches 1 and 2. As shown in Figure 30, the plume primarily oscillates north to south with the tides, which is reflective in the oscillatory pattern of the 10-25 mg/L (yellow) concentrations relative to the route centerline. Concentrations ≥10 mg/L have a maximum excursion of approximately 1.7 km from the route centerline. Figure 31 shows segmented areas of exposure of the water column to TSS concentrations ≥10 mg/L, with most locations experiencing exposures of less than 3 hours. Few areas experience exposure between 4 and 6 hours. As shown in Figure 32, the deposition between 1 and 5 mm tends to stay central to the route centerline, with discontinuous patches between 5 and 10 mm.

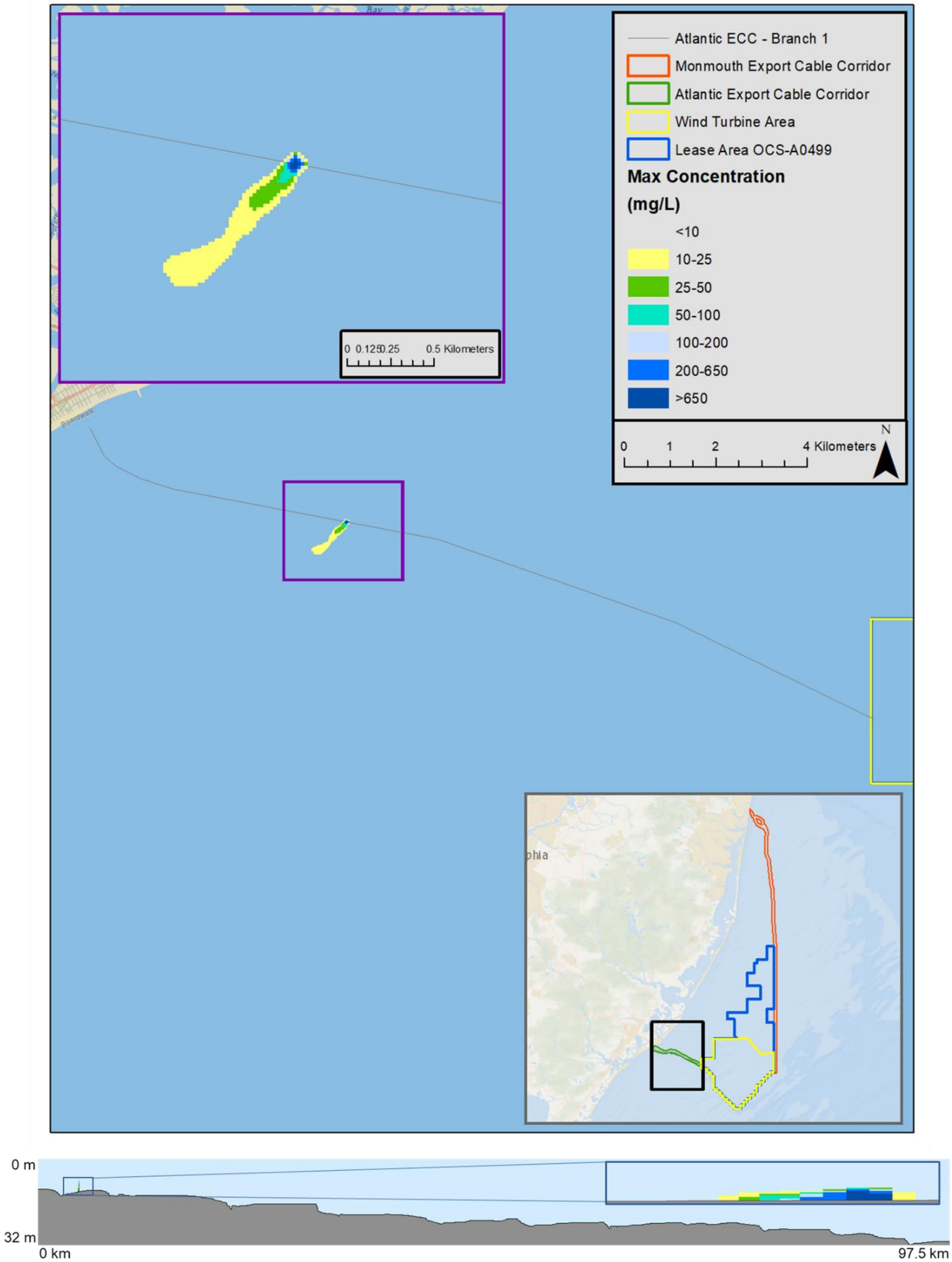

Figure 29. Snapshot of Instantaneous TSS Concentrations Associated with Cable Burial along the Atlantic ECC – Branch 1 .

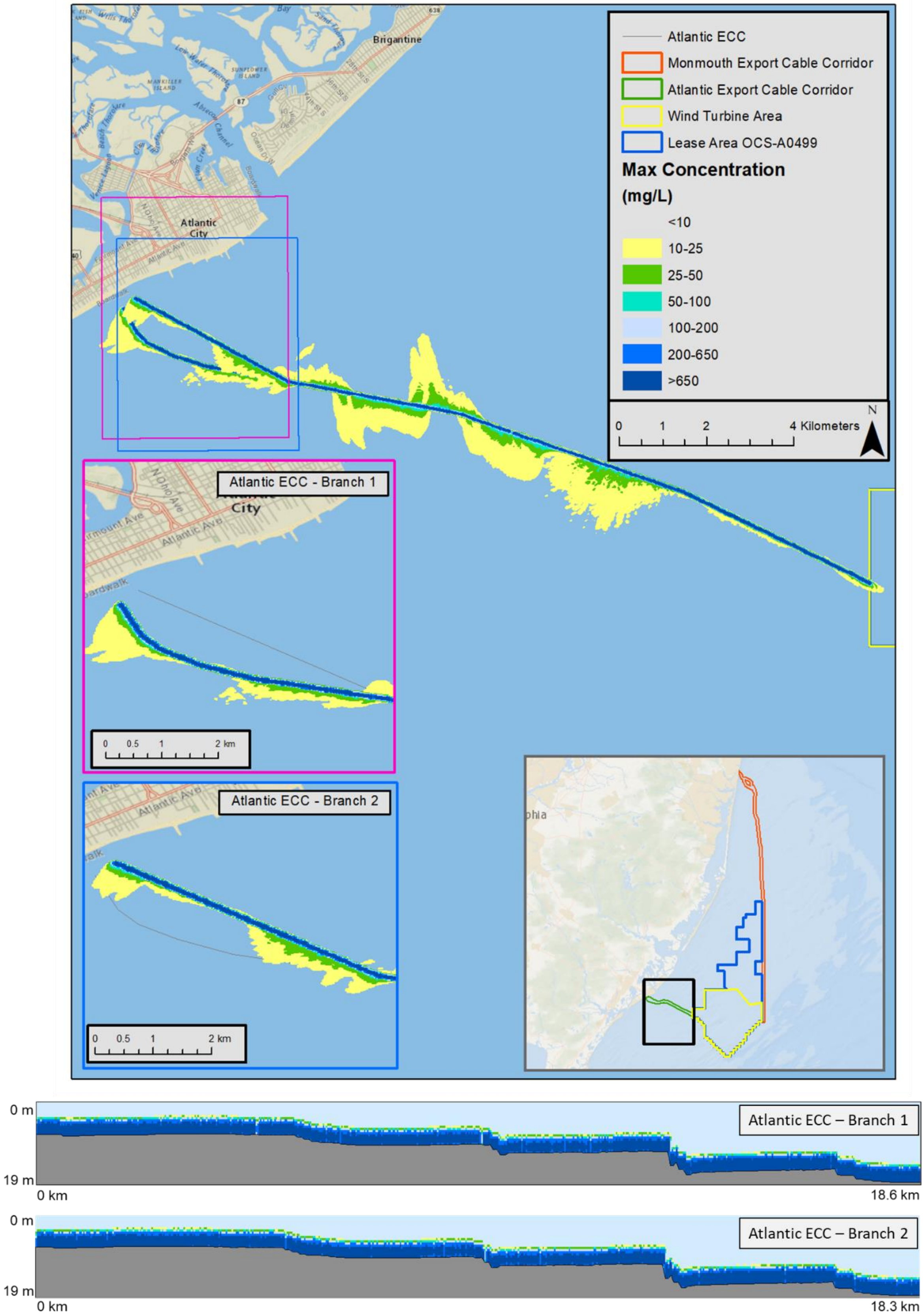

Figure 30. Map of Time-Integrated Maximum TSS Concentrations Associated with Cable Burial along the Atlantic ECC for Branch 1 and Branch 2.

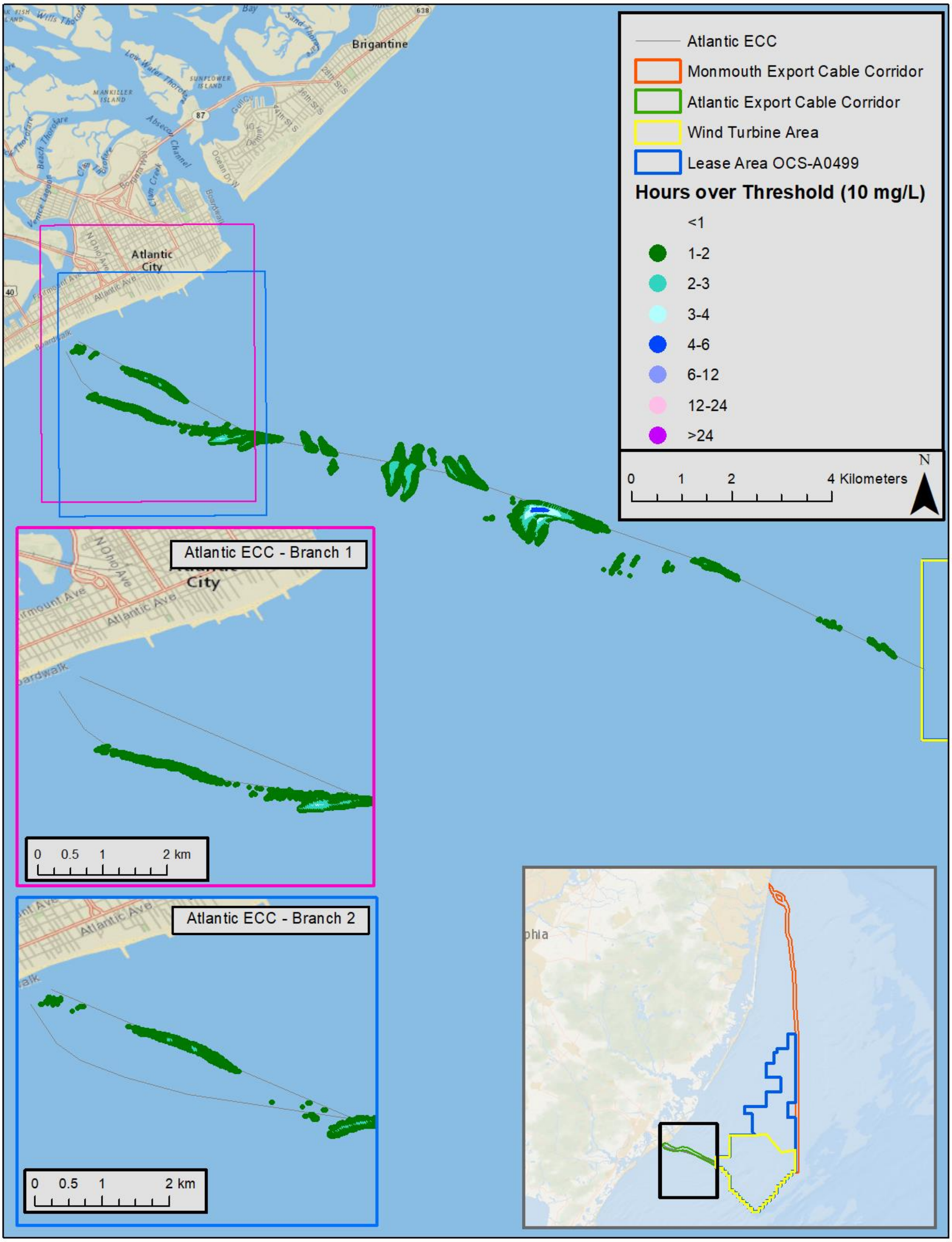

Figure 31. Map of Duration of TSS ≥10 mg/L Associated with Cable Burial along the Atlantic ECC for Branch 1 and Branch 2.

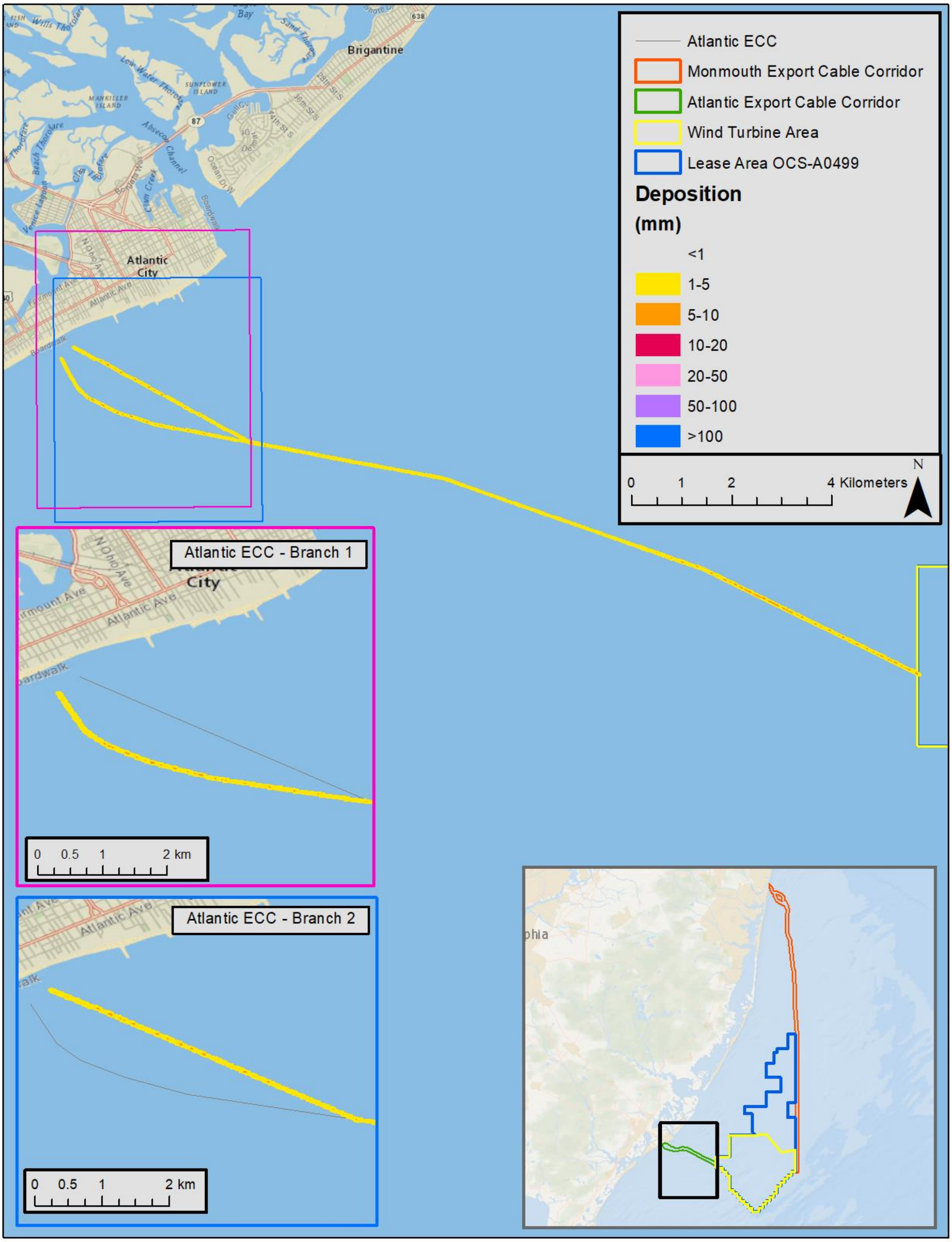

Figure 32. Map of Deposition Thickness Associated with Cable Burial along the Atlantic ECC for Branch 1 and Branch 2.

4.3.3 Landfall Approaches

This section presents SSFATE modeling and results associated with TSS generation and sediment deposition from the simulations of HDD pit activities for the Monmouth and Atlantic ECC landfall approaches.

Monmouth ECC – Representative Landfall Approach Scenario

The representative Monmouth ECC HDD pit excavation was modeled as a point source near the landward end of the Monmouth ECC in a location with representative environmental forcing conditions and bathymetry. A map of time-integrated TSS concentrations and a cross-section showing sediment introduction at the water surface are presented in Figure 33. This figure illustrates that the highest water column concentrations were centered around the HDD pit, with concentrations decreasing radially from the point source. Rather than forming concentric circles of decreasing concentrations around the HDD pit, the north to south oscillating currents created an oblong plume. The tail of the plume, with maximum concentrations ranging from 10-25 mg/L, was predicted to extend 3.3 km south of the HDD pit. The maximum excursion to the ≥10 mg/L contour can be attributed to sediment being introduced to the water column at the surface rather than close to the seabed, and the conservative assumption that no cofferdam or mitigation technique would be used during construction. Introduction at the surface increases the time it takes for sediment to deposit on the seabed, thus subjecting it to more tidal oscillations. As shown in Figure 34, most locations within the plume experienced exposures ≥10 mg/L for less than 6 to 12 hours with a maximum duration of exposure ≥10 mg/L centered at the HDD pit lasting 12 to 24 hours. Some sediment was transported south by the currents and temporarily entered the Manasquan Inlet. While the map of durations (Figure 34) indicates sediment may remain in the inlet for up to 4 hours, this value is cumulative over the entire simulation and does not indicate sediment remains continuously suspended in the inlet for this length of time. However, due to stronger currents in the channel, the sediment was unable to deposit. Depositional patterns were centered around the HDD pit (Figure 35), with maximum depositional thicknesses ranging between 10-20 mm.

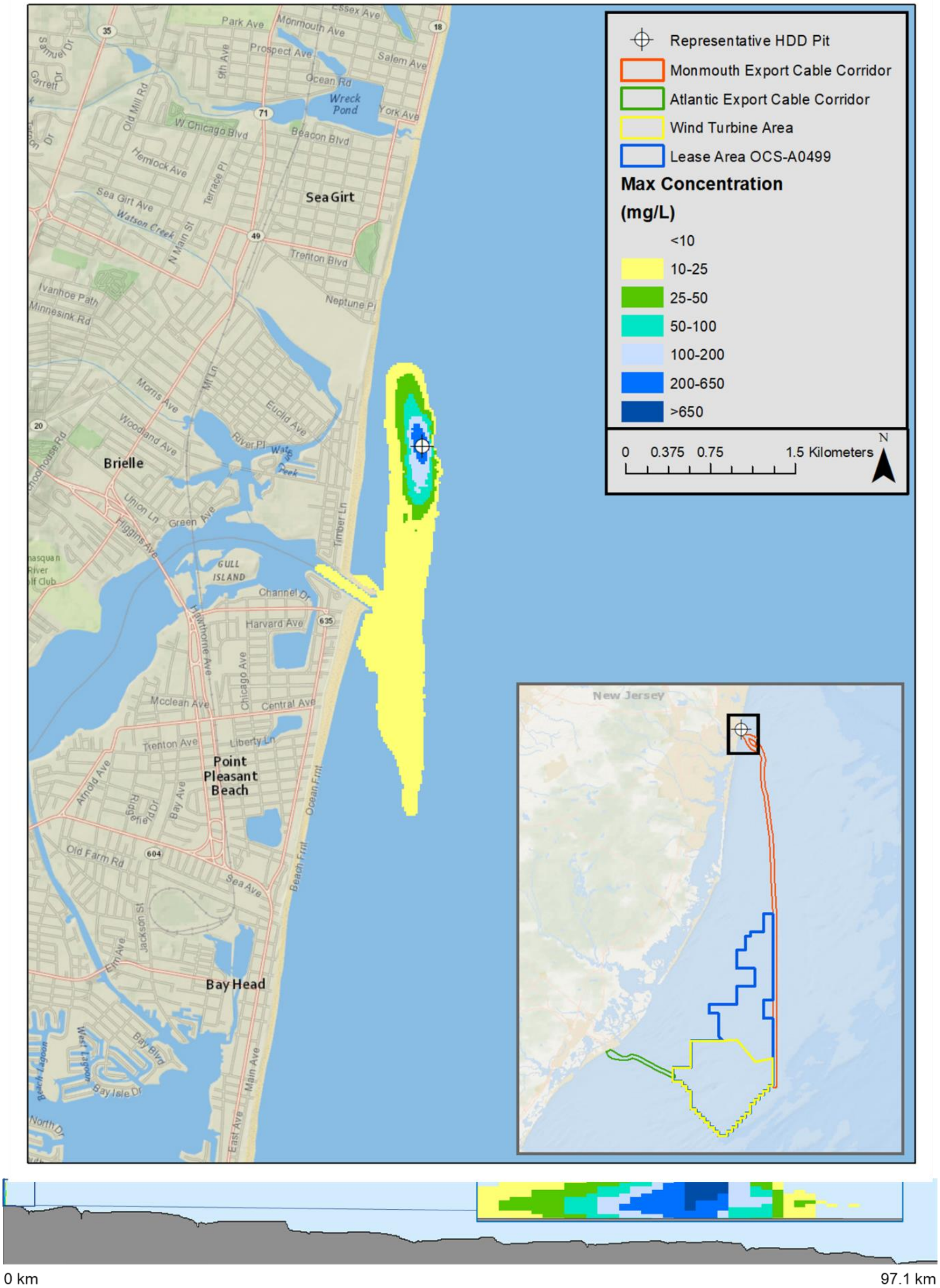

Figure 33. Map of Time-Integrated TSS Concentrations Associated with Monmouth ECC Representative HDD Pit Excavation.

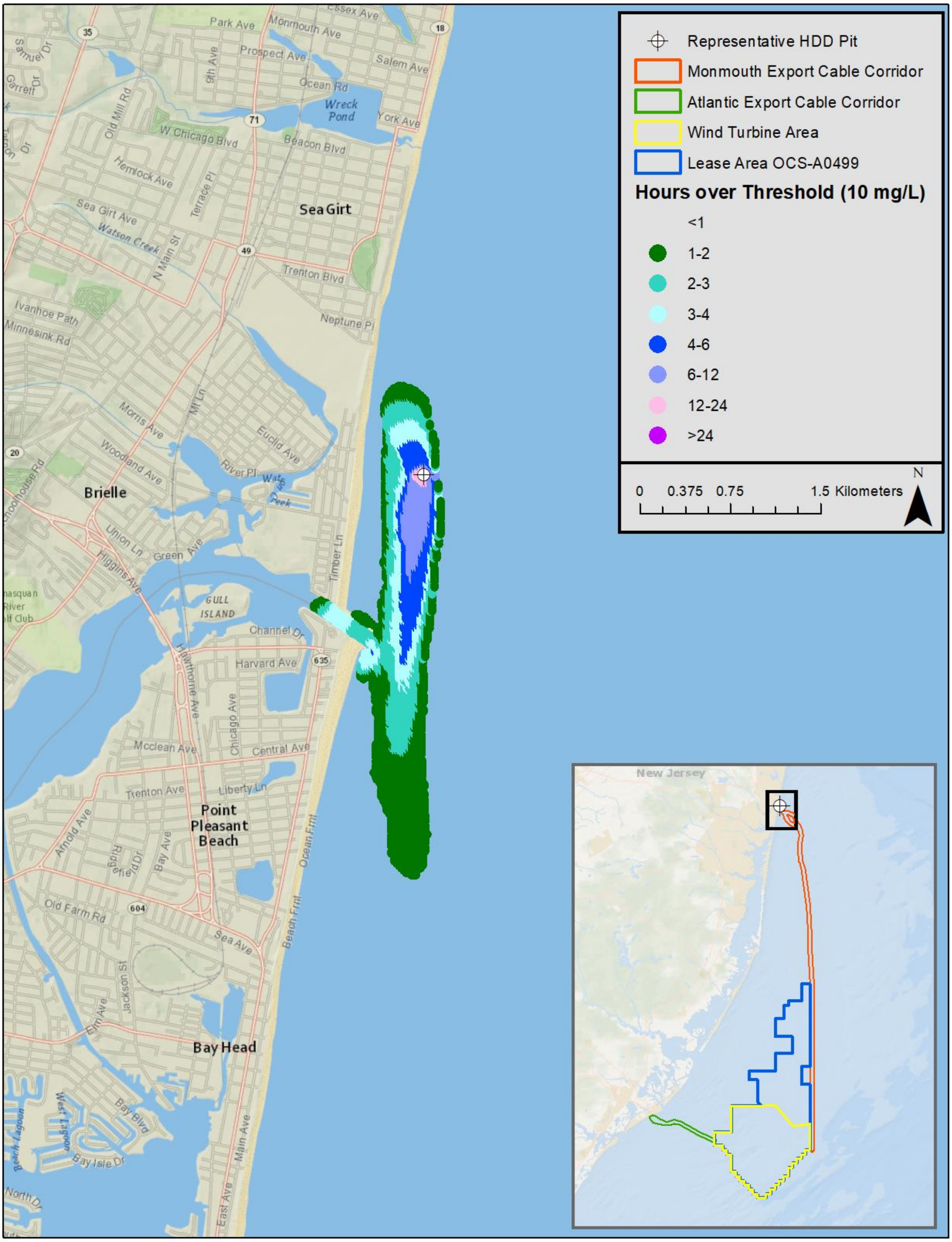

Figure 34. Map of Duration of TSS ≥10 mg/L Associated with Monmouth ECC Representative HDD Pit Excavation.

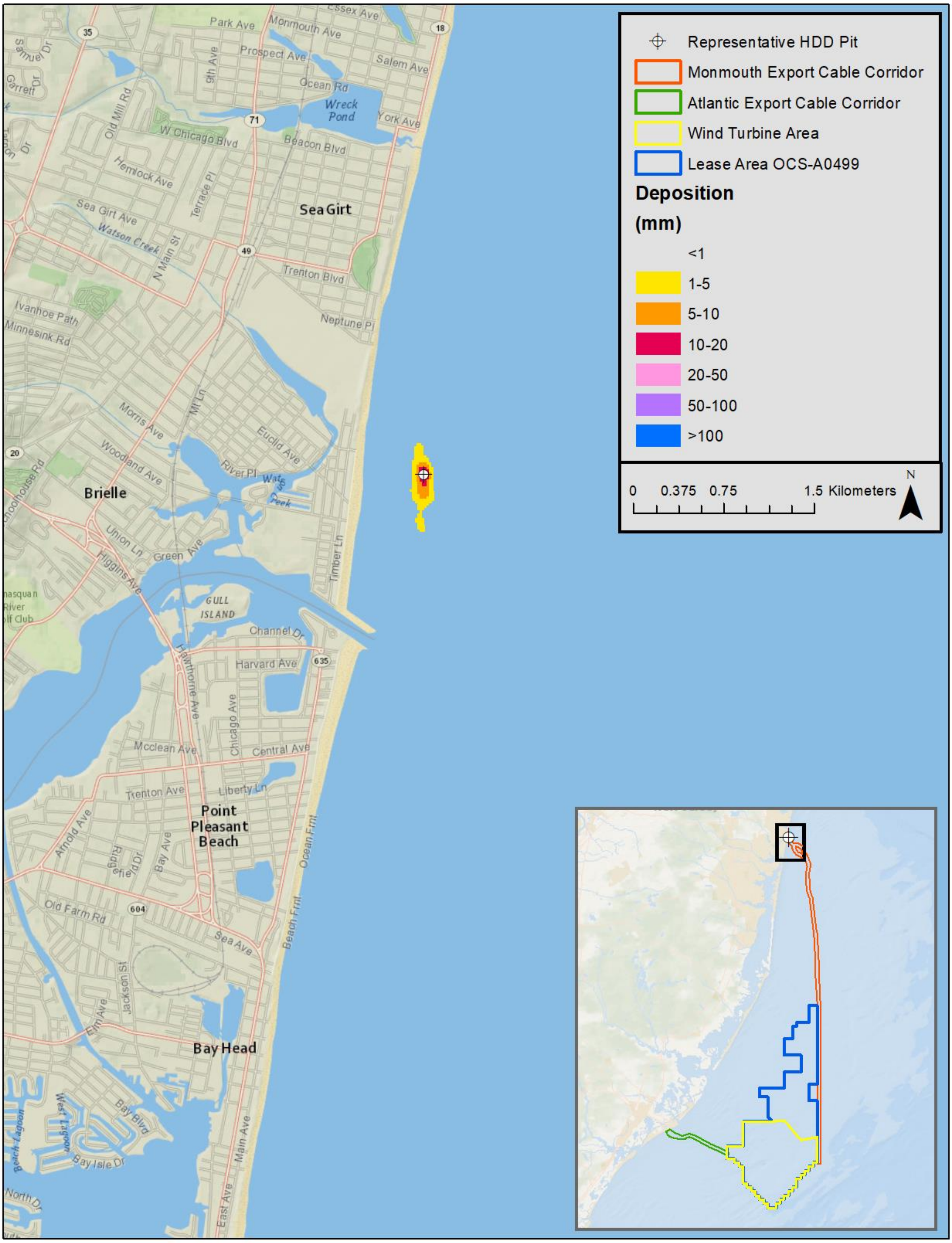

Figure 35. Map of Deposition Thickness Associated with Monmouth ECC Representative HDD Pit Excavation.

Atlantic ECC – Representative Landfall Approach Scenario

The representative Atlantic ECC HDD pit excavation was modeled as a point source near the landward end of the Atlantic ECC in a location with representative environmental forcing conditions and bathymetry. A map of the time-integrated TSS concentration and a cross-section showing sediment introduced at the water surface are presented in Figure 36. From this figure it is evident that the highest water column concentrations occurred at the HDD pit and decreased with increasing distance from the source. The currents biased the plume concentrations towards the southeast, parallel with the coastline, resulting in a maximum excursion to the ≥10 mg/L concentration contour of approximately 1.9 km. As with the Monmouth ECC landfall approach, because sediment was introduced at the water surface, the suspended sediment likely took longer to settle and underwent more tidal oscillations, and the conservative assumption that no cofferdam or mitigation technique would be used during construction. Figure 37 shows that the tail of the plume experienced water column concentrations ≥10 mg/L for less than 1 hour, while the rest of the plume experienced ≥10 mg/L concentrations for no more than 6 to 12 hours. Depositional patterns were centered around the HDD pit (Figure 38), with maximum depositional thicknesses ranging between 50 to 100 mm.

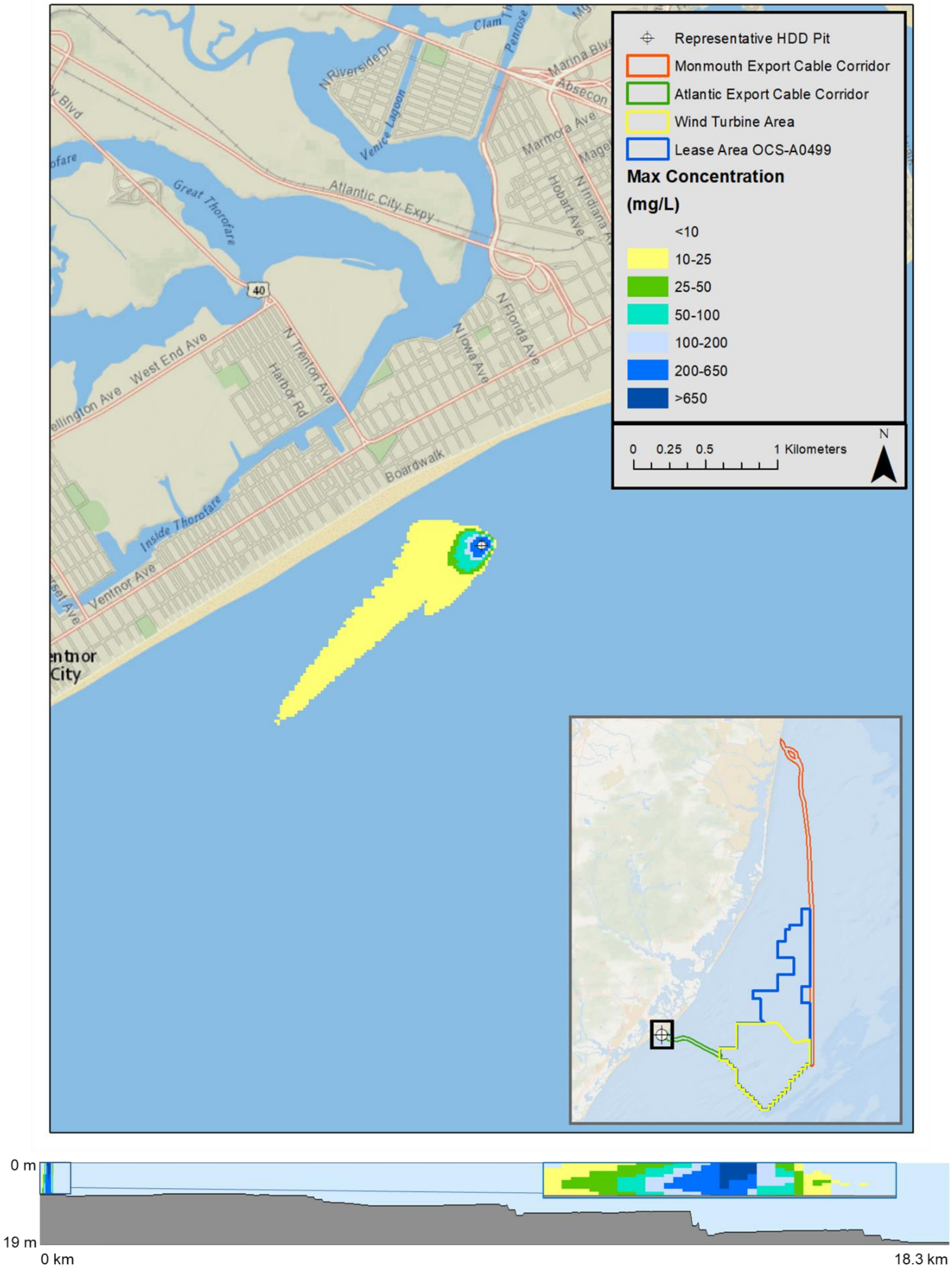

Figure 36. Map of Time-Integrated TSS Concentrations Associated with Atlantic ECC Representative HDD Pit Excavation.

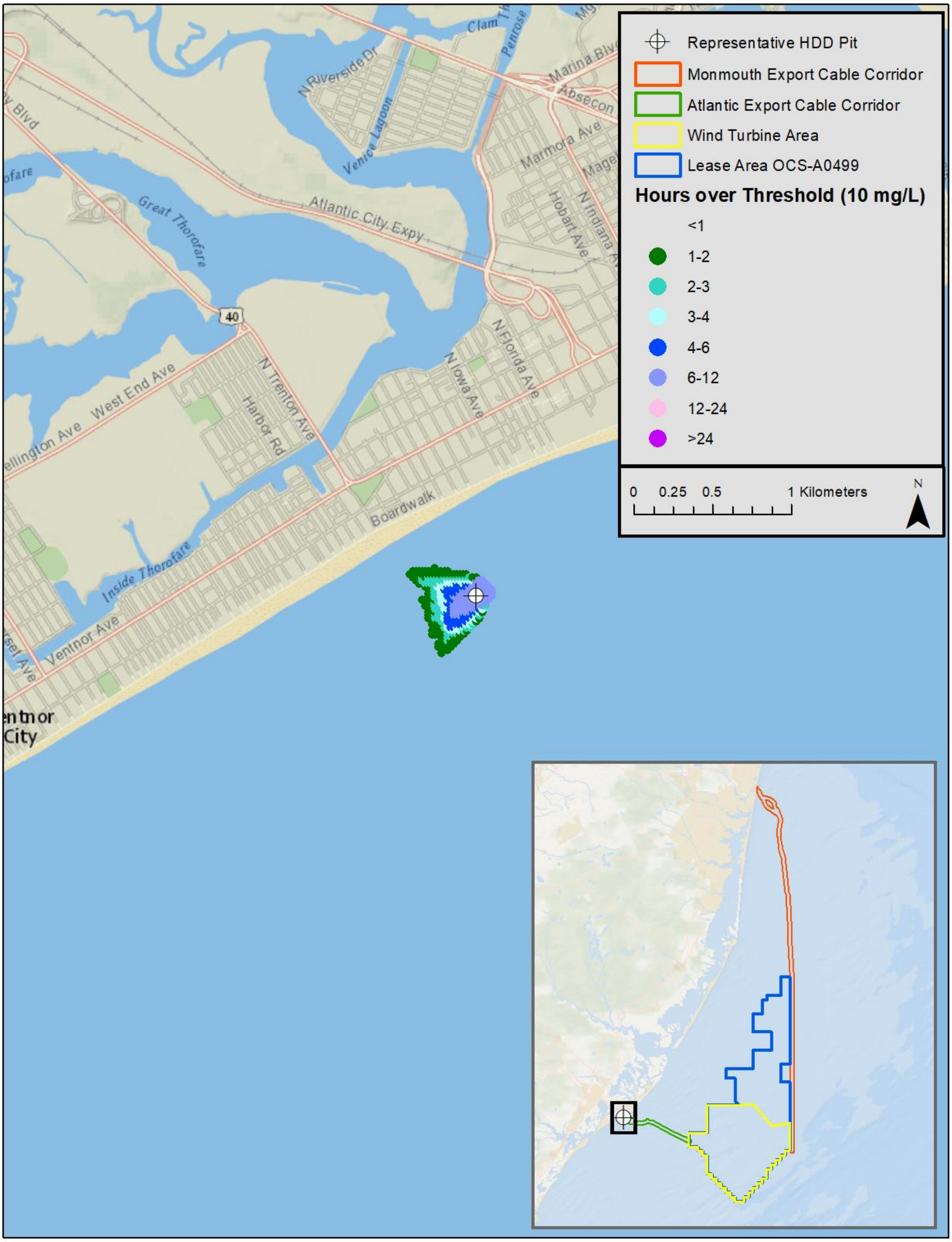

Figure 37. Map of Duration of TSS ≥10 mg/L Associated with Atlantic ECC Representative HDD Pit Excavation.

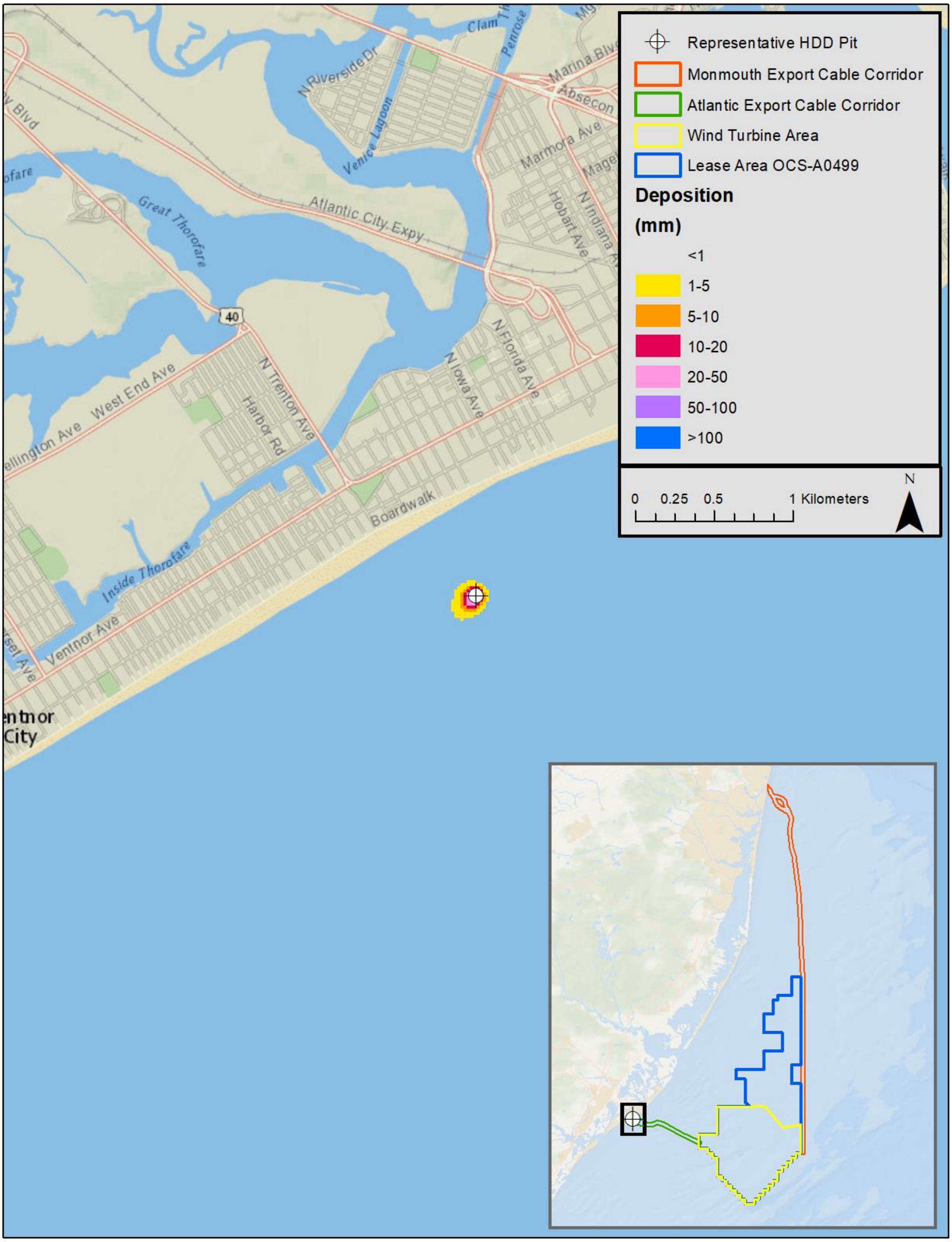

Figure 38. Map of Deposition Thickness Associated with Atlantic ECC Representative HDD Pit Excavation.

4.3.4 Results Summary Tables

Results from all modeled scenarios were analyzed to determine the spatial area, generally not contiguous, and maximum extents of TSS concentration, duration, and deposition thresholds. The time-integrated results provide a sum of all individual concentration grid cells that exceeded a threshold anywhere in the water column. Due to the similarity in results for each of the ECC branches, only one value was reported in the summary tables for the Monmouth and Atlantic ECC modeling. The values reported and discussed reflect the scenario predicted to have the maximum effect (i.e., maximum effects scenario) for each of the respective ECC branches.

Post-processing included calculations of areas above multiple TSS concentration thresholds and duration thresholds (Table 9 to Table 12). The areas in these tables are the total areas from the entire simulation, and therefore reflect the sum of different instances of smaller areas throughout the entire route and do not occur simultaneously. The tables illustrate that areas exposed to above-ambient TSS concentrations were largest when assessing concentrations above 10 mg/L, and that the areas rapidly decreased in size as the concentration threshold or duration increased. For example, as shown in Table 9, the Monmouth ECC scenario had a total area throughout the entire route of 33.73 km^2 ≥10 mg/L for more than 2 hours, but only 0.02 km^2 of this area was ≥200 mg/L for more than 2 hours. Above-ambient TSS concentrations also decreased with time. For the same example scenario (Monmouth ECC), concentrations ≥10 mg/L decreased from 33.73 km^2 for 2 hours (Table 9), to 11.33 km^2 for 4 hours (Table 10), to 3.17 km^2 for 6 hours (Table 11), and 0.04 km^2 for 12 hours (Table 12). Additionally, TSS concentrations ≥50 mg/L did not endure for periods >12 hours. Similar trends of rapid decrease of area with increasing time and/or increasing threshold are noted for all other routes presented.

Table 13 summarizes the maximum extent of the 10 mg/L and 100 mg/L concentrations as measured perpendicular to the route centerline and the maximum duration of TSS exposure ≥10 mg/L and ≥100 mg/L for each scenario. This table shows that the two representative IAC scenario extents are relatively similar, and that the Monmouth ECC activities are predicted to have 10 mg/L and 100 mg/L plumes that extend further than the Atlantic ECC activities. A larger plume extent can be attributed to the route orientation, timing of the currents, advance rate, and, for the Monmouth ECC, a higher volume of suspended sediment and higher fraction of fine sediment, causing the sediments to take longer to settle. The plumes are not expected to be of these sizes contiguously from the release, but rather it shows the potential trajectory the sediment plumes may follow. As described in the preceding paragraphs, the plumes were temporary and dissipated to 10 mg/L or less within 12 hours.

Table 14 summarizes the areas affected by sediment deposition over various thickness thresholds. The IAC installation had deposition less than 5 mm for both the jet and mechanical trenching scenarios. Comparing the two scenarios, the maximum distance to the 1 mm thickness contour was greater for the jet trenching installation parameters (110 m versus 50 m). Areas over deposition thresholds were also greater for the jet trenching installation parameters. The Monmouth ECC cable installation scenarios resulted in a maximum thickness between 10-20 mm. The Atlantic ECC cable installation scenarios resulted in a maximum thickness between 5-10 mm. Due to deposition thicknesses being less than 10 mm for the Atlantic ECC, no area was predicted to have deposition ≥10 mm and thus a maximum extent associated with the 10 mm threshold was not reported.

Table 9. Areas over Above-Ambient TSS Threshold Concentrations for Longer than 2 Hours for Each Scenario.

Scenario	Concentration Thresholds in mg/L					
	10	25	50	100	200	650
	Areas Above Concentration Threshold (km^2)					
Representative IAC – Jet Trencher	5.68	2.20	0.45	0.04	N/A	N/A
Representative IAC – Mechanical Trencher	9.35	3.44	0.48	0.04	N/A	N/A
Monmouth Export Cable – Jet Trencher *	33.73	15.43	6.42	1.32	0.02	N/A
Atlantic Export Cable – Jet Trencher *	0.43	0.02	N/A	N/A	N/A	N/A
Monmouth ECC Landfall Approach, Representative HDD Pit	1.13	0.28	0.14	0.07	0.03	<0.01
Atlantic ECC Landfall Approach, Representative HDD Pit	0.12	0.07	0.04	0.02	0.01	<0.01

**Both branches of the ECC were modeled and results were very similar. Of the two modeled ECC branches only results from the maximum effect scenario was reported for simplicity and to be conservative.*

Table 10. Areas over Above-ambient TSS Threshold Concentrations for Longer than 4 Hours for Each Scenario.

Scenario	Concentration Thresholds in mg/L					
	10	25	50	100	200	650
	Areas Above Concentration Threshold (km^2)					
Representative IAC – Jet Trencher	0.40	0.02	N/A	N/A	N/A	N/A
Representative IAC – Mechanical Trencher	2.87	N/A	N/A	N/A	N/A	N/A
Monmouth Export Cable – Jet Trencher *	11.33	3.48	0.79	0.10	N/A	N/A
Atlantic Export Cable – Jet Trencher *	0.04	N/A	N/A	N/A	N/A	N/A
Monmouth ECC Landfall Approach, Representative HDD Pit	0.41	0.15	0.07	0.03	0.01	<0.01
Atlantic ECC Landfall Approach, Representative HDD Pit	0.07	0.04	0.03	0.02	0.01	<0.01

**Both branches of the ECC were modeled and results were very similar. Of the two modeled ECC branches only results from the maximum effect scenario was reported for simplicity and to be conservative.*

Table 11. Areas over Above-ambient TSS Threshold Concentrations for Longer than 6 Hours for Each Scenario.

Scenario	Concentration Thresholds in mg/L					
	10	25	50	100	200	650
	Areas Above Concentration Threshold (km^2)					
Representative IAC – Jet Trencher	N/A	N/A	N/A	N/A	N/A	N/A
Representative IAC – Mechanical Trencher	0.05	N/A	N/A	N/A	N/A	N/A
Monmouth Export Cable – Jet Trencher *	3.17	0.62	0.16	N/A	N/A	N/A
Atlantic Export Cable – Jet Trencher *	N/A	N/A	N/A	N/A	N/A	N/A
Monmouth ECC Landfall Approach, Representative HDD Pit	0.17	0.08	0.04	0.02	0.01	<0.01
Atlantic ECC Landfall Approach, Representative HDD Pit	0.04	0.03	0.02	0.01	0.01	<0.01

**Both branches of the ECC were modeled and results were very similar. Of the two modeled ECC branches only results from the maximum effect scenario was reported for simplicity and to be conservative.*

Table 12. Areas over Above-ambient TSS Threshold Concentrations for Longer than 12 Hours for Each Scenario.

Scenario	Concentration Thresholds in mg/L					
	10	25	50	100	200	650
	Areas Above Concentration Threshold (km^2)					
Representative IAC – Jet Trencher	N/A	N/A	N/A	N/A	N/A	N/A
Representative IAC – Mechanical Trencher	N/A	N/A	N/A	N/A	N/A	N/A
Monmouth Export Cable – Jet Trencher *	0.04	N/A	N/A	N/A	N/A	N/A
Atlantic Export Cable – Jet Trencher *	N/A	N/A	N/A	N/A	N/A	N/A
Monmouth ECC Landfall Approach, Representative HDD Pit	0.02	<0.1	N/A	N/A	N/A	N/A
Atlantic ECC Landfall Approach, Representative HDD Pit	N/A	N/A	N/A	N/A	N/A	N/A

**Both branches of the ECC were modeled and results were very similar. Of the two modeled ECC branches only results from the maximum effect scenario was reported for simplicity and to be conservative.*

Table 13. Maximum Extent to the 10 mg/L and 100 mg/L TSS Contours from the Route Centerline and Maximum Duration of Exposure to TSS >10 mg/L and >100 mg/L for Each Scenario.

Scenario	Maximum Duration (hrs) of TSS >10 mg/L	Maximum Distance (km) to 10 mg/L Contour	Maximum Duration (hrs) of TSS >100 mg/L	Maximum Distance (km) to 100 mg/L Contour
Representative IAC – Jet Trencher	5.7	2.6	2.5	1.5
Representative IAC – Mechanical Trencher	6.3	2.9	2.7	0.9
Monmouth Export Cable – Jet Trencher *	12.8	2.6	6.0	1.5
Atlantic Export Cable – Jet Trencher *	5.5	1.7	0.8	<0.1
Monmouth ECC Landfall Approach, Representative HDD Pit	12.3	3.3	11	0.4
Atlantic ECC Landfall Approach, Representative HDD Pit	10.7	1.9	10.3	0.1

**Both branches of the ECC were modeled and results were very similar. Of the two modeled ECC branches only results from the maximum effect scenario was reported for simplicity and to be conservative.*

Table 14. Deposition over Thresholds for Each Scenario.

Scenario	Max Extent (m) of Deposition ≥1 mm	Max Extent (m) of Deposition ≥10 mm	Area (km^2) over Deposition Threshold				
			1 mm	5 mm	10 mm	20 mm	100 mm
Representative IAC – Jet Trencher	110	N/A	0.60	N/A	N/A	N/A	N/A
Representative IAC – Mechanical Trencher	50	N/A	0.42	N/A	N/A	N/A	N/A
Monmouth Export Cable – Jet Trencher *	200	30	8.32	0.75	0.02	N/A	N/A
Atlantic Export Cable – Jet Trencher *	50	N/A	1.39	0.07	N/A	N/A	N/A
Monmouth ECC Landfall Approach, Representative HDD Pit	479	102	0.09	0.03	0.01	N/A	N/A
Atlantic ECC Landfall Approach, Representative HDD Pit	200	103	0.04	0.02	0.02	0.01	N/A

**Both branches of the ECC were modeled and results were very similar. Of the two modeled ECC branches only results from the maximum effect scenario was reported for simplicity and to be conservative.*

4.3.5 Results Discussion

Simulations of several possible IAC or offshore export cable installation methods using either jet trenching installation parameters (for IAC and export cable installation) or mechanical trenching installation parameters (for IAC installation only) predicted above-ambient TSS ≥10 mg/L and deposition ≥1 mm stayed relatively close to the route centerline. This is due to sediments being introduced to the water column closer to the seabed. TSS concentrations ≥10 mg/L traveled a maximum distance of approximately 2.9 km, 2.6 km, and 1.7 km for IAC, Monmouth ECC, and Atlantic ECC cable installation, respectively. For the landfall approach scenarios, it was assumed that no cofferdam was deployed during construction activities, an excavator was used, and sediment was introduced at the surface. This resulted in a maximum distance for the predicted above-ambient TSS concentrations ≥10 mg/L of approximately 3.3 km and 1.9 km for the Monmouth and Atlantic HDD pits, respectively.

Above-ambient TSS concentrations stemming from cable installation for the IAC, Monmouth ECC, and Atlantic ECC model scenarios remained relatively close to the route centerline, were constrained to the bottom of the water column, and were short-lived. For the IAC and Atlantic ECC model scenarios, above-ambient TSS concentrations substantially dissipated within 2 to 4 hours and fully dissipated in less than 6 hours. For the Monmouth ECC model scenarios, above-ambient TSS concentrations substantially dissipated within 2 to 6 hours but required between 12 and 24 hours to fully dissipate, likely due to the relatively longer route (i.e., larger volume of suspended sediment), route orientation in relation to currents, and more frequent occurrence of fine sediment. For the landfall approach scenarios, the tails of the plumes, with concentrations ≥10 mg/L, were transported away from the source and were short-lived, while concentrations around the HDD pits dissipated within 6 to 24 hours for the Monmouth HDD pit and 6 to 12 hours for the Atlantic HDD pit. The larger areas of TSS concentrations above thresholds and the longer time for the plume to diminish to ambient conditions for the Monmouth HDD pit may be attributed to sediments being released in deeper water, the higher fraction of fine sediments taking longer to settle, and slightly stronger currents transporting the sediments parallel with the shore. For the HDD modeling, a conservative approach was used by assuming no mitigation techniques (e.g., cofferdam, silt screen) would be deployed during construction activities. Use of a cofferdam would likely reduce the extent of the plume and minimize transport of the plume by currents, thus resulting in more localized settling of sediment around the release location.

Deposition ≥1 mm was limited to 110 m from the IAC centerline for jet trenching installation parameters and to 50 m for mechanical trenching installation parameters. Variations in plume extent and duration for IAC installation can be attributed to differences in cross-sectional area and advance rates, which impacted the timing of the currents. Deposition ≥1 mm was limited to 200 m from the Monmouth ECC centerline and to 50 m of the Atlantic ECC centerline. The maximum deposition associated with IAC, Atlantic ECC, and Monmouth ECC model scenarios was less than 5 mm, between 5-10 mm, and between 10-20 mm, respectively. For the Monmouth and Atlantic HDD pit excavations, deposition ≥1 mm was predicted to extend a maximum distance of 479 m and 200 m, respectively. The Atlantic landfall approach scenario was predicted to have higher areas of deposition for the 10 mm and 20 mm thresholds due to a higher fraction of coarse sediment. In combination with the sediment type and the relatively more shore-perpendicular nature of the currents at the Atlantic HDD pit, more sediment remained close to the pit and settled to the bottom rather than lingering in the water column or being transported as a suspended sediment plume.

While the plume patterns for the respective representative IAC scenarios, offshore export cable scenarios, and landfall approach scenarios were generally similar, differences in the extent and persistence of the plumes and the extent and thickness of deposition may be attributed to route orientation relative to currents, timing of currents, installation parameters, volume suspended, and sediment grain size distribution.

5 REFERENCES

Anderson, EP, Mackas, DL. 1986. Lethal and sublethal effects of a molybdenum mine tailing on marine zooplankton: mortality, respiration, feeding and swimming behavior in *Calanus marshallae, Metridia pacifica* and *Euphausia pacifica.* Mar Environ Res. 19(2):131-155.

Anderson, E., Johnson, B., Isaji, T., & Howlett, E. 2001. SSFATE (Suspended Sediment FATE), a model of sediment movement from dredging operations. In WODCON XVI World Dredging Congress (pp. 2-5).

Anchor QEA. 2003. Literature Review of Effects of Resuspended Sediments Due to Dredging Operations. Prepared for the Los Angeles Contaminated Sediments Task Force.

Berry, WJ, Rubinstein, NI, Hinchey, EH, Klein-MacPhee, G, Clarke, DG. 2011. Assessment of dredging-induced sedimentation effects on Winter Flounder (*Pseudopleuronectes americanus*) hatching success: results of laboratory investigations. Paper presented at: WEDA, 2011. Proceedings of the Western Dredging Association Technical Conference and Texas A&M Dredging Seminar; Nashville, Tennessee.

Cake, EW, Jr (Gulf Coast Research Laboratory). 1983. Habitat suitability index models: Gulf of Mexico American oyster. U.S. Fish and Wildlife Service. Report nr FWS-OBS 82/10.57. 37 p.

Egbert, G. D., Bennett, A. F., & Foreman, M. G. 1994. TOPEX/POSEIDON tides estimated using a global inverse model. Journal of Geophysical Research: Oceans, 99(C12), 24821-24852.

Egbert, G. D., & Erofeeva, S. Y. 2002. Efficient inverse modeling of barotropic ocean tides. Journal of Atmospheric and Oceanic Technology, 19(2), 183-204.

Essink, K. 1999. Ecological effects of dumping of dredged sediments; options for management. J Coast Conserv. 5:69–80.

Fabricius, KE. 2005. Effects of terrestrial runoff on the ecology of corals and coral reefs: review and synthesis. Mar Pollut Bull. 50:125-146.

Foreman, J. 2002. Resuspension of sediment by the jet plow during submarine cable installation. Submitted to GenPower, LLC, Needham, MA. Submitted by Engineering Technology Applications, Ltd, Romsey, Great Britain.

General Bathymetric Chart of the Oceans (GEBCO). GEBCO_2020 Grid. Accessed 2020. Retrieved from https://www.gebco.net/data_and_products/gridded_bathymetry_data/gebco_2020/.

Gilmour, J. 1999. Experimental investigation into the effects of suspended sediment on fertilization, larval survival, and settlement in a scleractinian coral. Mar Biol. 135:451-462.

Hendrick, VJ, Hutchison, ZL, Last, KS. Sediment Burial Intolerance of Marine Macroinvertebrates. PLos ONE. 2016; 11(2): e0149114.

Huang, W. and M. Spaulding, 1995. 3D Model of Estuarine Circulation and Water Quality Induced by Surface Discharges. Journal of Hydraulic Engineering 121: 300-311.

Johnson, B. H., Andersen, E., Isaji, T., Teeter, A. M., & Clarke, D. G. 2000. Description of the SSFATE numerical modeling system (No. ERDC-TN-DOER-E10). Army Engineer Waterways Experiment Station Vicksburg MS Engineer Research And Development Center.

Kemps, H., & Masini, R. 2017. Estimating dredge source terms–a review of contemporary practice in the context of Environmental Impact Assessment in Western Australia. Report of Theme.

Lin, J., Wang, H. V., Oh, J. H., Park, K., Kim, S. C., Shen, J., & Kuo, A. Y. 2003. A new approach to model sediment resuspension in tidal estuaries. Journal of coastal research, 76-88.

Mid-Atlantic Regional Association Coastal Ocean Observing System (MARACOOS). Accessed 2020. Retrieved from http://erddap.maracoos.org/erddap/info/index.html?page=1&itemsPerPage=1000.

Mendelsohn, D., E. Howlett, and J.C. Swanson, 1995. WQMAP in a Windows Environment. In: Proceedings of the 4th International Conference on Estuarine and Coastal Modeling, October 26-28, 1995, San Diego, CA.

Mendelsohn, D., S. Peene, W. Saunders and M. Goodrich, 2003. Three-Dimensional Modeling Of Anthropogenic Impacts To Dissolved Oxygen In A Stratified Estuarine Environment: Savannah River Estuary. In: Proceedings, TMDL 2003, Chicago, Ill, Nov 16-19, 2003. Water Environment Federation.

Mid-Atlantic Regional Ocean Assessment (MAROA). 2020. Oceanographic setting and processes; [accessed 2020 August 5]. https://roa.midatlanticocean.org/ ocean-ecosystem-and-resources/characterizing-the-mid-atlantic-ocean-ecosystem/oceanographic-setting-and-processes/

Muin, M. and M.L. Spaulding, 1997. Three-dimensional boundary fitted circulation model. In: Journal of Hydraulic Engineering, Vol. 123, No. 1, January 1997, p. 2-12.

Muin, M., 1993. A three dimensional boundary fitted circulation model in spherical coordinates. Ph.D. Thesis, Department of Ocean Engineering, University of Rhode Island, Kingston, RI.

Murphy RC. 1985. Factors affecting the distribution of the introduced bivalve, *Mercenaria*, in a California lagoon- the importance of bioturbation. J Mar Res. 43:673-692.

National Data Buoy Center (NDBC). Accessed 2017. Historic Meteorological Observations [ASCII Text Files]. Retrieved from http://www.ndbc.noaa.gov/station_page.php?station=buzm3.

New Jersey Department of Environmental Protection (NJDEP). NJ Geographic Information Network. Accessed 2020. Coastline_2012_of_New_Jersey.shp [Shapefile]. Retrieved from https://njogis-newjersey.opendata.arcgis.com/datasets/njdep::coastline-2012-of-new-jersey?geometry=-82.160%2C38.666%2C-67.339%2C41.605.

New York State Department of State (NYSDOS). NY GIS Clearinghouse. Accessed 2020. NYS_Coastal_Boundary.shp [Shapefile]. Retrieved from https://gis.ny.gov/gisdata/inventories/details.cfm?DSID=317.

National Oceanic and Atmospheric Administration (NOAA). Bathymetric Data Viewer. Accessed 2020a. Retrieved from https://maps.ngdc.noaa.gov/viewers/bathymetry/.

NOAA. Accessed 2020b. Harmonic Constituents for Multiple Locations [ASCII Data]. Retrieved from https://tidesandcurrents.noaa.gov/.

NOAA. National Data Buoy Center (NDBC). Accessed 2020c. Meteorological Data for Multiple Locations. Retrieved from https://www.ndbc.noaa.gov/.

Rayment, WJ. 2002. Semi-permanent tube-building amphipods and polychaetes in sublittoral mud or muddy sand. Plymouth: Marine Biological Association of the United Kingdom. Marine Life Information Network: Biology and Sensitivity Key Information Sub-programme Available from: http://www.marlin.ac.uk.

Read, PA, Anderson, KJ, Matthews, JE, Watson, PG, Halliday, MC, Shiells, GM. 1982. Water quality in the Firth of Forth. Mar Pollut Bull. 13:421-425.

Read, PA, Anderson, KJ, Matthews, JE, Watson, PG, Halliday, MC, Shiells, GM. 1983. Effects of pollution on the benthos of Firth of Forth. Mar Pollut Bull. 14:12-16.

Rogers, AD (British Antarctic Survey). 2004. The biology, ecology and vulnerability of seamount communities. Gland, Switzerland, International Union for Conservation of Nature & Natural Resources. 12 p.

Soulsby, R.L. 1998. Dynamics of Marine Sands. Thomas Telford, England.

Spaulding, M.L., 1984. A vertically averaged circulation model using boundary fitted coordinates. Journal of Physical Oceanography, May, pp. 973 982.

Swanson, C., D. Mendelsohn, D. Crowley, and Y. Kim, 2012. Monitoring and modeling the thermal plume from the Indian Point Energy Center in the Hudson River. Proceedings of the Electric Power Research Institute Third Thermal Ecology and Regulation Workshop, Maple Grove, MN, 11-12 October 2011.

Swanson, J. C., Isaji, T., Ward, M., Johnson, B. H., Teeter, A., & Clarke, D. G. 2000. Demonstration of the SSFATE numerical modeling system. DOER Technical Notes Collection (TN DOER-E12). US Army Engineer Research and Development Center, Vicksburg, MS. http://www.wes.army.mil/el/dots/doer/pdf/doere12. pdf.

Swanson, J. C., & Isaji, T. 2006. Modeling dredge-induced suspended sediment transport and deposition in the Taunton River and Mt. Hope Bay, Massachusetts. In WEDA XXVI/38th TAMU Dredging Seminar, June (pp. 25-28).

Swanson, J. C., Isaji, T., Clarke, D., & Dickerson, C. 2004. Simulations of dredging and dredged material disposal operations in Chesapeake Bay, Maryland and Saint Andrew Bay, Florida. In WEDA XXIV/36th TAMU Dredging Seminar (pp. 7-9).

Swanson, J. C., Isaji, T., & Galagan, C. 2007. Modeling the ultimate transport and fate of dredge-induced suspended sediment transport and deposition. Proceedings of the WODCON XVIII, 27.

Swanson, J.C., M. Spaulding, J-P Mathisen and O.O. Jenssen, 1989. A Three Dimensional Boundary-fitted Coordinate Hydrodynamic Model, Part I: Development and Testing. Dt. Hydrog, Z.42, 1989, p. 169-186.

Swanson, J. C., 1986. A three dimensional numerical model system of coastal circulation and water quality. Ph.D. Thesis, Dept. of Ocean Engineering, University of Rhode Island, Kingston, RI.

Teeter, A. M. 1998.Cohesive sediment modeling using multiple grain classes, Part I: settling and deposition. Proceedings of INTERCOH.

Turner, EJ. Miller, DC. 1991. Behavior and growth of Mercenaria during simulated storm events. Mar Biol. 111:55-64.

United States Geological Survey (USGS). Water Data for Multiple Locations. Accessed 2020. Retrieved from https://waterdata.usgs.gov/nwis.

United States Department of the Interior (USDOI). 1982. Final environmental impact statement OCS SALE No.76 Outer continental shelf oil and gas lease sale offshore the Mid-Atlantic States.

Van Rijn, L. C. 1989. Handbook sediment transport by currents and waves. Delft Hydraulics Laboratory.

Wilber, DH, Clarke, DG. 2001. Biological effects of suspended sediments: a review of suspended sediment impacts on fish and shellfish with relation to dredging activities in estuaries. N Am J Fish Manag. 21(4): 855-875.

ATTACHMENT A

SEDIMENT TRANSPORT MODELING

Atlantic Shores Offshore Project Area Sandwave Clearance

Prepared by:

RPS

Jill Rowe, Heather Weitzner, Missy Gloekler

55 Village Square Drive
South Kingstown RI 02879

T +1 401 789 6224
E Jill.Rowe@rpsgroup.com

Prepared for:

EDR

RPS Project: P-19-208506
Attachment Version: 2
December 16, 2021

Contents

Figures

Tables

List of Acronyms

BOEM	Bureau of Ocean Energy Management
COP	Construction and Operations Plan
ECC	Export Cable Corridor
EDR	Environmental Design & Research
GIS	Geographic Information System
NOAA	National Oceanic and Atmospheric Administration
OCS	Outer Continental Shelf
O&M	Operations and Maintenance
PDE	Project Design Envelope
SSFATE	Suspended Sediment FATE
TSS	Total Suspended Solids
WEA	Wind Energy Area
WTA	Wind Turbine Area

1 INTRODUCTION

This attachment documents the sediment transport modeling assessment of the sediment-disturbing sandwave clearance activities associated with the development of the Project. The clearance methods are described in detail in the COP and the model inputs relative to the sandwave clearance modeling are documented in this attachment. To be consistent with the Project Design Envelope (PDE), this study bounded the potential effects associated with seabed preparation, prior to cable installation, by assuming conservative installation parameters associated with the anticipated equipment. Sandwave clearance was modeled using a trailing suction hopper dredger (TSHD) along a representative portion of the Monmouth ECC. It is expected that there will be sufficient time between sandwave clearance and cable installation such that the effects from sandwave clearance do not compound or influence effects from cable installation activities. The general study area, environmental data collected and used for modeling, and hydrodynamic modeling results are detailed in the main technical report. An illustration of the Atlantic Shores Offshore Project Region (Offshore Project Region) and relevant study components is presented in Figure 1.

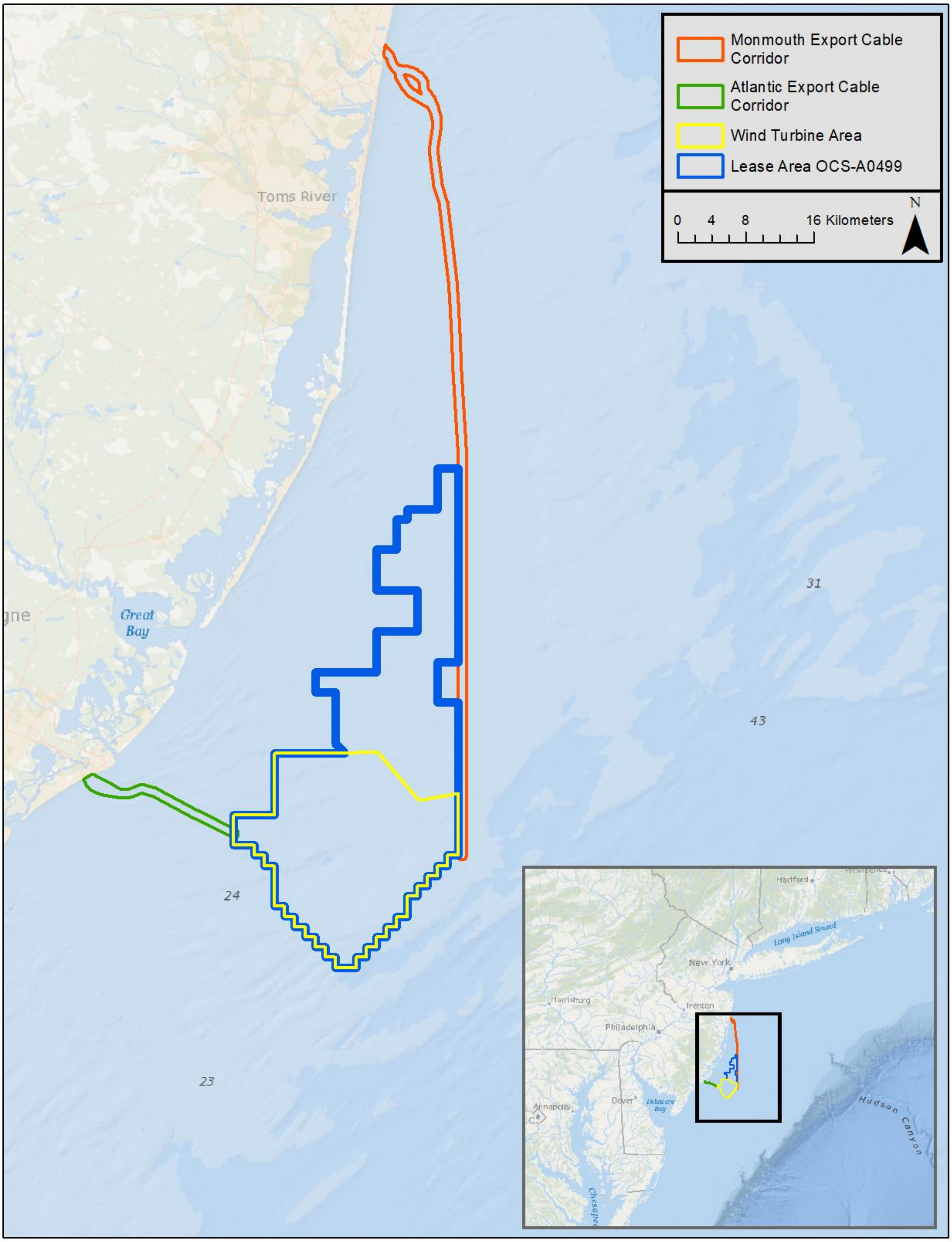

Figure 1. Map of Atlantic Shores Offshore Project Region with Offshore Components.

1.1 Study Scope and Objectives

RPS applied customized hydrodynamic and sediment transport models to assess potential effects from sediment suspension and dispersion during sandwave clearance activities. This approach is consistent with the modeling approach used for similar studies that have been accepted by state and federal regulatory agencies for pipeline and cable installation as well as harbor dredging and land reclamation activities. Specifically, the analysis includes two interconnected modeling tasks as listed below. Details of the hydrodynamic model application and sediment transport model theory are provided in the main technical report.

1. Using the BFHYDRO modeling system, development of a three-dimensional hydrodynamic model application of a domain encompassing the Project's activities; and
2. Using the SSFATE modeling system, simulations of the fate and transport of the suspended sediment (including evaluation of seabed deposition and suspended sediment plumes) associated with sandwave clearance activities. Velocity fields developed using the BFHYDRO model were used as the primary forcing for SSFATE.

The sandwave clearance activities were modeled using a TSHD for a representative segment of the Monmouth ECC. Given the larger sandwaves observed within the Monmouth ECC, the conservative installation parameters, and similar hydrodynamic forcing conditions, the modeling conducted along the Monmouth ECC can be considered representative of sandwave clearance along the Atlantic ECC. It is expected that there will be sufficient time between sandwave clearance and cable installation such that the effects from sandwave clearance do not compound or influence effects from cable installation activities. While several corridors may be cleared of sandwaves, each corridor would be cleared at different timeframes. Therefore, the simulation modeled for a single corridor in this study can be considered representative of other sandwave clearance activities in proximity to the Monmouth ECC and Atlantic ECC.

The effects of sandwave clearance activities were quantified using water column concentrations of total suspended sediment (TSS) and sediment deposition thickness on the seabed as a result of the suspended sediment settling over time. Results are presented with respect to the thresholds listed below, which were selected either because they are thresholds of biological significance or because they provide an effective means of demonstrating the physical effects. Thresholds associated with biological significance are documented in Sections 4.5.2.1 and 4.6.2.1 of the COP, which are the benthic and finfish and invertebrate sections, respectively.

- Water column concentrations thresholds: 10, 25, 50, 100, 200, and 650 milligrams per liter (mg/L)
- Water column exposure durations: 2, 4, 6, and 12 hours
- Seabed deposition: 1, 5, 10, 20, and 100 millimeters (mm)

This attachment to the main technical report describes the modeling approach and results of the sandwave clearance study. A description of environmental data sources used, the BFHYDRO hydrodynamic model and its application, and the SSFATE sediment dispersion model theory are provided in the main technical report.

2 SEDIMENT MODELING

The sediment transport modeling was conducted using SSFATE, an in-house model co-developed and maintained by RPS. A description of the model theory is provided in the main technical report. A representative SSFATE model scenario was run to simulate sandwave clearance. The following sections describe the route and associated modeling inputs.

2.1 SSFATE Study Model Application

2.1.1 Scenario Components: Routes and Approaches

Because a greater number of sandwaves are predicted to be present along the northern end of the Monmouth ECC, and the PDE indicates 20% of the ECC may require sandwave clearance, a representative sandwave clearance route (Figure 2) was selected. The route begins at the northern end of the Monmouth ECC, near the shoreline, and extends 20 km south along the modeled Monmouth ECC – Branch 2 cable route. Sandwave clearance along this route was modeled using a TSHD and a sediment sample representative of typical sandwave composition (Table 1). As a conservative approach, a representative sample with a higher fraction of fine sediment was selected and applied to the route. Fine sediments (e.g., clays, silts) tend to last longer in the water column, whereas coarse sediment (e.g., fine sand, coarse sand) will settle at a faster rate.

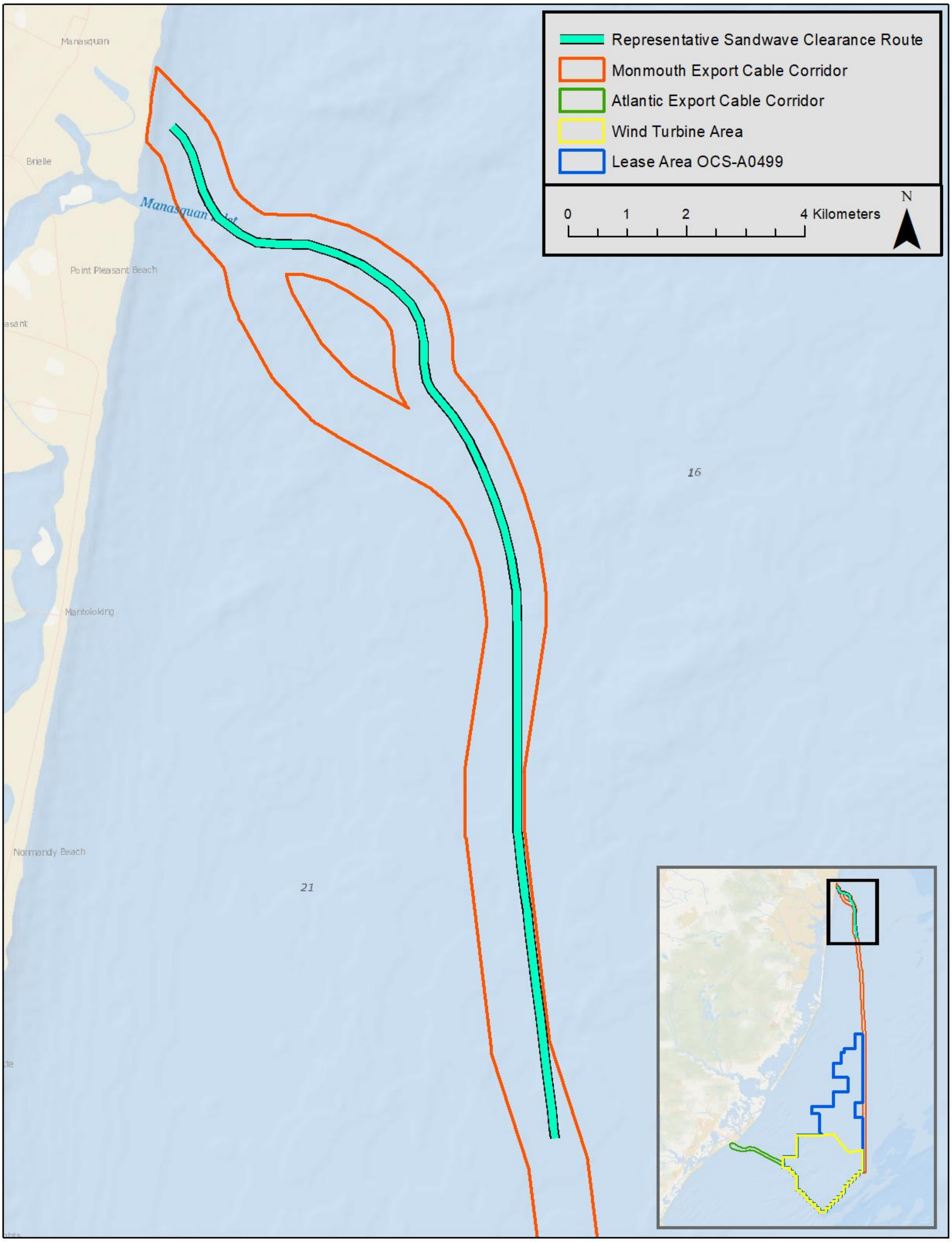

Figure 2. Modeled Representative Sandwave Clearance Route.

Table 1. Construction Activities Modeled.

Component	Equipment Type	Total Route Length (km)
Representative Sandwave Clearance, Monmouth ECC	TSHD	20

2.1.2 Project Components: Construction Activities

Sandwave clearance activities were modeled using TSHD, conservative equipment parameters, and average sandwave dimensions found along the route (Table 2). As a conservative approach and to bound potential TSHD disposal methods, 100% of the sediment was mobilized into the water column at the water surface. Because a disposal location had not been selected at the time of modeling, disposal at the water surface was modeled along the route.

Table 2. Construction Activity Modeling Parameters.

Component	Equipment Type	Corridor Width (m)	Corridor Depth (m)	Cross-Sectional Area (m^2)	Production Rate (m^3/hr)	Percent Mobilized (%)
Representative Sandwave Clearance, Monmouth ECC	TSHD	30	0.9	27	1,850	100

2.2 Sediment Modeling Results

To capture the unique results of the representative sandwave clearance scenario, sediment concentrations were computed on a grid with a 30 m resolution in the horizontal dimension and 1 m resolution in the vertical dimension. Model-predicted concentrations are considered as above ambient or as “excess” concentrations above background levels (i.e., a concentration of 0 mg/L is assumed for the ambient concentration).

Results are presented as a set of figures and tables. Maps of maximum above-ambient TSS concentrations, duration of above-ambient TSS ≥10 mg/L, seabed deposition, and a snapshot of instantaneous TSS concentrations are provided for each modeled scenario. Tables quantifying the area exceeding TSS thresholds for specific durations and areas of seabed deposition exceeding thickness thresholds are also presented.

Additional information about standard graphical outputs are provided below:

- **Maps of Instantaneous TSS Concentrations**: These figures show the instantaneous TSS concentrations at a moment in time. The concentrations are shown as contours using mg/L. The plan view shows the maximum concentration throughout the water column and the vertical cross-section shows the cross-sectional variability of concentrations along a transect.
- **Maps of Time-integrated Maximum TSS Concentrations**: These figures show the maximum time-integrated water column concentration from the entire water column in scaled plan view, including a vertical cross-sectional view of maximum TSS concentrations in the water column. The concentrations are shown as contours using mg/L. The entire area within the contour is at or above the concentration defined by the contour itself. Most importantly, it should be noted that these maps show the maximum TSS concentration that occurred throughout the entire simulation and that: (1) these concentrations do not persist throughout the entire simulation and may be just one time step; and (2) these concentrations do not occur concurrently throughout the entire modeled area but are the time-integrated spatial views of maximum predicted concentrations.
- **Maps of Duration of TSS Concentrations ≥10 mg/L:** These figures show the number of hours that the TSS concentrations are expected to be ≥10 mg/L.

- **Maps of Seabed Deposition**: These figures show the deposition on the seabed that would occur once the activity has been completed. The thickness levels are shown as contours (in mm) and the entire area within the contour is at or above the thickness defined by the contour itself.

2.2.1 Sandwave Clearance

This section presents SSFATE modeling results associated with TSS generation and sediment deposition from the simulation of sandwave clearance.

A snapshot of the instantaneous concentrations is presented in Figure 3 with the vertical cross-section along the route. This figure illustrates that higher concentrations were contained around the route centerline, with lower concentrations biased towards the south due to bottom currents. The cross-section shows that the plume extended throughout the water column due to the sediment being introduced at the surface. The map of maximum time-integrated concentrations is presented in Figure 4 with the vertical cross-section along the route, the duration of exposure to TSS ≥10 mg/L is presented in Figure 5, and the seabed deposition is shown in Figure 6. Figure 4 illustrates how the plume oscillated with the tides, which is reflective in the oscillatory pattern of the concentrations relative to the route centerline. The oscillatory pattern was less evident in regions where the route is parallel to local currents. In sections where the route is parallel to the currents, the plumes from the periodic dumping locations interact with each other more than in sections where the currents are perpendicular to the route. The interaction of the plumes resulted in areas with prolonged durations of exposure to TSS concentrations ≥10 mg/L. Concentrations ≥10 mg/L had a maximum excursion of approximately 3.2 km from the route centerline. The map of duration of exposure to TSS ≥10 mg/L (Figure 5) shows a pattern similar to the maximum concentration, with most locations exposed for less than 12 hours and a small area exposed for a little over 12 hours. Because the sediment is predominantly coarse, which tends to settle out of the water column relatively quickly, the deposition tended to remain close to the route centerline near locations associated with the periodic dumping of sediment at the surface (Figure 6). The deposition close to the route centerline was relatively high due to the coarse sediment settling near the source and large volume of sediment introduced within a short period of time and in a small area.

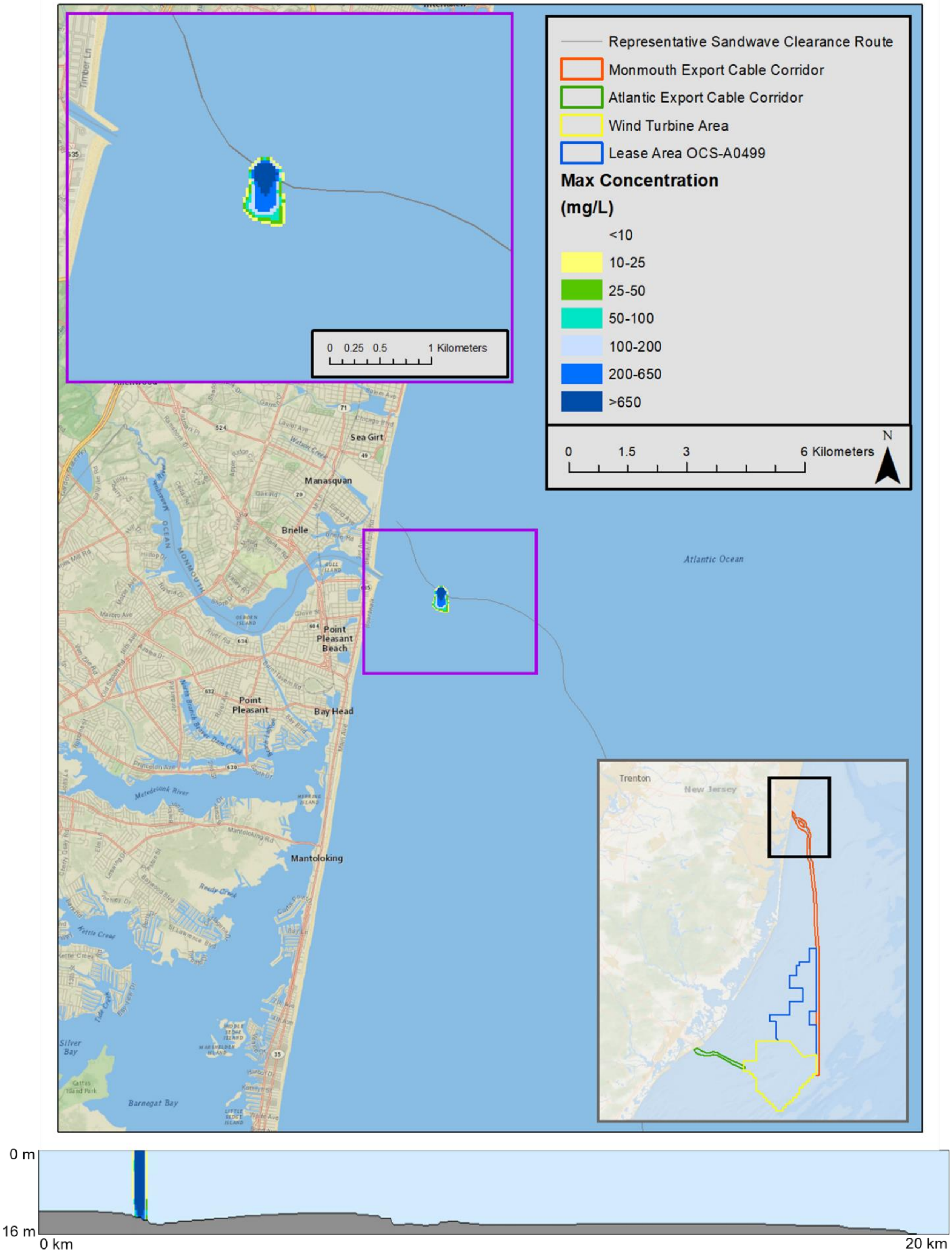

Figure 3. Snapshot of Instantaneous TSS Concentrations Associated with Sandwave Clearance along the Monmouth ECC.

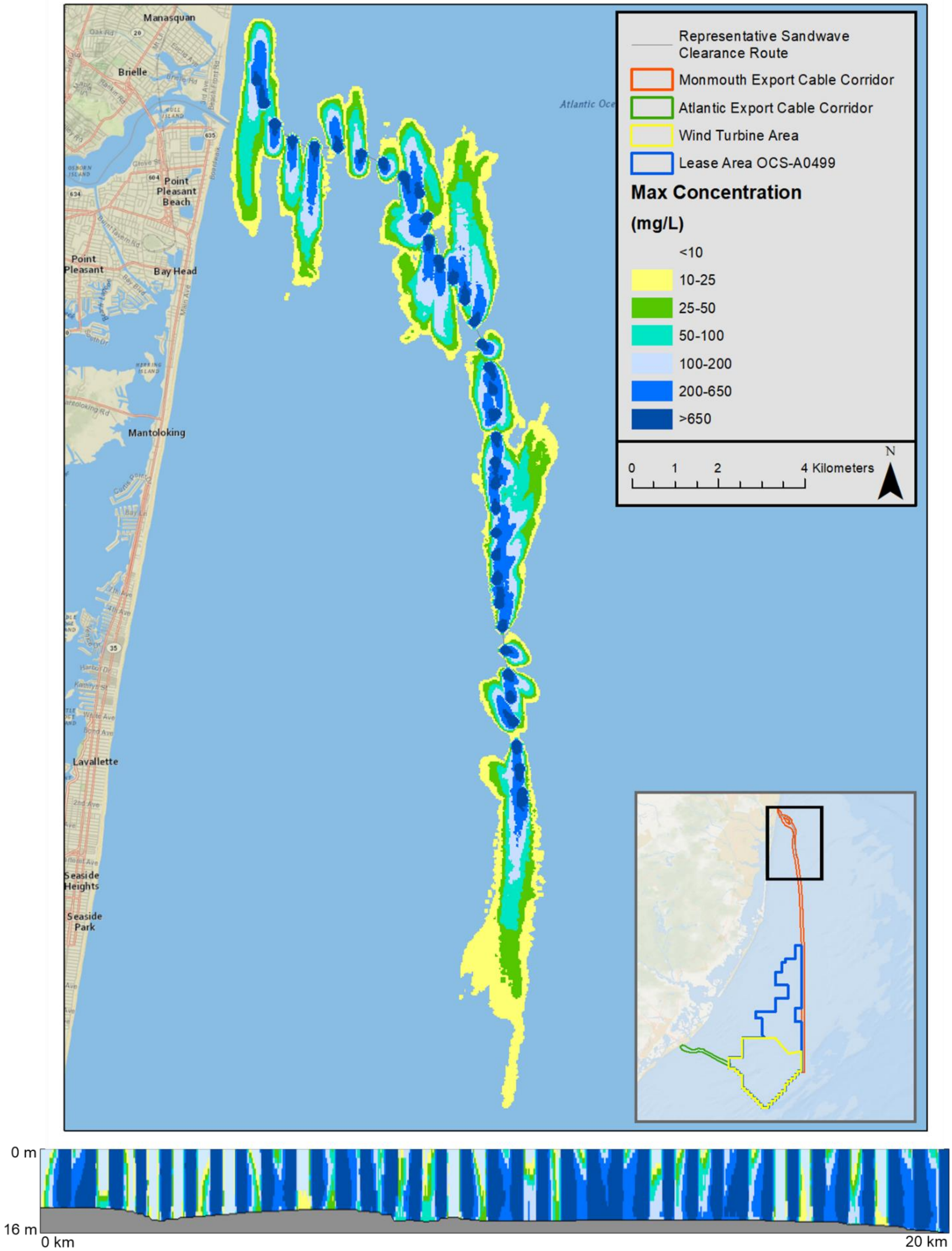

Figure 4. Map of Time-Integrated Maximum TSS Concentrations Associated with Sandwave Clearance along the Monmouth ECC.

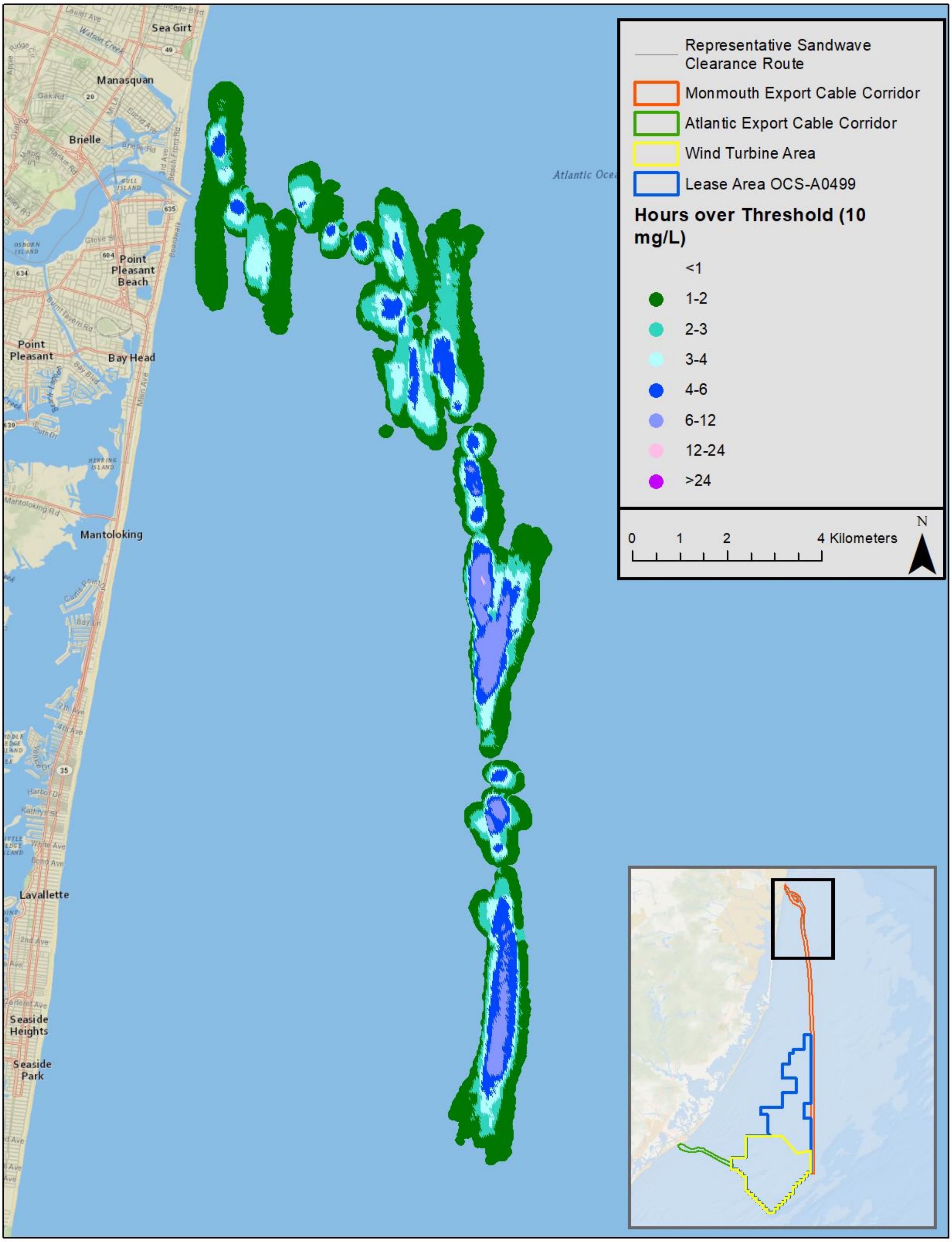

Figure 5. Map of Duration of TSS ≥10 mg/L Associated with Sandwave Clearance along the Monmouth ECC.

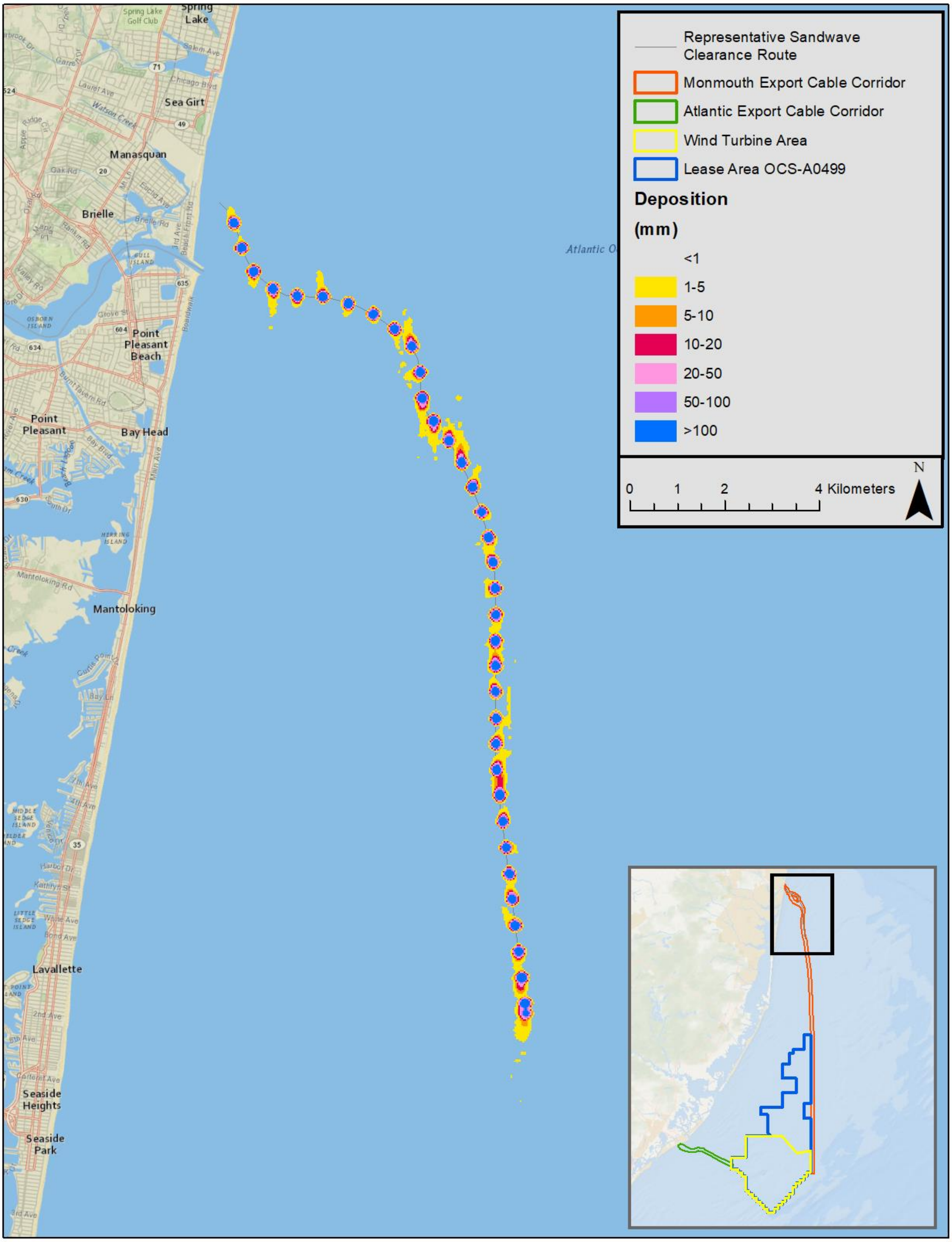

Figure 6. Map of Deposition Thickness Associated with Sandwave Clearance along the Monmouth ECC.

2.2.2 Results Summary Tables

Results were analyzed to determine the spatial area and maximum extents of TSS concentration, duration to TSS exposure, and deposition thresholds. The areas in these tables are the total areas from the entire simulation, and therefore reflect the sum of different instances of smaller areas throughout the entire route and do not occur simultaneously. These areas are not always contiguous. The results provide a sum of all individual concentration grid cells that exceeded a threshold anywhere in the water column.

Post-processing included calculations of areas above six TSS concentration thresholds for duration thresholds of 2, 4, 6, and 12 hours (Table 3 through Table 6). The tables illustrate that areas exposed to above-ambient TSS concentrations were largest when assessing concentrations above 10 mg/L, and that the areas rapidly decreased in size as the concentration threshold or duration increased. For example, as shown in Table 3, the total area throughout the entire route was 16.44 km^2 over 10 mg/L for more than two hours, but only 1.34 km^2 of this area was over 200 mg/L for more than two hours. Above-ambient TSS concentrations also decreased with time. Concentrations over 10 mg/L decreased from 16.44 km^2 for two hours (Table 3), to 5.97 km^2 for four hours (Table 4), to 2.05 km^2 for six hours (Table 5), to <0.01 km^2 for 12 hours (Table 6). In addition, TSS concentrations ≥25 mg/L did not endure for periods >12 hours.

Table 7 shows that the sandwave clearance activities are predicted to have 10 mg/L and 100 mg/L plumes that extend 3.2 km and 2.1 km from the route centerline, respectively. The plumes are not expected to be of these sizes contiguously from the release, but rather it shows the potential trajectory the sediment plumes may follow. As described in the preceding paragraphs, the plumes were temporary and dissipated to 10 mg/L or less within 12 hours.

Table 8 summarizes the areas affected by sediment deposition over various thickness thresholds. The maximum distance to the 1 mm and 10 mm thickness contours were 855 m and 165 m, respectively. Areas over deposition thresholds tended to decrease somewhat rapidly with increasing thresholds. The deposition close to the route centerline was relatively high due to the coarse sediment and large volume of sediment deposited in small areas.

Table 3. Areas over Above-Ambient TSS Threshold Concentrations for Longer than Two Hours.

	Concentration Thresholds in mg/L					
	10	25	50	100	200	650
Scenario	Areas Above Concentration Threshold (km^2)					
Representative Sandwave Clearance, Monmouth ECC	16.44	10.42	6.45	3.39	1.34	0.18

Table 4. Areas over Above-ambient TSS Threshold Concentrations for Longer than Four Hours.

Scenario	Concentration Thresholds in mg/L					
	10	25	50	100	200	650
	Areas Above Concentration Threshold (km^2)					
Representative Sandwave Clearance, Monmouth ECC	5.97	3.00	1.37	0.47	0.05	N/A

Table 5. Areas over Above-ambient TSS Threshold Concentrations for Longer than Six Hours.

Scenario	Concentration Thresholds in mg/L					
	10	25	50	100	200	650
	Areas Above Concentration Threshold (km^2)					
Representative Sandwave Clearance, Monmouth ECC	2.05	0.56	0.22	0.05	N/A	N/A

Table 6. Areas over Above-ambient TSS Threshold Concentrations for Longer than 12 Hours.

Scenario	Concentration Thresholds in mg/L					
	10	25	50	100	200	650
	Areas Above Concentration Threshold (km^2)					
Representative Sandwave Clearance, Monmouth ECC	<0.01	N/A	N/A	N/A	N/A	N/A

Table 7. Maximum Extent to the 10 mg/L and 100 mg/L TSS Contours from the Route Centerline.

Scenario	Maximum Duration (hrs) of TSS >10 mg/L	Maximum Distance (km) to 10 mg/L Contour	Maximum Duration (hrs) of TSS >100 mg/L	Maximum Distance (km) to 100 mg/L Contour
Representative Sandwave Clearance, Monmouth ECC	12.5	3.2	7.0	2.1

Table 8. Deposition over Thresholds.

Scenario	Max Extent (m) of Deposition ≥1 mm	Max Extent (m) of Deposition ≥10 mm	Area (km^2) over Deposition Threshold				
			1 mm	5 mm	10 mm	20 mm	100 mm
Representative Sandwave Clearance, Monmouth ECC	855	165	5.20	2.86	2.34	1.90	1.06

Results Discussion

For sandwave clearance activities, the plume footprint was largely influenced by the higher fraction of coarse sediment and large amount of sediment introduction at the water surface. Due to the periodic disposal of coarse sediment, the resulting footprint exhibited periodic plumes of higher concentrations and deposition along the route, especially when currents were parallel with the route.

Above-ambient TSS concentrations stemming from sandwave clearance activities remained relatively close to the route centerline and were short-lived. The maximum distances for the predicted above-ambient TSS concentrations ≥10 mg/L and 100 mg/L were approximately 3.2 km and 2.1 km, respectively. Above-ambient TSS concentrations substantially dissipated within four to six hours and fully dissipated in less than 12 hours for most areas. Deposition ≥1 mm and ≥10 mm was limited to 855 m and 165 m from the route centerline, respectively. The maximum deposition was >100 mm and predicted to extend a maximum distance of 20 m from the route centerline. While the extent and persistence of the plume and the extent and thickness of deposition were largely influenced by sediment grain size distribution, volume of sediment suspended, and location of sediment introduction within the water column, other factors of influence include route orientation relative to currents, timing of currents, and installation parameters.